University of Nevada

Reno

Earthquake Probability Models: Recurrence Curves, Aftershocks, and Clusters

A dissertation submitted in partial fulfillment of the requirements for the degree of Doctor of Philosophy in Geophysics

by

William Underwood Savage

December 1975

The dissertation of William Underwood Savage is approved:

Alan Rigall 12/18/75
Dissertation advisor

Lawrence L. Lamm
Department chairman

L R O'Brien
Dean, Graduate School

University of Nevada

Reno

December 1975

ACKNOWLEDGMENTS

It is with gratitude and pleasure that I acknowledge the guidance and advice provided by Dr. Alan S. Ryall during my graduate studies. I also thank Dr. Stephen D. Malone and Karen McNally for their encouragement and helpful comments. The many instances of assistance and support from friends and colleagues at the University of Nevada, the University of California at Berkeley, the National Center for Earthquake Research, and Woodward-Clyde Consultants are gratefully acknowledged. This work would not have been possible without the assistance of my wife, Lyn.

Portions of this work were supported by the Advanced Research Projects Agency and were monitored by the Air Force Office of Scientific Research under grant AFOSR-71-2041. It was also partly supported by the Atomic Energy Commission under contract AT(26-1)-454.

ABSTRACT

The application of the one-dimensional Poisson probability model to magnitude- and time-series of earthquakes can be an important aid in further understanding of the physics of earthquake occurrence, yet there are many features of earthquake sequences that are not described by the simple Poisson model. From a detailed examination of the axiomatic basis of the Poisson process in the context of observed earthquake magnitude-frequency and occurrence-frequency distributions, specific non-Poisson earthquake behavior patterns are identified and isolated for further study. Emphasis is placed on understanding the process of earthquake occurrence rather than on the determination of accurate mathematical models.

The frequency distribution of magnitude has been extensively discussed in terms of the linear relationship log N = a - bM. The Poisson basis of the law is reviewed so as to apply proper statistical procedures to evaluate data samples consistently and accurately. In studying the Poisson behavior of magnitude distributions, three non-Poisson elements must be considered in order to perform a mathematically valid analysis of b-values: determination of the minimum magnitude cutoff needed to define a complete catalog, possible non-random characteristics of the largest events, and magnitude-value biases or other sources of nonlinear magnitude-frequency distributions. Close examination of the cumulative

magnitude-frequency plot combined with use of the maximum likelihood estimator of b is the best b-value analysis technique. In the analysis of specific samples of foreshocks and aftershocks, it is found that the proposed dependence on compressive stress level within a fracture zone is not statistically supported at a high confidence level.

For earthquake time-series, three processes based on the Poisson model appear to describe earthquake behavior. The first is a simple Poisson occurrence of independent earthquakes that has a stationary or slowly time-varying occurrence rate. The second is the triggered process of aftershock occurrence, in which one of the independent events in the simple Poisson process initiates a single sequence or multiple sequences of aftershocks. Each aftershock sequence is composed of Poisson-distributed independent events that follow an approximately hyperbolically decaying rate law, with the trigger event generally of magnitude 4.0 or larger. The third process is that of microearthquake clustering, occurring among earthquakes of magnitude up to between 3.0 and 4.0. Clustering is defined by spatial and temporal relatedness among earthquakes and is identified in the seismically active regions of Nevada and central California. A cluster is not characterized by a trigger event, but each cluster is composed of events with magnitudes independent of one another. The cluster-size frequency distribution is described by an inverse power law with exponent near 3.5. Spatial and temporal statistical

features of clustering are analogous to those of the aftershock process in most respects, but the pattern of energy release is symmetric about the center of the cluster in constrast to the major energy release occurring with the trigger event of an aftershock sequence. Comparisons with laboratory experiments suggest that the predominant occurrence of clusters of earthquakes containing events differing by less than one-half magnitude unit is associated with the small size of the source volumes of the clustered events and apparent rapid viscoelastic reloading of the initial slip surface.

TABLE OF CONTENTS

CHAPTER I. INTRODUCTION

The proliferation of accurate and extensive earthquake catalogs has encouraged the use of earthquake statistics in fitting mathematical models to the patterns of earthquake occurrence. Such statistical probability models may be useful in developing more understanding of the mechanisms whereby earthquakes occur. However, the physics of the occurrence of earthquakes presently is not well understood in a deterministic sense. The collection and study of extensive earthquake data catalogs have occurred in an attempt to increase understanding of earthquake physics because of the inaccessibility of earthquake sources to direct experiments and measurements.

The use of probabilistic models in lieu of deterministic ones can be subject to a number of both mathematical and seismological (physical) errors and subtleties. In many earlier studies of earthquake statistics, the attempt often was made to find a mathematical model that accurately described the observed distribution of one or more variables of an earthquake data set. Then values of the parameters of the model were related to a physical interpretation of the mechanisms governing the occurrence of the data set. In this study, the weaknesses of such straightforward modeling procedures are discussed. In general, it is not reasonable to assume that simple probability models can describe the complexity of features of earthquake occurrence. In an

effort to develop mathematically accurate models, the more significant information and understanding from the seismological point of view can be obscured or neglected.

Poisson processes and derivations therefrom have proven applicable to many physical processes characterized by independently occurring events. In this paper, a critical review will be presented of the usage of the Poisson-based class of mathematical models in seismology. It will be shown that at the present time the primary value of the models discussed here is in identifying and isolating basic earthquake occurrence patterns for further analysis and thereby establishing constraints for the testing and evaluation of deterministic laboratory and theoretical physical models. The approach used in this study involves (1) explicit consideration of the mathematical assumptions made; (2) careful evaluation of the composition of the data sets used, particularly of the measurement of the parameters; (3) detailed examination of the ability of the models used to adequately or inadequately represent the observed earthquake parameters; and (4) interpretation of the probability models and their inadequacies in terms of the processes of earthquake occurrence.

The key to this approach lies in the attempt to identify and investigate the details of any disagreement between the models used and the data they are trying to describe probabilistically. This perspective on the use of probability models in seismology is taken so as to maximize the

seismological understanding gained rather than demonstrate the application of statistical probability theory.

Poisson Processes

For modeling purposes, an earthquake is defined as a point event described by its focal coordinates, occurrence time, and magnitude. Procedures for measuring these parameters vary individually for the specific data sets used. There are certainly other parameters that may be used to describe earthquakes, such as focal mechanism, stress orientation, slip area, stress drop, ambient stress, and geologic setting. But for an initial model that will be applied generally, the least complex and most widely and uniformly observed parameters are most suitable for mathematical treatment. The models and data samples that will be discussed will be related to other parameters of earthquake occurrence to the greatest extent possible.

The most mathematically tractable examination of the earthquake point process is in terms of one-dimensional frequency distributions. A cursory examination of the chronological catalogs of many earthquake data sets suggests a somewhat random distribution of location, magnitude, and occurrence time. The class of probability models to which such random data is applied is the stochastic process. Several authors (Cox and Lewis, 1966; Parzen, 1962; and Vere-Jones, 1970) have presented the theory of one- and multi-dimensional stochastic processes. Common usage applies the

term "stochastic" to mathematical models and "random" to the data variable being discussed.

The simplest one-dimensional model of a series that is random over some parameter is the Poisson process, which can be derived from the following axioms (Parzen, 1962). Let q be a continuous coordinate with events taking place at q_1, q_2, q_3, ..., and let N(q) be the number of events which have occurred in the interval (0,q]. The Poisson process is usually defined over the coordinate of time but, for the sake of generality, an arbitrary coordinate q is used in this definition.

Axiom 1. The process N(q), $q \geq 0$, has independent increments; that is, the number of events in any interval (q_i, q_j) is independent of the number of events in any other nonoverlapping interval. Thus, the events composing N(q) are assumed to have no causal connection.

Axiom 2. For any $q \geq 0$, the probability that an event will occur in a given interval dq, no matter how small, is greater than zero and is, in fact, equal to λdq, where λ is a constant over q. λ corresponds to the average number of events per unit q.

Axiom 3. For $q \geq 0$,

$$\lim_{h \to 0} \frac{P[N(q+h) - N(q) > 1]}{P[N(q+h) - N(q) = 1]} = 0 \quad ; \tag{1-1}$$

or, it is not possible for events to happen at exactly the same value of q.

Axiom 4. N(q) has stationary increments. That is, for any two values of q, $q_2 > q_1 > 0$, and any $h \geq 0$, the random variables $N(q_2) - N(q_1)$ and $N(q_2+h) - N(q_1+h)$ are identically distributed. Thus, the distribution is constant over q.

These axioms lead directly to a differential equation whose solution is the Poisson distribution (Parzen, 1962),

$$P(x,q) = \frac{e^{-\lambda q} (\lambda q)^x}{x!} , \qquad (1\text{-}2)$$

where λ is the mean number of events per unit q, and P(x,q) is the probability of occurrence of x events in interval q. The mean of equation (1-2) is λq and is the most probable number of events in interval q.

It is also shown (Parzen, 1962) that, for random events that are Poisson distributed in time, the occurrence intervals between successive events (q_2-q_1, q_3-q_2, ...) are independent, exponentially distributed random variables with cumulative distribution function

$$F(q) = 1 - e^{-\lambda q} , \qquad (1\text{-}3)$$

and density function

$$f(q) = dF/dq = \lambda e^{-\lambda q} . \qquad (1\text{-}4)$$

It is not necessarily true, however, that events with exponentially distributed occurrence intervals are Poisson distributed. As an extreme example, the exponentially distributed occurrence intervals could be sequentially distributed according to size, having the intervals increasing from smallest to largest. This would certainly contravene axioms 1 and 4, yet satisfy equation (1-3).

An additional useful property of the Poisson process is its additivity. That is, the sum of two independent Poisson processes with rate λ_1 and λ_2 is a Poisson process with parameter $\lambda_s = \lambda_1 + \lambda_2$ (Parzen, 1962). This may be extended to the sum of any number of independent Poisson processes.

In order to model certain kinds of statistical behavior, several modifications of these axioms can be made so as to describe specific features of earthquake occurrence. The resulting generalized Poisson processes are powerful modeling tools, but the increased mathematical sophistication also holds the possibility of obscuring a greater understanding of the physics of earthquake occurrence.

In the following chapters, the Poisson process model will be used to analyze the sequence of earthquakes in time, N(t), and the sequence of earthquakes in magnitude, N(M). For both one-dimensional processes, the analysis will involve the discussion and application of the relevant statistical techniques to find parameters of Poisson models to fit various data sets. From this base, the more significant aspects of the modeling procedure will be investigated, namely, the details of any inadequacies of the Poisson model. It is remarkable to find that the simple, one-dimensional Poisson model represents the statistical features of earthquakes from so many differing geologic and tectonic settings. The power of the model as discussed herein, however, lies in its usefulness in allowing the discrimination of some more subtle features of earthquake occurrence.

Sources of Earthquake Data

Earlier statistical studies by a variety of authors have used earthquake catalog data taken from many local sources, as well as worldwide catalogs such as the Hypocenter Data File prepared by the National Oceanic and Atmospheric Administration (NOAA). As many of these studies are reviewed and reanalyzed in the following chapters, the data sources will be described.

Three additional earthquake data samples that are discussed in this paper have not been previously analyzed.* These samples are briefly described here.

Beginning in October, 1969, a state-wide telemetry network covering the central portion of Nevada was put into operation. Stations are indicated by triangles in Figure 1-1, and the events recorded and located during the period up to the end of 1971 are shown. Events in the six quadrilateral zones were selected for particular analysis. Locations were revised to obtain the best possible epicenters. Magnitudes for the events have not been determined in general; however, for specific events, in order to obtain magnitude estimates, comparisons were made between amplitudes obtained from the Wood-Anderson instruments at Reno, and amplitudes recorded on three-component, short-period Benioff

*Some of the material for this paper has been taken from a publication by the author, "Microearthquake clustering near Fairview Peak, Nevada, and in the Nevada Seismic Zone," Journal of Geophysical Research, vol. 77, pp.7049-7056 (1971).

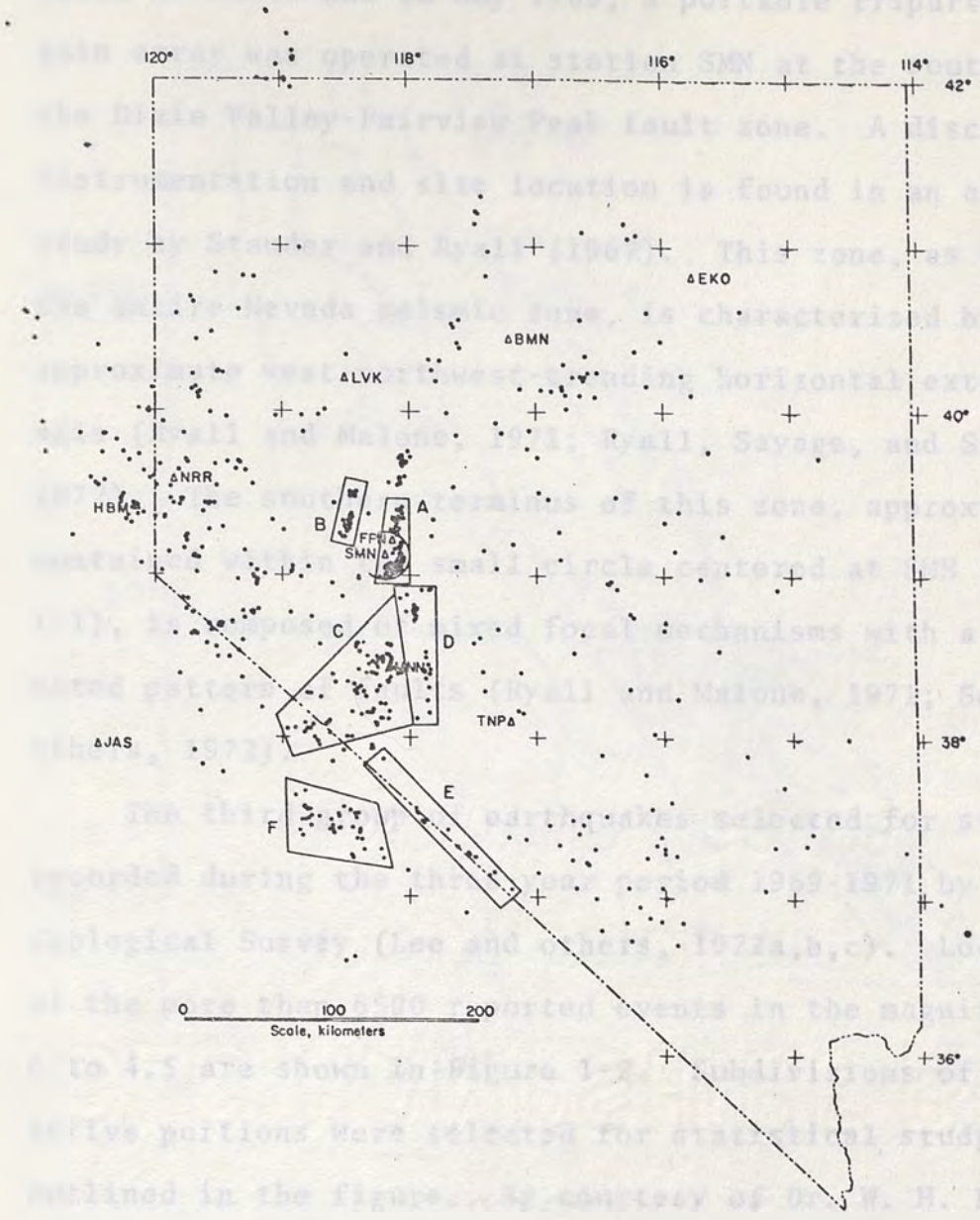

Figure 1-1. Study areas in the Nevada Seismic Zone. (A) Fairview Peak zone; (B) Rainbow Mountain zone; (C) Mina zone; (D) Cedar Mountains zone; (E) Fish Lake Valley zone; (F) Bishop zone. Circular zone around station SMN contains events used in detailed microearthquake study.

instruments at Tonopah (TNP) and Battle Mountain (BMN).

Just prior to operation of the state-wide network, between 17 March and 16 May 1969, a portable tripartite high-gain array was operated at station SMN at the south end of the Dixie Valley-Fairview Peak fault zone. A discussion of instrumentation and site location is found in an earlier study by Stauder and Ryall (1967). This zone, as well as the entire Nevada seismic zone, is characterized by an approximate west-northwest-trending horizontal extension axis (Ryall and Malone, 1971; Ryall, Savage, and Slemmons, 1972). The southern terminus of this zone, approximately contained within the small circle centered at SMN (Figure 1-1), is composed of mixed focal mechanisms with a complicated pattern of faults (Ryall and Malone, 1971; Smith and others, 1972).

The third group of earthquakes selected for study was recorded during the three-year period 1969-1971 by the U. S. Geological Survey (Lee and others, 1972a,b,c). Locations of the more than 6500 reported events in the magnitude range 0 to 4.5 are shown in Figure 1-2. Subdivisions of the most active portions were selected for statistical study and are outlined in the figure. By courtesy of Dr. W. H. K. Lee of the U. S. Geological Survey, a magnetic tape containing all event focal locations, magnitudes, and other location information was provided, by means of which the analysis was conducted.

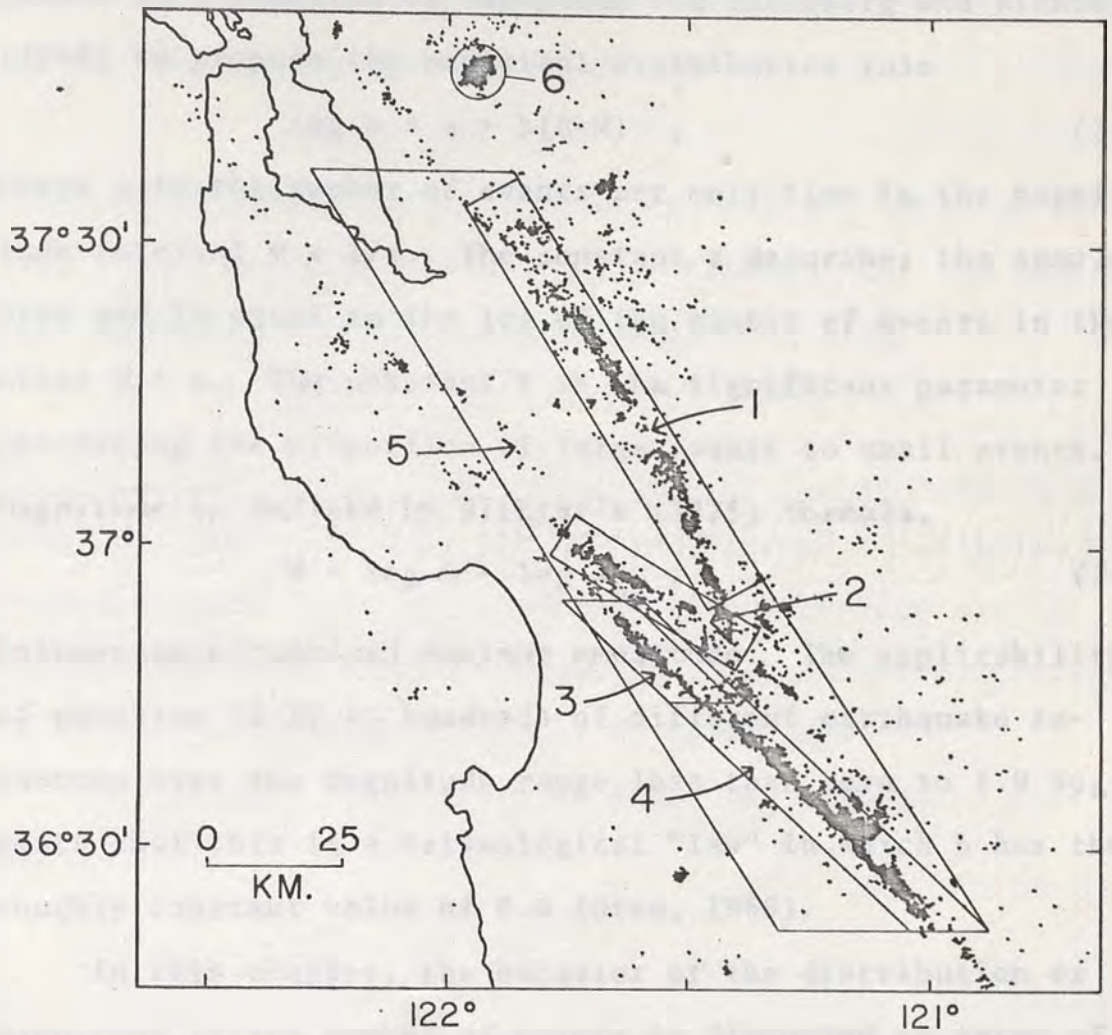

Figure 1-2. Study areas in Central California. (1) Calaveras zone; (2) Sargent zone; (3) San Andreas North zone; (4) San Andreas zone; (5) Central California zone; and (6) Danville swarm zone.

CHAPTER II. MAGNITUDE-FREQUENCY RELATIONSHIPS

Introduction

The examination of the frequency of occurrence of earthquakes as a function of magnitude led Gutenberg and Richter (1944) to propose the empirical distribution rule

$$\log n = a + b(8-M) \quad , \tag{2-1}$$

where n is the number of events per unit time in the magnitude interval M ± 1/4. The constant a describes the sample size and is equal to the log of the number of events in the class M = 8. The constant b is the significant parameter describing the proportion of large events to small events. Magnitude is defined by Richter's (1935) formula,

$$M = \log A - \log A_o \quad , \tag{2-2}$$

between magnitude and maximum amplitude. The applicability of equation (2-1) to hundreds of different earthquake sequences over the magnitude range less than zero to 8.9 suggests that this is a seismological "law" in which b has the roughly constant value of 0.9 (Utsu, 1969).

In this chapter, the behavior of the distribution of magnitude versus number of events is discussed in terms of the simple Poisson process reviewed in Chapter I. The analysis of magnitude distributions is examined in terms of proper techniques for determining statistical significance. Poisson and non-Poisson aspects of several distributions are then evaluated as properties of earthquake occurrence as well as products of the measurement of magnitude.

Theoretical Review

In common usage, equation (2-1) is usually rewritten as

$$\log n(M) = a' - bM \quad , \tag{2-3}$$

where n(M) is the number of events with magnitude between M and M + dM. In exponential form, this is

$$n(M) = 10^{a'}\ 10^{-bM} \quad . \tag{2-4}$$

Prior to Gutenberg and Richter's publication, Ishimoto and Iida (1939) presented an equivalent relation for the number n(a) of events in the amplitude range a to a+da,

$$n(a) = Ka^{-m} \quad . \tag{2-5}$$

The constant m-1 was shown equal to b in equation (2-4) by Asada and others (1951). The Gutenberg-Richter relation has been more generally applied due to the widespread use of Richter magnitude values. Equation (2-3) is often referred to as the "recurrence curve" or "b-value curve."

Integrating equation (2-4) gives the cumulative form of the law,

$$N(M) = 10^{A}\ 10^{-bM} \quad , \tag{2-6}$$

or, in logarithmic form,

$$\log N(M) = A - bM \quad , \tag{2-7}$$

where N(M) is the number of events greater than or equal to the magnitude M. In accumulating magnitude statistics, intervals of magnitude are typically used, in which the value M is assigned to the group of magnitudes falling between M-ΔM and M+ΔM. Thus, for the discrete case, the interval and cumulative equations are easily related:

$$n(M) = N(M-\Delta M) - N(M+\Delta M) = 10^{a}\, 10^{-bM} . \quad (2\text{-}8)$$

The value of b is often determined by fitting either equation (2-3) or (2-7) to the data using linear or weighted least-squares methods or using "eye-ball" techniques.

An alternate method of determining b has been noted by Utsu (1965) and Lomnitz (1966). For a given sample, they calculated the value of the mean magnitude of all the events larger than some minimum M_o:

$$\overline{M}(M_o) = \frac{\sum_i M_i n(M_i)}{\sum_i n(M_i)} = M_o + \frac{1}{b \ell n 10} . \quad (2\text{-}9)$$

From this, the value of b is easily calculated:

$$b = \frac{.4343}{\overline{M}(M_o) - M_o} . \quad (2\text{-}10)$$

Note that M_o has the exact value $M_o = M_1 - \Delta M$, where M_1 is the first magnitude class.

Aki (1965) demonstrated that equation (2-10) has an alternate derivation and is, in fact, the maximum likelihood estimator of b.

Before presenting the derivation of the maximum likelihood technique, it is necessary to determine the probability density function for M. Equation (2-6) is normalized so that its intergral from M - 0 to infinity is one and is origin-translated so that the new function, N'(M), gives the cumulative distribution of magnitudes less than M:

$$N'(M) = 1 - e^{-(b \ell n 10)M} . \quad (2\text{-}11)$$

Also, if the minimum magnitude is 0.0, from equation (2-9),

$$M = \frac{1}{b\ell n10} \quad . \tag{2-12}$$

At this point it is important to recognize that the formulae developed through equation (2-12) indicate that the sequence of magnitudes described by equation (2-3) can be shown to be Poisson distributed. N'(M) in equation (2-11) is in the form of equation (1-3) with mean given by $b\ell n10$. The continuous variable q has been replaced by the discontinuous variable M. M is associated with each point event in the same way that the quantity $(q_{i+1} - q_i)$ is. According to Theorem 2B of Parzen (1962), if the occurrence intervals (the values of M) are exponentially distributed with mean $1/\lambda$, and if the occurrence intervals are independent, identically distributed positive random variables, then the process N'(M) is a Poisson process with intensity λ. The two conditions of this theorem are well satisfied by the general success with which the exponential distribution of equation (2-4) describes any time-sequential grouping of magnitudes.

The recognition that earthquake magnitudes may be described by the Poisson process, with all its attendant mathematics, suggests that the four axioms of Chapter I should be applicable. Reformulated in terms of magnitude, the assumptions are as follows:

1_M. there is no causal connection between events of different magnitudes;

2_M. the probability of occurrence of an event is a small constant greater than zero;

3_M. there is a minimum magnitude for the data set considered; and

4_M. the distribution of magnitude is constant over the order of occurrence in the sequence.

Although these axioms and the Poisson process are found to apply generally to all earthquake magnitudes, instances exist when one or more axioms do not apply, as for aftershock sequences. These cases will be examined in detail later in this chapter.

It may then be concluded from the foregoing that for a given sequence of magnitudes, the number of events within each magnitude class is a Poisson-distributed random variable. From equation (1-2), the probability distribution of the number n of events with magnitude $M_i \pm \Delta M$ is given by

$$P(n) = \frac{e^{-n(M_i)} n(M_i)^n}{n!} \quad . \qquad (2\text{-}13)$$

$n(M_i)$ is the mean number of events obtained from equation (2-8). Using the additive property of Poisson processes, the number of events with $M \geq M_i - \Delta M$ is also Poisson distributed. This distribution was noted to be empirically true by Utsu (1961) after Suzuki (1958).

The maximum likelihood estimator of b and its confidence limits can now be derived. From the distribution function

equation (2-11), the probability density function f(M) is obtained:

$$f(M) = \frac{dN'}{dM} = b'e^{-b'M} \quad , \tag{2-14}$$

in which $b' = b\ell n10$. Since magnitude will again be measured in finite classes, successive integration over the limits $(M-\Delta M)$, $(M+\Delta M)$ between M_o and M_m results in the discrete equation

$$f(M_i) = \frac{(e^{b'\Delta M} - e^{-b'\Delta M})e^{-b'M_i}}{e^{-b'M_o} - e^{-b'M_m}} \quad . \tag{2-15}$$

Again, M_i is the central value of each class, and, for $i = (1,\ldots,k)$, $M_o = M_i - \Delta M$, and $M_m = M_k + \Delta M$.

For large samples, the parameter b calculated by maximizing its joint probability distribution (equation 2-15) is at least as good as other estimates of b (von Mises, 1964).

It will be found later that, even for very small samples, the maximum likelihood technique is accurate but with large error limits. By finding

$$\frac{\partial f}{\partial b'} = 0$$

the maximum probability with respect to b' can be found for each magnitude M_i. Since $f(M_i)$ is an exponential function, it will be computationally easier to first take the logarithm:

$$y_i = \frac{\partial}{\partial b'} \ell n f(M_i) \quad . \tag{2-16}$$

For all the values of M_i, the maximum joint likelihood becomes

$$\sum_i y_i = \frac{\partial}{\partial b'} \ln \prod_i f(M_i) = 0 \quad . \qquad (2\text{-}17)$$

When evaluated using equation (2-15),

$$\Delta M \frac{e^{2b'\Delta M} + 1}{e^{2b'\Delta M} - 1} + \frac{M_o e^{-b'M_o} - M_m e^{-b'M_m}}{e^{-b'M_o} - e^{-b'M_m}} - \frac{\sum M_i}{N} = 0 \quad , \qquad (2\text{-}18)$$

is obtained. This equation may be solved directly for the maximum likelihood estimator of b', but several simplifications are possible. In the first term, the quotient of exponentials may be expanded in a power series. When evaluated for a range of values of $2b'\Delta M$, this term may be replaced by $1/Kb'$ with K listed in Table 2-1 (after Utsu, 1971). No correction is needed for $2b\Delta M$ less than about 0.4. When the magnitude range $M_m - M_o$ is larger than 2.0, the second term may be set equal to M_o with less than a few percent error in b'. Thus, for a large magnitude range, equation (2-18) reduces to

$$Kb = \frac{.4343}{\bar{M}(M_o) - M_o} \quad . \qquad (2\text{-}19)$$

For small magnitude intervals, K = 1, and this equation is the same as equation (2-10) obtained by calculating the average magnitude.

As Aki (1965) showed, confidence limits for b are easily derived. The central limit theorem (Hahn and Shapiro, 1967) states that "the distribution of the standardized mean of n independent observations from any distribution with finite mean and variance approaches a standard normal distribution

TABLE 2-1

$2b\Delta M$	K
0.0	1.000
0.1	1.004
0.2	1.017
0.3	1.039
0.4	1.070
0.5	1.108
0.6	1.154
0.7	1.208
0.8	1.268
0.9	1.344
1.0	1.407

as the number of observations in the sample becomes large." The mean of y_i is zero, using equation (2-16).

The variance is found to be

$$\sigma^2 = \frac{1}{k^2 b'^2} + \frac{(M_m - M_o)^2}{2 - e^{b'(M_m - M_o)} - e^{b'(M_o - M_m)}} \quad . \tag{2-20}$$

Then, from the central limit theorem, the function

$$\frac{\frac{\Sigma y_i}{n}}{\sqrt{\frac{\sigma^2}{n}}} = \frac{\Sigma y_i}{\sigma\sqrt{n}} \tag{2-21}$$

is distributed according to the standard normal distribution, with mean equal to zero and standard deviation equal to one. The confidence limits are then given by (Hahn and Shapiro, 1967):

$$\frac{\Sigma y_i}{\sigma\sqrt{n}} \leq t_{c\ell,n-1} \quad . \tag{2-22}$$

The expression (equation 2-18) is inserted for Σy_i to obtain (after Page, 1968)

$$\frac{1}{\sqrt{n}} \left[\frac{1}{Kb'} + \frac{M_o e^{-b'M_o} - M_m e^{-b'M_m}}{e^{-b'M_o} - e^{-b'M_m}} - \frac{\Sigma M_i}{N}\right] \Big/$$

$$\left[\frac{1}{K^2 b'^2} + \frac{(M_m - M_o)^2}{2 - e^{+b'(M_m - M_o)} - e^{b'(M_o - M_m)}}\right]^{1/2}$$

$$\leq t_{c\ell,n-1} \quad . \tag{2-23}$$

The inequality (equation (2-23) is solved for b' to obtain the limits. Typically, 95% confidence limits are used, thus

giving the range of value of b' such that the probability is 0.95 that the "true" value of b' lies within the range.

Confidence limits permit the estimation of fluctuation of the value of b due to random variations in $n(M_i)$, the number of events per magnitude class. The approximation made in calculating the confidence limits was that $n(M_i)$ is normally distributed. As was found earlier, the distribution is actually Poisson; but near the mean, even for quite small numbers, the two distributions are quite similar with no extreme deviations. Thus, the confidence limit calculations should be correct for arbitrarily small numbers of events.

A statistically proper test to compare b-values from two sets of data was discussed by Utsu (1966). For two sequences with b-values b_a and b_b, $b_b<b_a$, which were calculated with numbers of events n_a and n_b, the ratio b_b/b_a is tested for the hypothesis that the b-values are equal. Utsu (1966) showed that the ratio is distributed according to the F distribution with $2n_a$ and $2n_b$ degrees of freedom. Thus, the difference in b-value is significant at the 100α% level if

$$\frac{b_a}{b_b} > F_{\alpha}(2n_b, 2n_a) \quad . \tag{2-24}$$

The preceding method for comparing b-values is not necessarily sensitive to the seismologically significant difference in b-value. For example, two pairs of b-values, (0.5, 0.8) and (0.9, 1.2), have the same arithmetic difference but ratios of 1.6 and 1.33, respectively. In later

discussions in this chapter, several factors which could affect the "baseline" level of b are discussed. In principle, comparisons with different baselines should be performed with a b_a-b_b test rather than a b_b/b_a test. Cox and Lewis (1966) discuss a different test appropriate for Poisson parameters. The confidence limits are given by

$$\frac{b_a - b_b}{\frac{b_a^2 \ell n 10}{n_a} + \frac{b_b^2 \ell n 10}{n_b}} \pm t_{c\ell,n-1} \quad . \tag{2-25}$$

For large sample sizes, this quantity can be assumed to have zero mean and unit variance. Cox and Lewis (1966) suggest that this distribution is well behaved even when the number of events is small.

Magnitude-Frequency Analysis: Techniques and Interpretations

The calculation of b-values is important in several research areas. Scholz (1968), following Mogi (1962), noticed an inverse relationship between compressive stress and b-value in laboratory fracturing experiments. Thus, the determination of a statistically significant low b-value for certain earthquake sets may be an indicator of high stress and, therefore, a predictive factor for large earthquakes. The good fit of an earthquake sequence to the linear recurrence law can also allow the selection of a complete earthquake sample. If it can be demonstrated that the low-magnitude

curvature often observed for recurrence curves is caused by the incomplete recording of small events, then a statistically complete sample (i.e. a sample including all events larger than a cutoff magnitude M_o) can be obtained by determining the magnitude at which curvature begins. The definition of M_o for each data sample must satisfy Poisson axiom 3_M. Complete samples are important in the study of earthquake time-interval distributions and of earthquake triggering hypotheses.

The assumed linearity of the magnitude-frequency distribution must also be evaluated for each sample. Curvature of "knees" may indicate an anomalous seismic region, or simply a bias or error in calculating magnitude. Axioms 1_M, 2_M, and 4_M of the Poisson process are violated by the occurrence of curvature. The behavior of the distribution for large earthquakes is often difficult to evaluate: should the largest events be included or excluded from a sample; is there a "maximum magnitude" for a particular region; do mainshocks belong to the same statistical population as aftershocks? The inclusion of "trigger" events violates axioms 1_M and 4_M, but because of the small number of large events typically involved, there is often no significant distinction that can be made in terms of Poisson behavior.

All of the preceding examples depend on recognizing the occurrence of and deviation from Poisson behavior of the magnitude distribution of earthquake data sets. In many earlier

studies, emphasis has been placed on determining b-values by various methods. The consideration here will also include examination of the detail of deviations from purely Poisson distributions of magnitude.

The methods available to calculate b-values, namely, visually fitting or least-squares fitting of straight lines to data samples plotted according to equations (2-3) or (2-7) or estimating b by the maximum likelihood technique, are used and evaluated in the following sections of this chapter. There are particular features of earthquake magnitude distributions which are of critical importance in applying the assumptions of Poisson behavior. In order of discussion these are: large-magnitude distributions, small-magnitude distributions, statistics of data grouping, and magnitude determination. Earthquake data sets from the literature are interpreted with respect to the details of their Poisson behavior.

Effect of Large Events. The largest events in an earthquake sample present several special problems for recurrence curve parameterization depending on the randomness or nonrandomness of their occurrence. As was discussed earlier (equation 2-13), the number of events that occur in a fixed time interval within a fixed magnitude range is expected to be Poisson distributed. The Poisson curves superimposed on the two recurrence curves for n(M) and N(M) in Figure 2-1 illustrate the process of random variations in number of events. The

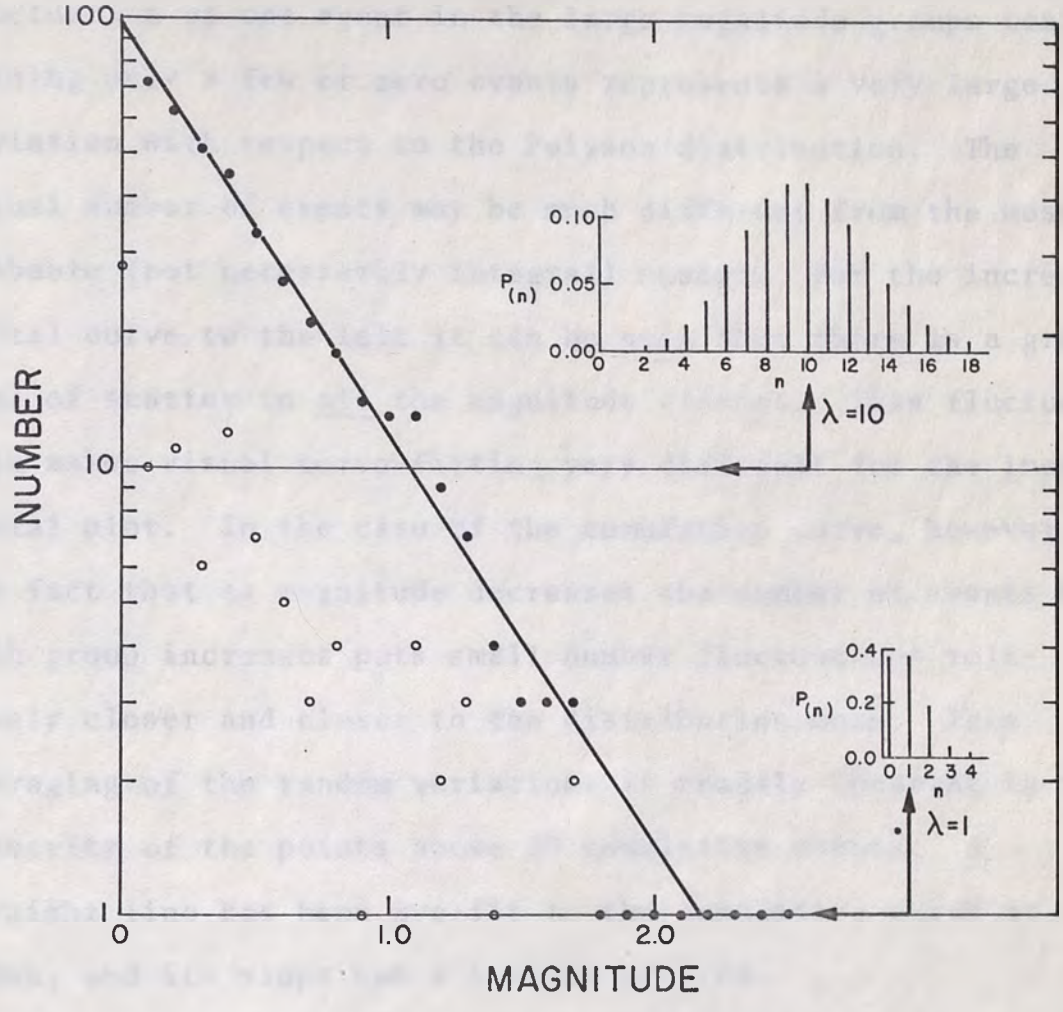

Figure 2-1. Magnitude-frequency curves for the random-number generated data in Table 2-2. Closed circles are for cumulative plot and open circles are for incremental plot. The Poisson distributions also shown are calculated for the values $\lambda = 1$ and $\lambda = 10$.

data composing the curves are taken from a random-number generated set of magnitude-frequency data with b = 1.00 used by Utsu (1967) and listed in Table 2-2. Because the number of events per magnitude class varies in integral amounts, a fluctuation of one event in the large magnitude groups containing only a few or zero events represents a very large deviation with respect to the Poisson distribution. The actual number of events may be much different from the most probable (not necessarily integral) number. For the incremental curve to the left it can be seen that there is a great deal of scatter in all the magnitude classes. This fluctuation makes visual curve-fitting very difficult for the incremental plot. In the case of the cumulative curve, however, the fact that as magnitude decreases the number of events in each group increases puts small number fluctuations relatively closer and closer to the distribution mean. This averaging of the random variations is readily apparent in the linearity of the points above 20 cumulative events. A straight line has been eye-fit to the cumulative curve as shown, and its slope has a b-value of 1.08.

An alternative to using visual fitting to determine the slope of a recurrence curve is to apply a least-squares technique. In the case of the incremental plot, for all magnitude intervals the random variations are large. Also, the values of log n(M) cannot be included in the regression when n(M) = 0, so the data must be truncated to exclude such

TABLE 2-2

M	n(M)	N(M)	M	n(M)	N(M)
0.0	28	100	1.3	3	7
0.1	10	72	1.4	1	4
0.2	11	62	1.5	0	3
0.3	6	51	1.6	0	3
0.4	12	45	1.7	2	3
0.5	7	33	1.8	0	1
0.6	5	26	1.9	0	1
0.7	3	21	2.0	0	1
0.8	4	18	2.1	0	1
0.9	1	14	2.2	0	1
1.0	0	13	2.3	0	1
1.1	4	13	2.4	0	1
1.2	2	9	2.5	1	1

points. In this example, the truncation occurs at M = 0.9, leaving only 10 points to which a line could be fit. Yet the other 16 points certainly contain valid information. Also, using unweighted least-squares assigns equal significance to both large and small numbers of events. More weight should be assigned the intervals with larger numbers of events to minimize random fluctuations, as in the Deming least-squares technique discussed by Utsu (1967). However, the weights would need to be varied according to the number of events per group and the total number of groups, a rather complex and arbitrary procedure.

The cumulative plot is much more amenable to least-squares. Again, weights would have to be assigned to reduce the computational significance of large-magnitude groups. But the well-defined linearity of the smaller events suggests that an unweighted fit could be calculated for N(M) greater than 10 with fairly small standard deviation. The standard deviation does estimate the quality of the fit, but, since some data was not used in the computation, it is not a satisfactory measure of the accuracy of the b-value.

There is another difficulty with use of the cumulative plot. Although random errors in the magnitude intervals would approximately average out as M decreased, whatever small error did not disappear would accumulate as N(M) increased. Ryall and others (1968) tested the effect of removing the largest event from the 250-event Truckee sequence

with $M \geq 2.2$. They obtained an increase in the value of b from .77 to .81, which is to be expected from a decrease in the number of large events in a cumulative plot. An estimate of the possible cumulative effect of random fluctuations in each magnitude group can be taken from a table of cumulative Poisson probabilities (Hahn and Shapiro, 1967, p.157). Utsu (1961) used this random fluctuation to obtain error limits on the value of b; his limits were very large because he assigned equal weight to the numbers of large-magnitude events. As can be noticed in Figure 2-1, the high or low fluctuation in numbers of events per magnitude class is biased to the low side; that is, the random fluctuations would lead to a more probable low estimation of N(M) and a consequently higher value of b for the cumulative plot.

The method of maximum likelihood avoids some of these problems. Since it uses the incremental rather than cumulative values of n(M), cumulative random error biases do not occur. And since all values of n(M) are used, including zero, the data-fitting difficulties of regression techniques are avoided. The b-value obtained for Utsu's (1967) random-number data using the maximum likelihood estimator is .95, with confidence limits ±.19 giving a measure of the random data variation, not the quality of linear fit.

In interpreting the meaning of the confidence limits just given for b (.95 ± .19), it is important to recall that these limits were calculated on the assumption of normally

distributed events in each magnitude class. From Figure 2-1, it is apparent that the statistical behavior for small samples is not a good approximation to normal behavior. Thus, the assumption of normally distributed deviations used to calculate the confidence limits of b (equations 2-16, 2-17, and 2-21) is not necessarily accurate for the few largest events.

The question of the statistical behavior of the few largest events of a sequence and whether or not to include them in b-value calculations can be examined from an empirical basis. For aftershock sequences, Utsu (1969) notes that in many cases the main shock is too large to be included in the recurrence curve of the aftershocks. He suggests that the main-shock occurrence mode may be quite difference than that of the aftershocks. In fact, earthquakes with aftershocks are characterized by their nonrandom behavior with respect to the aftershock sequence: they determine the starting point of an exponentially decreasing rate of occurrence of events. However, Ryall and others (1966) pointed out that as a rule only the most active portion of an aftershock sequence is included in the recurrence curve. The events which occur many months and years before and after the main shock are not completely included and may account for the apparent exceptional behavior of the main shock. Long-term distributions of larger events in the western United States do not suggest that main-shock and aftershock

recurrence curves are significantly different (Ryall and others, 1966).

Other earthquake occurrence patterns, such as swarms and secondary aftershock sequences (Utsu, 1969), may present similar inclusion-exclusion questions with respect to the largest events. An example of this is a swarm of several thousand detected earthquakes which occurred near Danville, California, in 1970. Bufe (1970) analyzed the largest 986 of these events to investigate the possibility of time-varying b-values. Using the maximum likelihood estimator on successive groups of 50 events, Bufe found large fluctuations in b (from 0.6 to 1.17) with extreme values occurring near the times of large events.

To test this conclusion, a reanalysis was performed using the list of Danville events in Lee and others (1971). The 374 events in the magnitude range of 1.1 to 4.3 were divided into groups of 50 and are plotted cumulatively in Figure 2-2. The b-values associated with these curves are given in Table 2-3. Visually the curves are quite different, and Bufe's conclusion that significantly different values occur at the times of large events seems to be substantiated. However, if the large events greater than or equal to M = 3.1 are not included in the calculation, the b-values given in the second row of Table 2-3 are obtained. The b-value for the entire sequence is .70 (which was also that found by Lee and others, 1971, using visual fitting) with associated 95%

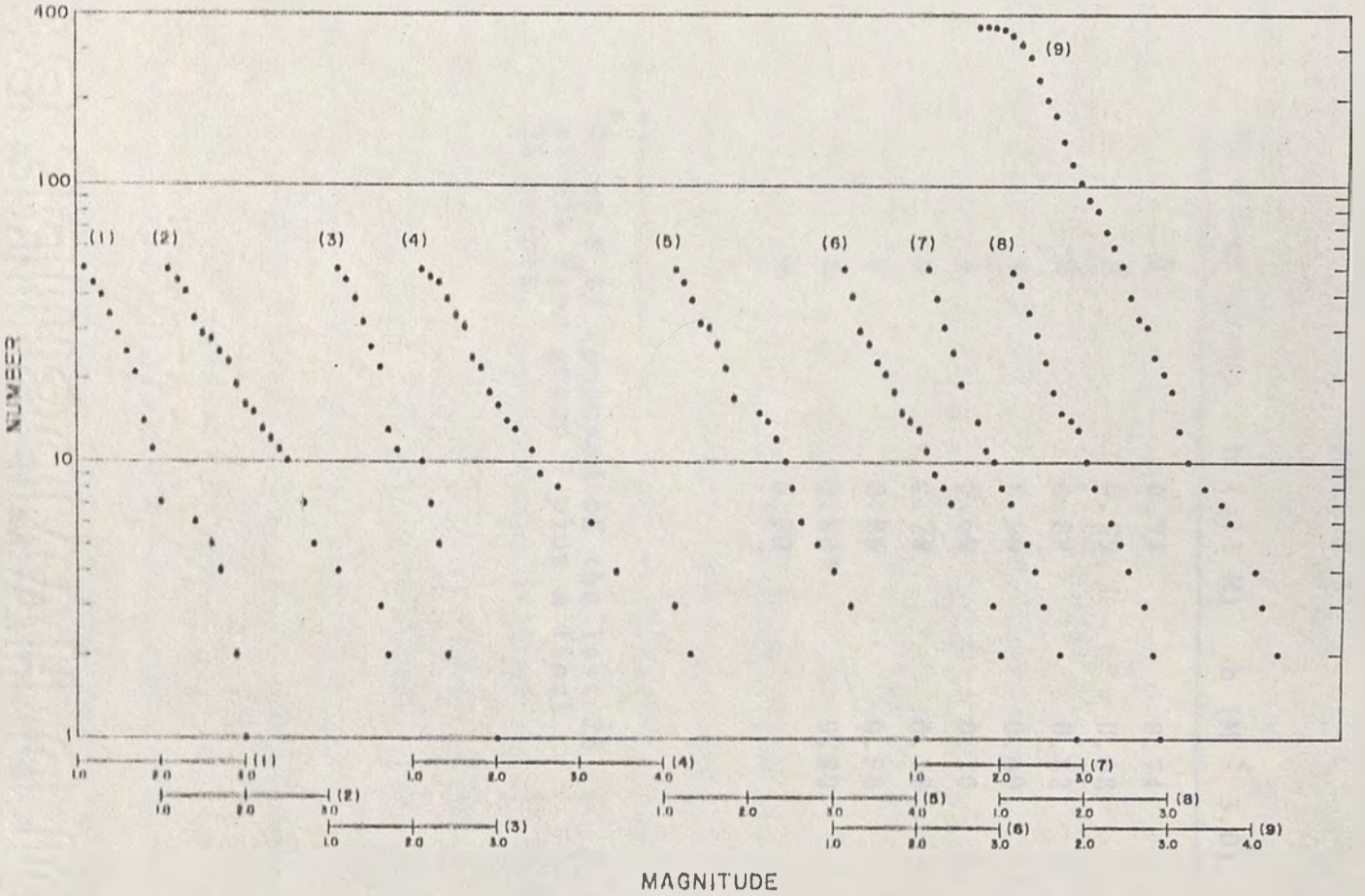

Figure 2-2. Cumulative magnitude-frequency plots for 50-event subsets of the Danville swarm. Subset 8 is composed of 25 events from subset 7 plus the last 25 events. Set 9 is the plot for all the data.

TABLE 2-3

50-event group	b (all M)	b ($M \leq 3.0$)
1	0.74	0.74
2	0.55	0.68
3	0.82	0.82
4	0.50	0.69
5	0.60	0.70
6	0.78	0.78
7	0.96	0.96
8	0.80*	0.80
9	0.70	

*Group 8 is composed of the last 25 events from group 7 plus a final 25 events.

confidence limits .58 and .89 for 50 events. Samples 2, 4, and 7 with large events included lie outside these limits; yet with large events excluded, only sample 7 is too large. Application of the F test for sample 7 indicates it also comes from the same distribution, with 95% certainty. Therefore, since none of the differences in b-value with the largest events excluded are statistically significant, the conclusion is drawn that the slope of the recurrence curve does not change significantly for the 50-event samples. For the Danville swarm, Bufe's conclusion is found to probably have resulted from the occurrence of the largest events within the swarm. From Table 2-3, there is a trend seen to higher values of b later in the swarm. The significance of this trend is a moot question, however, since it is not supported statistically. Another point of importance is that the maximum likelihood b-value calculated for the entire sequence does change somewhat when the largest events are excluded--it increases to .76, which is within the 95% confidence limits of .70 with 374 events. The change is not considered meaningful and is due to a slight reduction of the value of $\bar{M}(M_o)$ in equation (2-10) without the appropriate correction as in equation (2-19).

The preceding discussion has shown the mathematical ease and statistical value of using the maximum likelihood estimator to calculate b-values. From the example of the Danville sequence one can appreciate that the occurrence of

the larger events of a data set may perturb the magnitude distribution of subsets of that sequence. The use of equation (2-18) in its general form allows for specific consideration to be made of data sets truncated at their upper magnitude ends.

Small Events Distributions. The ability to determine complete catalogs of earthquakes is essential to the analysis of many aspects of earthquake occurrence patterns. A complete catalog is defined as the set of all events in a temporally continuous earthquake sample with magnitude larger than a cutoff magnitude, M_o. It has been noticed that there does not appear to be any minimum magnitude to which the exponential model, equation (2-7), does not apply (Page, 1968). That is, increasing the sensitivity of a recording system simply extends the magnitude range of the linear portion of the curve. Yet, in all cases, the frequency-magnitude curve deviates from linearity below some small value of magnitude. In the case of the Danville swarm (Figure 2-2), the point of deviation is easy to pick visually on the cumulative plot and is denoted M_o. Since the point M_o is usually quite near the minimum detectable size of earthquake for the recording system, it is concluded that the deviation from linearity is due to the incomplete detection of small-magnitude events. Thus, M_o defines the magnitude above which detection of earthquakes in a given region is complete.

Knopoff and Gardner (1972) have used another method to

find M_o. Using 10,400 events in a "Southern California Statistical Area," they tested the randomness of successive events occurring within 1/2 magnitude unit intervals. They found a sharp change from significant randomness to a significant nonrandomness for the catalog at M = 3-3/4, which is quite consistent with the network density and sensitivity for the 1934-1967 period. This technique has the disadvantage of requiring very large samples to which to apply the statistical test.

The incomplete recording of small events presents a serious difficulty in determining the slope of a recurrence curve when it is not possible to pick M_o and still leave a "complete" catalog which is large enough to be accurately analyzed. Determining M_o depends on two interrelated factors: magnitude class interval and magnitude range. Since a change in slope is being sought, there must be sufficient linear data to establish an accurate, stable value of b. Sufficiency in terms of total number of events will be discussed in the following section using confidence limits. The magnitude range must also be subdivided in such a manner that a point of slope change may be observed. Thus, the accuracy of determination should be within an interval $2\Delta M$ over the range of magnitude M_R. If M_o occurs in one of the intervals, there must be sufficient intervals with $M_i > M_o$ to establish a stable value of b. In practice, this condition means that there must be at least four points of linearity to clearly fix the reference slope against which a change may be observed. That is,

$$\frac{M_m - M_o}{2\Delta M} \geq 4 \quad . \qquad (2\text{-}26)$$

Ryall and others (1968) also noted the necessity of using small magnitude intervals (they recommended 0.1 unit intervals) to obtain accuracy in plotting cumulative magnitude distributions.

The data from the Danville sequence in Figure 2-2 represent an almost ideal case; it will usually be more difficult to pick the M_o. Using a cumulative plot is probably the most accurate method, provided the data are determined with a small ΔM so that any linearity can be easily recognized. Using Knopoff and Gardner's technique does not allow the analyst to take account of any possible anomalous fluctuations of the distribution.

Sample Size. Several authors have recently considered the statistical significance of varying numbers of events in samples used to determine b-values. Ryall and others (1968) empirically tested subsets of the 1966 Truckee aftershock sequence. They concluded that samples of 50 events could fluctuate in b-value by 30%, while samples of 100 or more events produced values which were closer to the true slope. Utsu (1967) also noted the increased accuracy associated with large sample sizes by measuring the random variations in b of a number of samples. He suggested using the standard deviations obtained for different sized groups as a method of comparing b-values.

As was discussed in the theoretical portion of this chapter, the maximum likelihood estimator easily leads to the calculation of confidence limits on b, which may be used for comparisons. Since these limits include the factor $\sqrt{n}$, the sample size explicitly determines the accuracy of the slope if the source of error is randomness in the probability distribution. Note that the number n represents the events actually used in the b-value determination, i.e. the number of events between M_o and M_m, which is often smaller than the total sample size. Similarly, the F-test, difference test, and ratio test allow other comparisons of estimation accuracy that depend on the number of events used in each sample.

While a statistically meaningful b-value may be obtained from virtually any size sample, the confidence limits for small samples are so huge that comparison of slopes is almost meaningless. For example Suyehiro (1966) examined, at teleseismic distances, the foreshocks and aftershocks occurring within 33 hours of the main Chilean earthquake of 1960. For 31 foreshocks and 122 aftershocks plotted in six magnitude intervals and fit with a straight line by least squares, the b-values he found were .55 for the foreshocks and 1.13 for the afterhsocks. When recalculated using the maximum likelihood estimator, the slopes obtained are .74 ± .25 and 1.33 ± .26 for the foreshocks and aftershocks with 95% confidence limits. The F-test concludes that these two values are significantly different at the 95% level. However, they are

not significantly different at the 99% level. The small number of events in the foreshock sample, as well as the large value of b for the aftershocks (the confidence limits are proportional to b), are the statistical sources of doubt about the significance of the b-value difference. In an earlier study (Asada and others, 1964) discussed by Suyehiro (1966), foreshocks and aftershocks of a magnitude 3.3 event were examined. Again, the small number of events (25 foreshocks) makes the difference (.35 to .76) not significant using the F-test at the 99% level. From yet another study (Suyehiro, 1970), b-values (.70 and .95) were recalculated for foreshocks and aftershocks of a magnitude 5.1 event and differed from Suyehiro's (1970) values of .59 and .89 for 171 and 876 events respectively. The recomputed values were just barely significantly different at the 99% level.

Suyehiro's analysis technique is poor in several respects, including the small numbers of events used. The principal factors affecting the recurrence curve slopes are Suyehiro's use of very wide magnitude intervals and the use of least-squares fitting. For the Chilean case, there were only five magnitude intervals over a completely recorded range of 1.5 units; the unweighted least-squares fit then produced a small value for b. For the magnitude 5.1 event, the range of data was large enough to compensate for the 0.3 magnitude unit intervals, but again the least-squares fit was biased by large events. Also, no attempt was made to

determine M_o and then exclude incomplete small-magnitude groups.

The effect that sample size has on b calculations is statistically considered by means of confidence limits or the F-test. But the effective sample size of a given sequence may be drastically changed by the cutoff magnitude M_o and inclusion or exclusion of large events. Because each case may present unique problems, individual examination like that done for Suyehiro's foreshock-aftershock examples will be necessary. From the standpoint of ease of calculation, the use of equation (2-19) with a magnitude range greater than two magnitude units and a number of events greater than the quantity 100b is optimum.

Magnitude Determination. The parameter magnitude was originally devised to allow comparison of earthquakes in terms of their energy. Richter (1958) has reviewed the development of magnitude scales and notes that estimates of seismic energy have been developed in the form

$$\log E = 11.8 + 1.5M \quad . \qquad (2\text{-}27)$$

In general, for larger events ($M \geq 4$) a unified magnitude scale incorporating both body-wave and surface-wave magnitudes determined at teleseismic distances is used. Although there may be some small systematic biases (Shlien and Toksoz, 1970), critical reviews of frequency-magnitude data (e.g. Isacks and Oliver, 1964; Utsu, 1969; Evernden, 1970) have generally established the validity of the magnitude scale in

terms of a linear, semi-logarithmic, frequency-magnitude distribution.

For smaller events, quite satisfactory results are obtained using Richter's local magnitude relation, equation (2-2). However, it has been pointed out by Eaton and others (1970), Thatcher (1973), and others that over a large range of distance, the maximum amplitude phase is not the same for all events. To empirically avoid such variations, the usual approach in microearthquake studies is to correlate a special local magnitude scale with Richter magnitudes based on Wood-Anderson seismograph measurements of the larger events of the sequence. Although such procedures are followed with good internal consistency in general, the comparison of studies based on different scales is often made questionable because of ignored or unnoticed biases in the magnitude values with respect to standard scales. Several examples will be considered here.

The most carefully and consistently developed Richter magnitude determinations are those for the 1966 Parkfield aftershock sequence (Eaton and others, 1970). The earthquake maximum amplitudes recorded by field seismograph systems were corrected for seismometer response, amplifier gain, and the use of vertical rather than horizontal instruments to give equivalent Wood-Anderson amplitudes, from which M_L's were calculated. The recurrence curves thus developed are linear over two units of magnitude. Following the Parkfield

earthquake study, the increasingly dense network of stations installed and operated by the U. S. Geological Survey resulted in the data sample from central California introduced in Chapter I. Magnitudes for these events were determined (Lee and others, 1972) by measuring the coda length (F - P time) of the events at many stations, then correlating these averages with Wood-Anderson magnitudes and magnitudes calculated by Eaton's technique. The F-P magnitude technique is principally an empirical one, though Aki's (1969) interpretation of local earthquake codas as scattered waves provides some theoretical support. Magnitudes greater than 3.5 for the central California data were obtained only from Wood-Anderson instruments in the area. The recurrence curves for various portions of the San Andreas fault system using this data are shown in Figure 2-3. For most samples, there is a pronounced curvature of the data, beginning at magnitude 3.5 and extending smoothly to the left, to M = 0, with no clearly defined M_o. This is surprising, since the Danville sequence to the north on the Calaveras fault (Figure 2-2) and the Parkfield area to the south are characterized by well-determined b and M_o values. Thus, the offset in the curve at M = 3.5, as well as the curvature itself over a magnitude range that should exhibit linearity, strongly suggest that there is a bias in the values of the magnitudes rather than a valid nonlinearity.

There are several factors which may explain the smooth

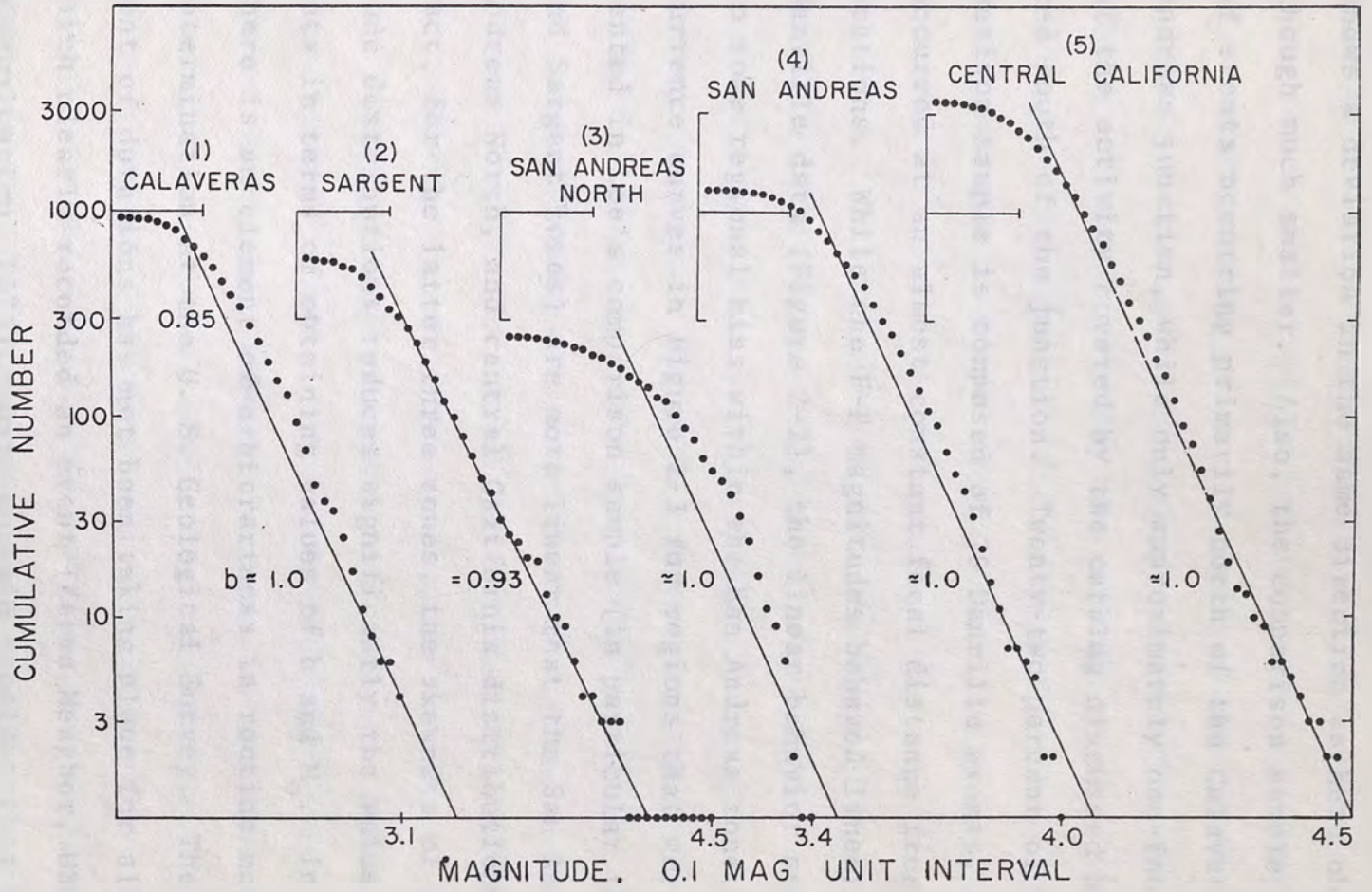

Figure 2-3. Cumulative magnitude-frequency plots for the five regions in central California shown in Figure 1-2. Horizontal scales at the top of each curve represent one magnitude unit; the vertical scales represent one-half order of magnitude change in number of earthquakes.

deviation. In Figure f of Lee and others (1972), the data sample from which the duration-magnitude rule was derived shows a deviation in the same direction as here observed, although much smaller. Also, the comparison sample is composed of events occurring primarily north of the Calaveras-San Andreas junction, while only approximately one-fourth (23%) of the activity covered by the catalog discussed here occurred south of the junction. Twenty-two percent of the comparison sample is composed of 79 Danville events, which occurred at an almost constant focal distance from the array stations. While the F-P magnitudes behaved linearly for the Danville data (Figure 2-2), the linear behavior seems subject to some regional bias within the San Andreas zone. The recurrence curves in Figure 2-3 for regions that were represented in Lee's comparison sample (in particular the Calaveras and Sargent zones) are more linear that the San Andreas, San Andreas North, and central California distributions. In fact, for the latter three zones, the skewness of the magnitude distributions reduces significantly the value of the data in terms of obtaining values of b and M_o. In addition, there is an element of arbitrariness in routine magnitude determination at the U. S. Geological Survey. The measurement of durations has not been taking place for all stations which clearly recorded an event (Karen Meagher, USGS, personal communication, 1973). Only certain stations that have been found to produce generally consistent duration magnitudes are used.

An alternate method is sometimes used that avoids the specific difficulties of calculating Richter magnitudes. Instead of using Richter's formula for magnitude (equation 2-2), the logarithm of the measured amplitude (either zero-to-peak, or peak-to-peak) is plotted with respect to number of events. Thus, the response characteristics of the recording system that differ from a Wood-Anderson horizontal seismometer are ignored. For several sequences recorded by the University of Nevada field systems, this was chosen as the easiest method for determining recurrence curves. The sequences from Adel and NTS shown in Figure 2-4 were recorded on the tripartite field system described in the introduction. The events were reproduced on a Geotech helicorder and were counted by maximum amplitude groups. To justify neglecting the system response, it was noted that for microearthquakes with magnitudes between approximately 0.5 and 2.5, the peak spectral frequencies lie within the flat (±3db) portion of the recording system response (Douglas and Ryall, 1972). This frequency range corresponds to the flat portion of the Wood-Anderson response. For a range of magnitude which is usually sufficient (about 2.0 units), no amplitude correction for variation in focal distance is necessary if the ratio of the focal distance range to the average focal distance is less than about 0.8. For larger distance ranges, a correction in amplitude due to geometrical spreading would have an effect over more than 0.3 units of magnitude, causing a

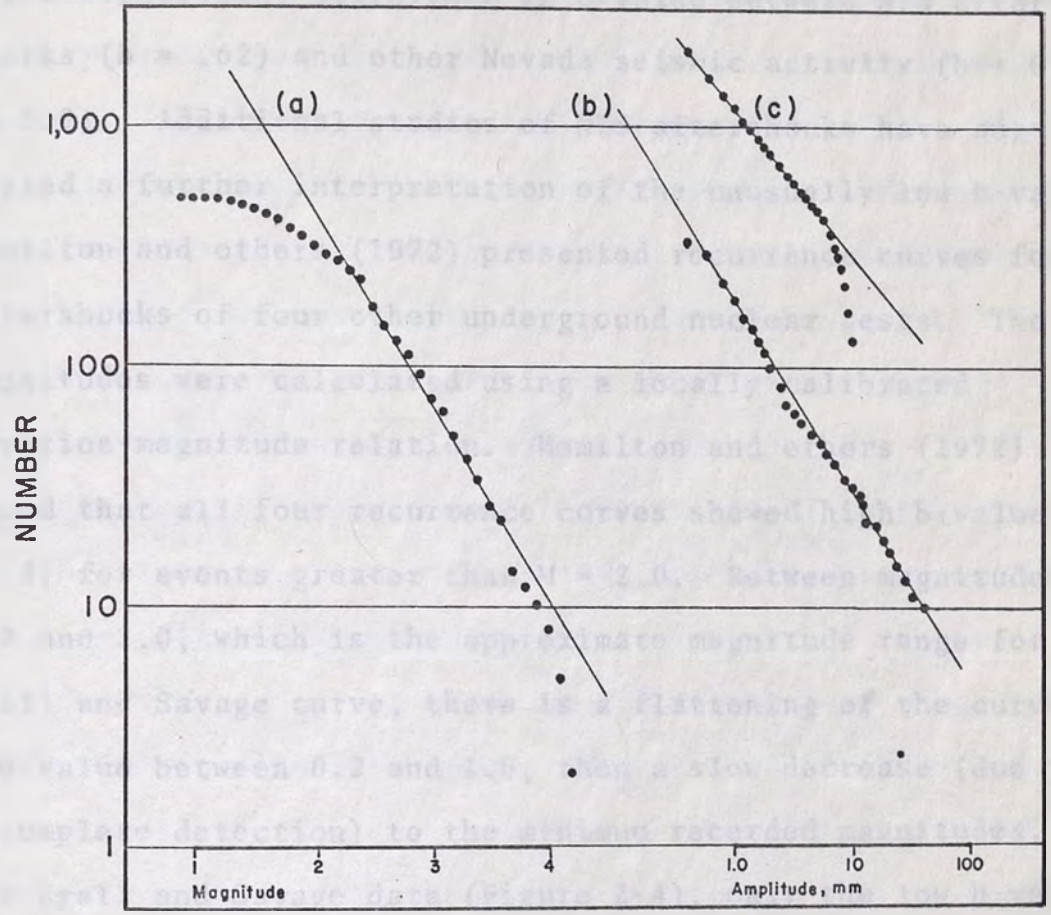

Figure 2-4. Cumulative magnitude-frequency plot for (a) the Truckee aftershock sequence. Cumulative amplitude-frequency plots for (b) Adel, Oregon, swarm earthquakes and (c) NTS Boxcar afterhshocks.

reduction by this amount in the usable magnitude range. For the NTS data, the ratio is one-third, causing magnitude errors over a range of 0.2 magnitude units, which is of little concern.

It was concluded by Ryall and Savage (1969) that there was a significant difference in b-value between NTS aftershocks (b = .62) and other Nevada seismic activity (b = 0.8 to 0.9). Additional studies of NTS aftershocks have suggested a further interpretation of the unusually low b-value. Hamilton and others (1972) presented recurrence curves for aftershocks of four other underground nuclear tests. The magnitudes were calculated using a locally calibrated duration-magnitude relation. Hamilton and others (1972) found that all four recurrence curves showed high b-values (1.4) for events greater than M = 2.0. Between magnitudes 1.0 and 2.0, which is the approximate magnitude range for the Ryall and Savage curve, there is a flattening of the curve to a b-value between 0.2 and 1.0, then a slow decrease (due to incomplete detection) to the minimum recorded magnitudes. In the Ryall and Savage data (Figure 2-4), only the low b-value range is apparent, with an increase in slope for larger magnitudes. While Hamilton and others (1972) suggest that the larger magnitudes may be underestimated so that the slope should be closer to 1.0, the abnormally low value for the range of 1.0 to 2.0 determined by two independent groups suggest that it is real. A discussion of this knee in the

recurrence curve as a possible indicator of fracture distribution will be presented at the end of this chapter.

The preceding several examples serve to illustrate the kinds of errors and the details of data evaluation associated with magnitude determination when doing a mathematically and seismologically proper magnitude-frequency analysis. A significant characteristic of a useful magnitude-determination procedure should be the fit of those magnitudes to a linear recursion curve. Instances of nonlinear distribution suggest either statistically incomplete data, biased magnitude values, or a highly atypical earthquake occurrence mechanism. The details of non-Poisson statistical behavior can provide the means of discriminating its source.

Physical Model. There remain the fundamental questions of what b-values mean and on what they depend. According to the fracture theory of earthquakes, a seismic event is caused by a sudden drop of stress level on a fault surface (Mogi, 1967; Brune, 1970). The Gutenberg-Richter law is an empirical observation of the fracture process, which may be examined from both laboratory and theoretical viewpoints.

Scholz (1968) has determined from fracturing of laboratory rock specimens that the value of b depends inversely on the level of compressive stress. He attributes high values of b in the laboratory (1.0 to 2.5) to crack closing and frictional sliding. Lower values (0.5 to 1.0) are considered to be due to the propagation of new fractures. In the

latter range, Scholz follows Mogi (1962) in relating this occurrence to that of earthquakes.

As a theoretical model, Scholz assumes a simple (approximately normal) distribution of local stress within an inhomogeneous medium subject to a uniform applied stress. This immediately leads to an exponential distribution of fracture area, r^2. Assuming simple relations between fracture area and strain energy, the Gutenberg-Richter law is derived, in which the parameter b is inversely proportional to stress. The fracture area distribution can then be written, using b, as

$$n(r^2) = G \cdot (r^2)^{-(b+1)} \quad . \qquad (2\text{-}28)$$

Finally, Scholz suggests that only the scale of the medium inhomogeneities may be different between microfractures and earthquakes, so variations in b-value for crustal fractures should represent differences in stress level.

An alternative approach to the meaning of recurrence curves may be taken from Brune's (1970) source model. Using this theoretical description of source function and energy propagation, it is possible to relate seismic energy and magnitude to other parameters. Hanks and Wyss (1972) summarize the use of earthquake spectral measures in Brune's (1970) model to determine source parameters. Using their results, with P-wave energy considered negligible, total energy is given by

$$E = (\text{const})\, M_{mo}^{\,2} f_o^{\,3} \left(\frac{2}{\varepsilon} - \frac{2}{3}\right) \qquad (2\text{-}29)$$

where

$$M_{mo} = \Delta\sigma r^3 \frac{16}{7};\quad f_o = \frac{G}{r};\quad \varepsilon = \frac{\Delta\sigma}{\varepsilon_{eff}} \qquad (2\text{-}30)$$

and where M_{mo} represents seismic moment. Converting energy to magnitude with equation (2-27), an equation relating magnitude and source parameters is found:

$$M = (\text{const})\, (\Delta\sigma)^{4/3} r^2 \left(\frac{2}{\varepsilon} - \frac{2}{3}\right)^{2/3} . \qquad (2\text{-}31)$$

Thus, in the Gutenberg-Richter relations,

$$\log N = A - b(\text{const})(\Delta\sigma)^{4/3} r^2 \left(\frac{2}{\varepsilon} - \frac{2}{3}\right)^{2/3} . \qquad (2\text{-}32)$$

This equation is similar to the distribution of crack area found by Scholz (equation 2-27), but it is the <u>product</u> of stress drop and source area which is exponentially distributed. Equation (2-32) is similar to the result obtained by Wyss (1972), in which he also noted the basic importance of the product of source dimension and stress drop.

Using the third of equation (2-30), it can be noticed that b is inversely proportional to effective stress level,

$$\log N = A - b(\text{const})(\varepsilon\sigma_{eff})^{4/3} r^2 \left(\frac{2}{\varepsilon} - \frac{2}{3}\right)^{2/3} \qquad (2\text{-}33)$$

for each value of log N.

Several results may be noted from equations (2-32) and (2-33). Although there is sparse data on stress drop, effective stress and source area, in the same region over large magnitude ranges, stress and stress drop may be assumed

constant or simple linear with r^2 (Wyss and Brune, 1968). From this, one finds that the distribution of crack size is exponential, and the constancy of b (~0.9) for most crustal earthquakes implies that the fracture distribution, or degree of inhomogeneity, is about the same for all fracture zones over the entire range of magnitude (Mogi, 1967). The exceptional knee in the NTS recurrence curve (Figure 2-4) may thus be interpreted as a structural regularity in the upper 5 kilometers of the crust. The regularity should be on the order of a kilometer in dimension based on the appropriate source size of a magnitude 2.0 earthquake (Douglas and Ryall, 1972). Mogi (1967) has noted such knees for several regions in Japan. Alternatively, with a given sequence, a change in the functional relationship (equation 2-31) at a particular magnitude could also be the source of non-Poisson features of the magnitude distribution. For the NTS data, a predominantly smaller stress drop for the larger events could also cause the knee. Accumulation of much more statistical data will be necessary prior to a clear understanding of the relation between stress, stress drop, and source dimension and their influence on earthquake b-values.

The parameter b has been found to theoretically and experimentally vary inversely with stress. From Scholz' (1968) measurements of the change in b for microfractures in rock samples under compressive stress, the maximum change is not more than a factor of two, in general. Smaller stress

changes produce a less obvious effect. In particular, Scholz found that the change in b-value between 80% of fracture stress and 100% fracture stress is as small as 2 to 8% for higher confining pressures in triaxial tests. The change in b between 50% and 100% of fracture stress is larger, 19 to 33%. Detecting such small differences at the 99% level with the F-test would require high and low stress samples with thousands of events for the 80% case and at least hundreds of events for the 50% case. The change in b for a large change in percent of fracture stress, for the laboratory case, is slight, and is statistically supportable only with large samples.

The earlier discussion considered several examples, namely, research by Bufe (1970) and Suyehiro (1966, 1970), in which low b-values were found. It was shown that in both cases there was some indication of low b prior to times of large energy release, but the statistical substantiation of differences in b was, at best, not conclusive. The Danville swarm showed a trend to higher b-value which was not statistically significant, and the greatest foreshock-aftershock differences were barely significant at the 99% level. In an additional example, variations in b-value were noted for several areal subdivisions of the 1966 Parkfield aftershock zone (Eaton and others, 1970). For events along the southeast portion of the slip surface, lower b (.73) was observed for events deeper than 6 kilometers, while higher b-value

(.94) was found for shallower aftershocks. This trend is not supported at 95% by a statistical significance test.

There is some question as to the reasonableness of lower stress observations expected for aftershocks. As was noticed for the Parkfield events (Eaton and others, 1970), aftershocks occurred chiefly on the edges of the slip surface, presumably where stress concentrations exist. Thus, the stress level for most aftershocks may not be significantly different than the pre-main-event stress level and consequently not detectable with recurrence curves. However, it may be that the effective stress level would increase with depth, which the tendency to lower b with depth at Parkfield supports. The trend to higher b with time during the Danville sequence suggests a lowering of stress in the focal zone, but the statistical fluctuations are so large that no interpretation can be firmly drawn.

Conclusions

On an empirical basis, Richter magnitude or an equivalent is found to be a generally independent variable which is Poisson distributed over all the events of a sequence. In the hundreds of existing studies of earthquake magnitude statistics, emphasis has been placed chiefly on the determination of the parameter b and the comparison of b-values among various data sets. The approach here has been, however, to focus on various non-Poisson aspects of magnitude distribution. Prior to use of the statistically best maximum

likelihood estimator of b, the following items should be evaluated:

1. The value of M_o, the smallest completely detected magnitude, must be determined. This satisfies Poisson axiom 3_M. The minimum detection level in the seismic recording system should be compatible with M_o.
2. The possible incompleteness of the largest events of the sample may require special consideration. The occurrence of a trigger event clearly violates axioms 1_M and 4_M. The general maximum likelihood estimator, equation (2-18), allows the sample to be restricted to exclude the largest events to improve the quality of the b-value estimation. Specific large magnitude problems include the question of inclusion of main-shocks in a sequence and the possibility of a maximum magnitude limit M_m in a geologic region.
3. Any nonlinearities in the magnitude distribution between M_o and M_m are contrary to axioms 1_M, 2_M, and 4_M of the fundamental Poisson assumptions allowing the use of equation (2-18). Evaluation of cumulative plot of magnitude versus number can reveal such nonlinearities as magnitude biases of "knees" in the recurrence curve.
4. There are a number of simplifications of equation (2-18) made possible by various data collection techniques and the use of large number of events.

5. The non-Poisson details summarized above have significance in gaining further understanding of the relationship that stress, stress drop, and source dimension have with magnitude-frequency distributions.

CHAPTER III. OCCURRENCE TIME MODELS AND AFTERSHOCKS

Introduction

In this chapter, time-series created by the occurrence of earthquakes are examined in detail. Previous research has indicated that within specific regions over differing time periods earthquake occurrence appears to be a generally random phenomenon. Yet there are many groups of shocks, such as aftershock sequences, that exhibit substantial nonrandomness. The general temporal distribution of earthquakes in complete catalogs is modeled here as the combination of three processes: (1) a steady-state or slowly rate-varying process of random events, (2) strongly time-dependent processes of random events (aftershocks and swarms), and (3) nonrandom clustering of closely related earthquakes. As in the preceding chapter, the aim of this investigation is to extract seismological understanding from the observed statistical behavior. In a historical review of time-series observations, the first two portions of the general temporal model are described and evaluated. The occurrence of clustering is then investigated in detail in Chapter IV using the data from Nevada and California discussed in Chapter I.

Historical Review

Earlier seismological investigators studied time-series patterns of earthquakes with the objective of discovering causal processes. Consequently, correlations were tested with every conceivable physical phenomenon, such as climatic

variations, sunspot cycles, barometric pressure, temperature, rainfall, solar and planetary influences, and tidal stresses. Since many of these phenomena are periodic or approximately so, a commonly used technique was to examine the earthquake series for periodicities, then correlate whatever significant periods were noticed with other occurrences with the same recurrence periods. Aki (1956), Van Wormer (1967), and Malone (1972) have comprehensively reviewed past literature discussing periodicities and external trigger phenomena.

In general, this approach is highly unsatisfactory, since a positive correlation of two time-series says little about any possible causal connection between the two phenomena except that their occurrence times happen to coincide. In particular, examination of earthquakes as a phenomenon "caused" by some physical process such as those listed above is fraught with many possible errors due to unknown ancillary relationships which may actually contain causal connections or to spuriously high correlations caused by internal statistical dependencies within the earthquake sample. With respect to the latter, Jeffreys (1938) pointed out that "any tendency of earthquakes to stimulate one another after short intervals of time will lead to an increase of the random amplitudes expected to be obtained in a Fourier analysis." Malone (1972) also noted an instance in which the observation of tidal periods within an aftershock sequence appears to have been the product of an unusual burst of activity in the sample used.

It has long been noticed that large earthquakes are usually accompanied by foreshocks and aftershocks. In 1894, Omori (discussed in Aki, 1956) observed that the number of aftershocks of the 1891 Nobi earthquake in Japan decreased hyperbolically with time. Later researchers corroborated this observation (Utsu, 1961), which has led to a general rule for the number of aftershocks occurring in a unit time interval given by

$$n(t) = A\ (t - \beta)^{-p} \quad , \qquad (3\text{-}1)$$

with A, β, and p constants for the sequence, and t the time after the main shock. Other less regular temporal patterns have also been investigated, but as Conrad concluded in 1932 (Aki, 1956), "besides the law of decrease of aftershocks, there is not a single trend that one can be certain of."

Beginning very early in the twentieth century in Japan, the hypothesis of independence among very large events was tested by comparing the given sequence with a simple Poisson distribution. The events in the catalog were counted in some arbitrary time interval, then plotted along with a Poisson distribution that was calculated using the rate parameter given by the total number of events divided by the total time interval of the catalog. Four examples of early comparisons from Aki (1956) are shown in Figure 3-1. Nonrandomness is pronounced and was remarked upon by the various authors.

Aki (1956) has compiled a bibliography of work pertaining to statistical analysis of many earthquake time-series,

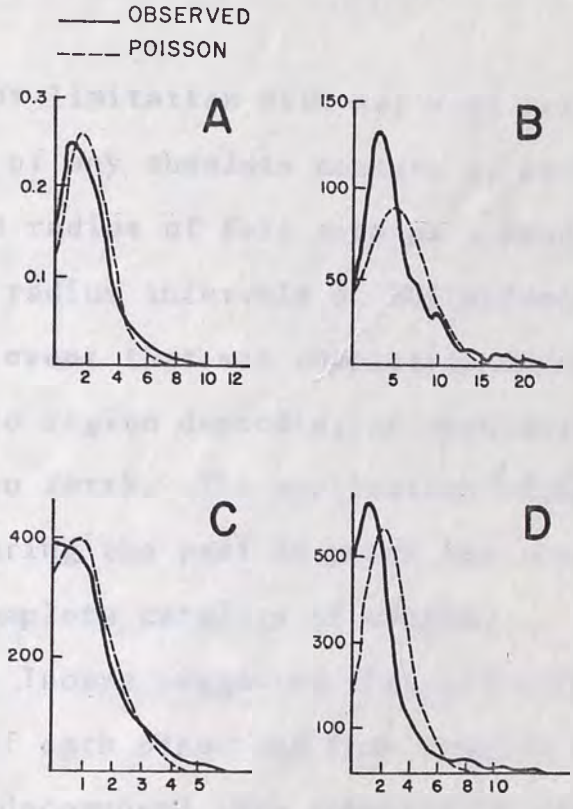

Figure 3-1. Frequency distributions and associated Poisson distributions for (a) strong earthquakes in Japan, 10-day counting interval (Inouye, 1932); (b) felt earthquakes in the Tokyo area, 1898-1947, monthly counting interval (Kishinouye, 1948); (c) small earthquakes in the Tokyo area, daily counting interval (Iida, 1939); (d) Oxford Catalogue earthquakes, 1925-1930, daily counting interval (Wanner, 1937a,b).

much of which was done in Japan. Aki notes from this survey that the Poisson distribution does not accurately describe all earthquake occurrence; there is quite often a tendency for earthquakes to occur in groups other than simple foreshock and aftershock sequences. Since several of these earlier studies do have significant results, two examples by Inouye (1937) and Jeffreys (1938) are considered in some detail.

One major limitation with all work prior to the 1940's was the lack of any absolute measure of earthquake size. The Japanese used radius of felt area as a means of grouping events, with radius intervals of 100 kilometers. Thus the minimum size event that was completely counted could vary from region to region depending on population density, time of day, and so forth. The application of the Richter magnitude scale during the past 30 years has resulted in much more rigorously complete catalogs of events.

In 1937, Inouye suggested that all earthquakes occur independently of each other and that complex time-series patterns may be decomposed into consecutive simple Poisson distributions with different rates. Several years earlier, Inouye (1932) noticed that felt events occurring during time intervals of a few years fit a Poisson distribution fairly well, but over longer periods the Poisson fit was poor. He proposed using a varying-rate Poisson distribution to model the complete occurrence pattern:

$$P(x) = \frac{e^{-f(x)} f(x)^x}{x!} \quad , \qquad (3\text{-}2)$$

where x is the number of events per unit time. In the later paper, he concluded that strongly felt events in Japan between 1912 and 1925 could be fit by the distribution

$$P(r) = \frac{10}{11} \frac{e^{-6.0} 6.0^x}{x!} + \frac{1}{10} \frac{e^{-15.0} 15.0^x}{x!} \quad . \qquad (3\text{-}3)$$

The two rates, 6.0 and 15.0, apply to different portions of the sequence, with the higher rate applying to the periods of greater event occurrence. Inouye (1932) also found that earthquake swarms in the Ito district could be roughly modeled by an exponentially decreasing rate of occurrence. As an alternative to the Poisson model, he applied the lognormal distribution,

$$\Phi(x) = \frac{1}{\sqrt{2\pi}\, \sigma(x+h)} e^{-\frac{(\log(x+h) - c)^2}{2\sigma^2}} \quad . \qquad (3\text{-}4)$$

Although it does fit some of the observed distributions more accurately than the Poisson curve, no discussion was made of the meaning of its parameters, c, h, and σ. The lognormal distribution is commonly applied to processes in which the value of an observed variable is a random proportion of the preceding value (Hahn and Shapiro, 1967, p.134). The significance of this model for earthquakes is not clear. Inouye also tested the correlation of successive monthly intervals and found a tendency for months with high occurrence rates to be followed by another month of high rate. Events which

occurred at somewhat greater depths (subcrustal) showed a lower monthly correlation.

Inouye's work exemplifies most other available papers from Japan during the 1930's. The randomness of earthquakes was tested by comparison with a Poisson model, but the only conclusions drawn were "yes, the sample is approximately random" or "no, the sample is not composed in independent events because there are aftershocks and swarms." The investigations were carried no further.

Concurrently, Jeffreys (1938) developed several significant results in earthquake statistics. He noted that in earlier analyses of periodicity in earthquake occurrence, the events were assumed independent of each other and no account was taken of aftershocks. Jeffreys showed that the occurrence of groups of dependent events in the sequences analyzed would create spuriously large amplitudes obtained by Fourier analysis. By counting the numbers of aftershocks present in four and one-half years of the International Seismological Summary catalog, Jeffreys found that the recurrent periods of earthquake activity previously determined by Davison (1938) could be explained by the occurrence of aftershocks rather than as a result of triggering influences. Jeffreys suggested that any analysis of periodicities in earthquakes should be applied only to independent series of events.

In the second portion of his paper Jeffreys examined the degree of independence among the 1071 reported aftershocks of

the Tango, Japan, earthquake of 1927. Nasu (1929) had shown that the Tango aftershocks were the sum of two Omori-law decaying sequences: one beginning with the main event, and one starting with the largest aftershock which occurred 24.5 days later. Jeffreys calculated the maximum likelihood values of β in equation (3-1) and obtained an excellent χ^2 fit; he found no reason to use a value of p different from 1.0. Jeffreys then proposed that, other than in the relationship given by equation (3-1), the aftershocks be independent. He roughly tested this using the error distribution of second differences of numbers of events per day and found that the aftershock sequences could indeed be described as random events fluctuating about hyperbolic decay curves. Jeffreys concluded his investigation by testing the aftershock sequence for periodicities, with negative results.

Recent Studies

Statistical studies made during the following 20 years were of the same genre as these just discussed, with no new results or techniques. In the 1960's, however, a renewed and continuing interest in statistical seismology appeared, due primarily to the existence of rapidly growing, high-quality data catalogs. The completion of many detailed local and regional studies in this period and the accumulation of increasingly complete worldwide data by the National Oceanic and Atmospheric Administration (NOAA) have made possible more conclusive analyses of earthquake time sequences. Vere-Jones

(1970) notes also that some of the statistical ideas needed to treat complicated point processes have only recently been developed. Unfortunately, much of the Japanese and European work earlier in the century was ignored, and the same discoveries have been made again. The more recent research using better data samples is certainly better substantiated, but the temporary disuse of such ideas as Inouye's varying-rate Poisson process and Jeffrey's discovery of the statistical independence of one set of aftershocks has probably hindered the development of statistical modeling of earthquakes. A key problem has been the approach to modeling foreshocks, aftershocks, and swarms.

In the same manner as earlier researchers (for example, Wanner, 1937a,b), Knopoff and Gardner (1972) and Shlien and Toksoz (1970a) removed aftershocks from the NOAA world data catalog using arbitrary criteria and found that the remaining sequence was approximately Poisson. To identify and eliminate nonrandom events Knopoff and Gardner (1972) manually scanned a portion of the NOAA catalog to define distances 2L and time T (both functions of magnitude) such that related events would occur within 2L and T of each other. Knopoff and Gardner (1972) also established (using the randomness test described by Knopoff and Gardner, 1969, and discussed in Chapter II) that the NOAA catalog is complete down to magnitude 4-3/4. These two procedures selected 5547 events from the total of 25,430 shocks between 24 March 1963

and 31 December 1968. By a χ^2 test of the hourly distribution of events, Knopoff and Gardner (1972) concluded that the catalog with aftershocks removed was random at the 99% level. For a cutoff magnitude of 5-1/4, the smaller sample of 19,429 events was random at the 95% level.

Shlien and Toksoz (1970a) used a slightly different technique to test the NOAA catalog for relatedness among events: using the property of Poisson events that their recurrence times are exponentially distributed (equation 1-3), they tested the catalog for such a distribution. Figure 3-2 is taken from Shlien and Toksoz (1972a) and shows the sequential distribution of numbers of events per day. Exponential distributions were tested for groups of 5016 events (separated by vertical bars) with associated probability P (significance level is 100[1 - P]). The procedure used to remove aftershocks for the lower figure is much like the method applied by Knopoff and Gardner (1972). For all the "aftershock-removed" samples, the Poisson model is acceptable at the 95% level. For only two of the "aftershock-included" groups is the behavior Poisson, with the others being excessively non-Poisson. Shlien and Toksoz note that the variability in occurrence of Poisson behavior in the raw data may explain earlier conflicting conclusions about the statistical nature of earthquakes.

A trend to higher activity may be noticed in the lower part of Figure 3-2; the daily rate increases from about seven

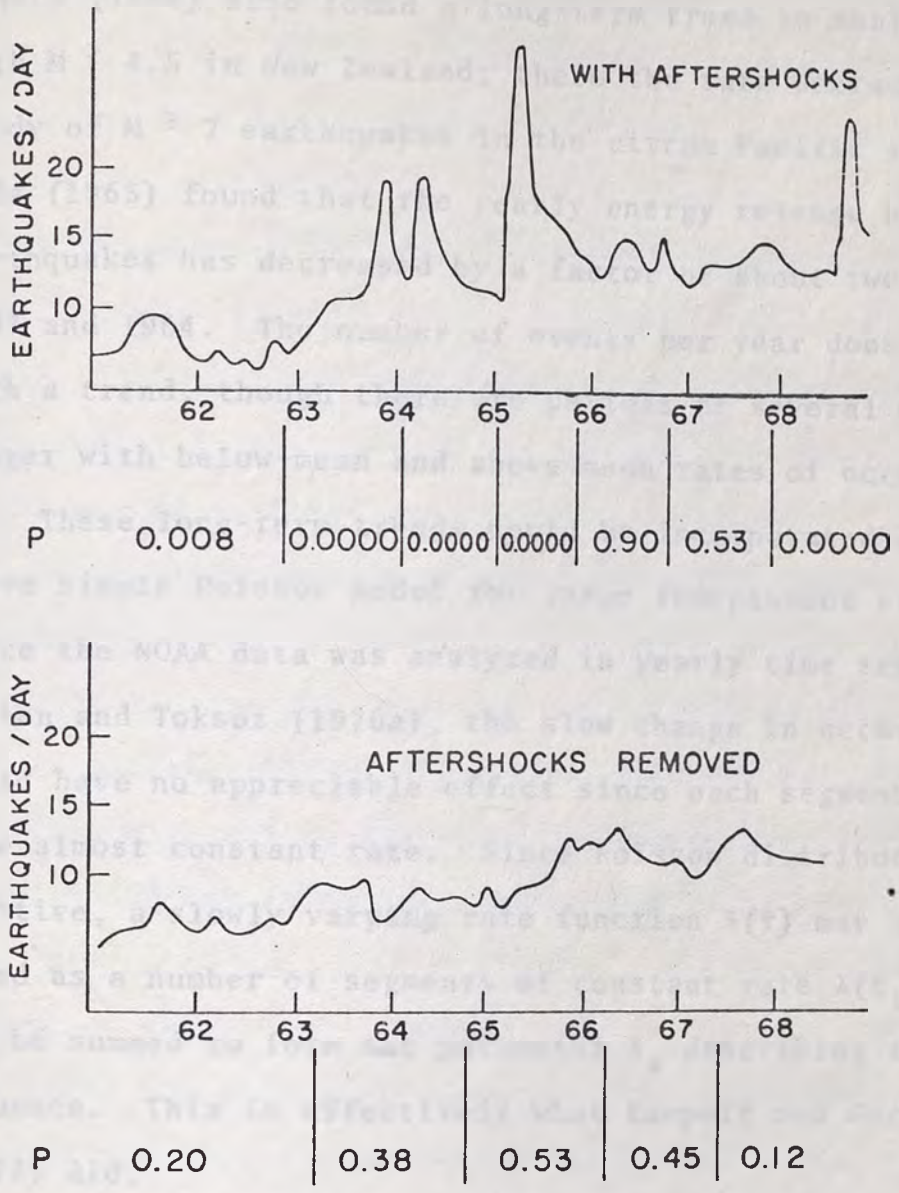

Figure 3-2. Daily earthquake frequency for the NOAA worldwide catalog, 1961-1968. P values are the probabilities that time intervals between earthquakes for consecutive groups of 5016 events are distributed exponentially.

events per day to more than ten over a period of seven years. It is possible that some or all of this increase may be due to increased coverage by the worldwide net. Vere-Jones and others (1964) also found a long-term trend in shallow events with $M \geq 4.5$ in New Zealand; there the rate decrased. In a study of $M \geq 7$ earthquakes in the circum-Pacific seismic belt Duda (1965) found that the yearly energy release by shallow earthquakes has decreased by a factor of about two between 1897 and 1964. The number of events per year does not show such a trend, though there are periods of several decades or longer with below-mean and above-mean rates of occurrence.

These long-term trends could be incorporated in the above simple Poisson model for large independent events. But since the NOAA data was analyzed in yearly time segments by Shlien and Toksoz (1970a), the slow change in occurrence rate would have no appreciable effect since each segment would have almost constant rate. Since Poisson distributions are additive, a slowly varying rate function $\lambda(t)$ may be considered as a number of segments of constant rate $\lambda(t_i)$ which may be summed to form the parameter λ_s describing the entire sequence. This is effectively what Knopoff and Gardner (1972) did.

While small rate variations may be considered as sequential short time intervals with differing constant rates, very rapid and large deviations from the mean occurrence rate cannot be successfully modeled by series of constant occurrence

rates. For example, the high peaks of activity in Figure 3-2 (top) represent an increase in the occurrence rate by a factor of three or more. When these peaks are examined in detail the fluctuations of the occurrence rate are recognized to be principally due to aftershock sequences. Utsu (1961, 1969) has found that the modified Omori's law (equation 3-1) describes the distribution of occurrence rates for most aftershock sequences. He notes, however, as does Mogi (1963), that there is great variability in the number of aftershocks which follow a given magnitude event, although events down to magnitude 5.5 (the lower limit of Utsu's reviewed main-shock data) may be followed by aftershock sequences.

It has also been observed on numerous occasions that aftershock sequences are compound; there may be secondary aftershock sequences following larger aftershocks. The procedure Jeffreys (1938) followed to analyze two overlapping aftershock sequences was discussed above (pp. 61 to 62). Lomnitz and Hax (1966) also used Omori's rate law to examine the interdependence of aftershocks. For three of the four sequences that they examined, Lomnitz and Hax concluded that the Omori law accurately described the occurrence rate changes and that the individual aftershocks were statistically independent of each other. For example, in the Kern County, 1952, aftershock sequence, the main event (M = 7.7) was followed 36 hours later by a magnitude 6.1 aftershock that triggered its own aftershock series. To transform this double sequence,

$$\tau = a_1 + b_1 \log t = H(t-t_o)(a_2 + b_2 \log(t-t_o)) \qquad (3\text{-}5)$$

was used to convert the time sequence of events N(t) into a stationary sequence, N(τ). Constants a_1, b_1, a_2, and b_2 were determined by stepwise linear regression with H the Heaviside step function and t_o the time of occurrence of the second main event. Figure 3-3 (top) indicates the success of the compound transformation.

To test each sequence for the degree of grouping among aftershocks, Lomnitz and Hax calculated the correlation coefficient between the number of events occurring in successive (transformed) time intervals. For the Kern County sequence, with cutoff magnitude $M_o = 4.0$, the correlation coefficient was not significantly different from zero as determined by a random control sequence. Similarly, two simple aftershock series were considered, the San Francisco, 1957, and Alaska, 1964. These two also were found to evidence no grouping among events larger than $M_o = 2.5$ and $M_o = 4.5$, following the M = 5.3 and M = 8.3 main shocks, respectively. The fourth sequence considered was the 1960 Chilean foreshocks and aftershocks. Lomnitz and Hax found this series to be composed of four different periods of activity occurring over a four-day period. They decided that the time sequence was too complicated to be fit by an equation of the form of equation (3-5)(see Figure 3-3, bottom), so further analysis was not done. Since this sequence was so distant from most recording centers, too few events were

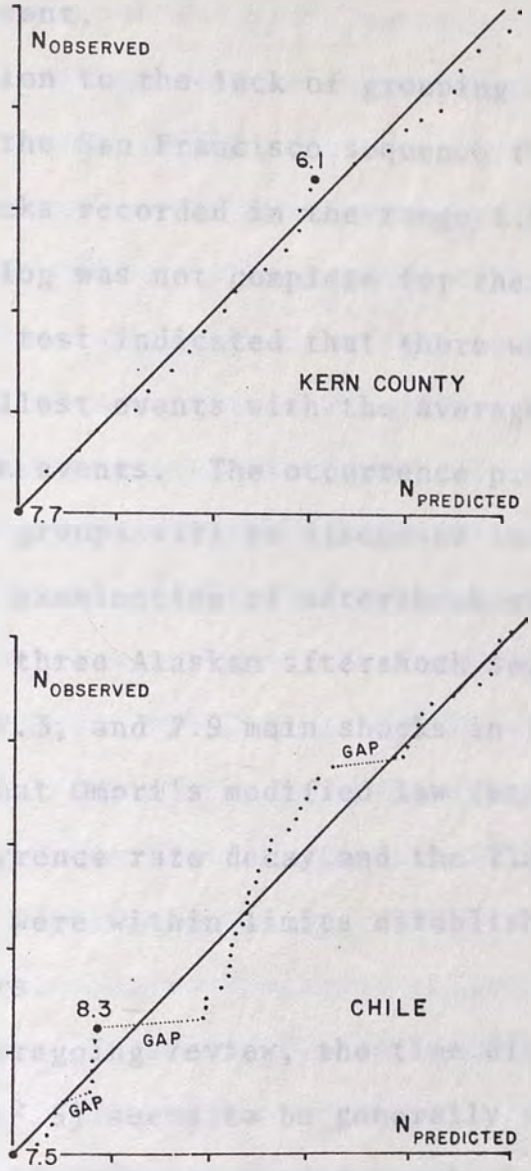

Figure 3-3. Cumulative number of aftershocks observed versus number predicted from equation (3-5) for the (a) 1952 Kern County earthquake and (b) 1960 Chilean earthquake sequence. Each division represents 20 aftershocks.

recorded (50 events are represented in Figure 3-3) to attempt any more complicated modeling. From the figure however there is a suggestion that there were at least three superposed sequences of activity, excluding the six foreshocks of the magnitude 8.3 event.

One exception to the lack of grouping among aftershocks was found: in the San Francisco sequence there were a number of aftershocks recorded in the range $1.6 \leq M \leq 2.5$, although the catalog was not complete for these small events. The correlation test indicated that there was some dependence among these smallest events with the average group containing fewer than seven events. The occurrence process of such microearthquake groups will be discussed in Chapter IV.

In another examination of aftershock grouping, Utsu (1962) examined three Alaskan aftershock sequences following magnitude 8.3, 7.3, and 7.9 main shocks in 1957 and 1958. He also found that Omori's modified law (equation 3-1) described the occurrence rate decay and the fluctuations in the occurrence rate were within limits established by a sequence of random numbers.

From the foregoing review, the time distribution of large events ($M \geq 5$) seems to be generally well described as a concurrent combination of random events occurring at a constant or slowly changing rate and occasional sequences of random events with approximately hyperbolically decaying rate whose occurrence is dependent on one or more trigger events.

There is only a general correlation between increasing magnitude of the main event and increasing number of aftershocks, which varies from region to region (Mogi, 1963; Utsu, 1969). The recurrence cycle of major displacements on plate boundaries is on the order of 100 years or more (Mogi, 1968), so the present observations are usually not sufficiently long to fully sample recurring seismic activity.

Some occurrence patterns are apparently not described by the above model and require further analysis. These include very complex foreshock-aftershock sequences, such as the 1960 Chile sequence, and swarms of events which lack a main event. These two patterns account for only 20% or so of all seismic activity (Mogi, 1963). It has already been noted for the Chilean events that the observed activity might be described by at least three separate exponential distributions. In general, it will be assumed here that all such complex aftershock series may be modeled by the combination of multiple Omori distributions with variable parameters. In addition, Utsu (1969) suggests that "large scale swarms in non-volcanic regions may be regarded as groups of aftershock sequences triggered by several large shocks of approximately equal magnitudes." Therefore swarms may also be modeled as sums of hyperbolic rate laws.

Generalized Poisson Models. The ability to model general earthquake occurrence in terms of a Poisson series plus individually modeled aftershock sequences is not satisfying in

that it is necessary to extract and individually determine model parameters for each aftershock sequence or swarm. An alternative approach to individual modeling is to select a multi-parametered model, then use appropriate statistical estimation techniques to obtain the best values of the parameters for the sequence. Vere-Jones and Davies (1966) have suggested the use of a "trigger" process, in which groups of events occur at times (cluster centers) defined by a simple Poisson process. The cluster center may or may not correspond to a particular trigger event. The probability that a shock will occur in a small time interval $(t + \tau, t + \tau + d\tau)$ following the occurrence time t of a trigger event is independent of t and denoted and equal to

$$P = X\Phi(\tau) \quad . \qquad (3\text{-}6)$$

X is an independent random variable denoting the size of each group, and has distribution q(N), where N is the number of events per group. It is also assumed that the triggered sequences of events are themselves independent. This then is the fundamental form of a generalized Poisson process (Parzen, 1962), a simple Poisson process in which the probability of more than one event occurring in a small time interval is finite instead of zero (see axiom 3).

Vere-Jones and Davies attempted to find a form of $\Phi(\tau)$ which described the long-term time series of $M \geq 4.5$ earthquakes in New Zealand. After testing exponential and hyperbolic decays, they concluded that neither form was adequate

for both long- and short-term intervals. The temporal dependence among shocks may last for many months, but is also evidenced by very strong short-term (1 to 5 days) grouping. Vere-Jones and Davies concluded that larger data samples and more detailed analysis must be made of the complex grouping process of shallow earthquakes.

Following Vere-Jones and Davies (1966), Shlien and Toksoz (1970a) also used the generalized Poisson model, with somewhat different assumptions. Shlien and Toksoz had noticed that the non-Poissonness of the worldwide earthquake time series was due to an excess number of time intervals with many events. To examine the distribution of events during these intervals, Shlien and Toksoz selected days during which the number of events which took place had a probability of occurrence less than .001 on the assumption of a simple Poisson process. Earthquake activity was broken into eight world regions for this examination, with consecutive days with highly improbable numbers of events combined into large clusters. The distribution of cluster sizes is shown in Figure 3-4; this is also the distribution of the random variable X in equation (3-6). Since an inverse cube law fits the histogram rather well, it was assumed that the cluster size probability distribution q(N) could be adequately described by a Zeta distribution,

$$q(N) = \frac{N^{-E}}{\zeta(E)} \quad . \qquad (3\text{-}7)$$

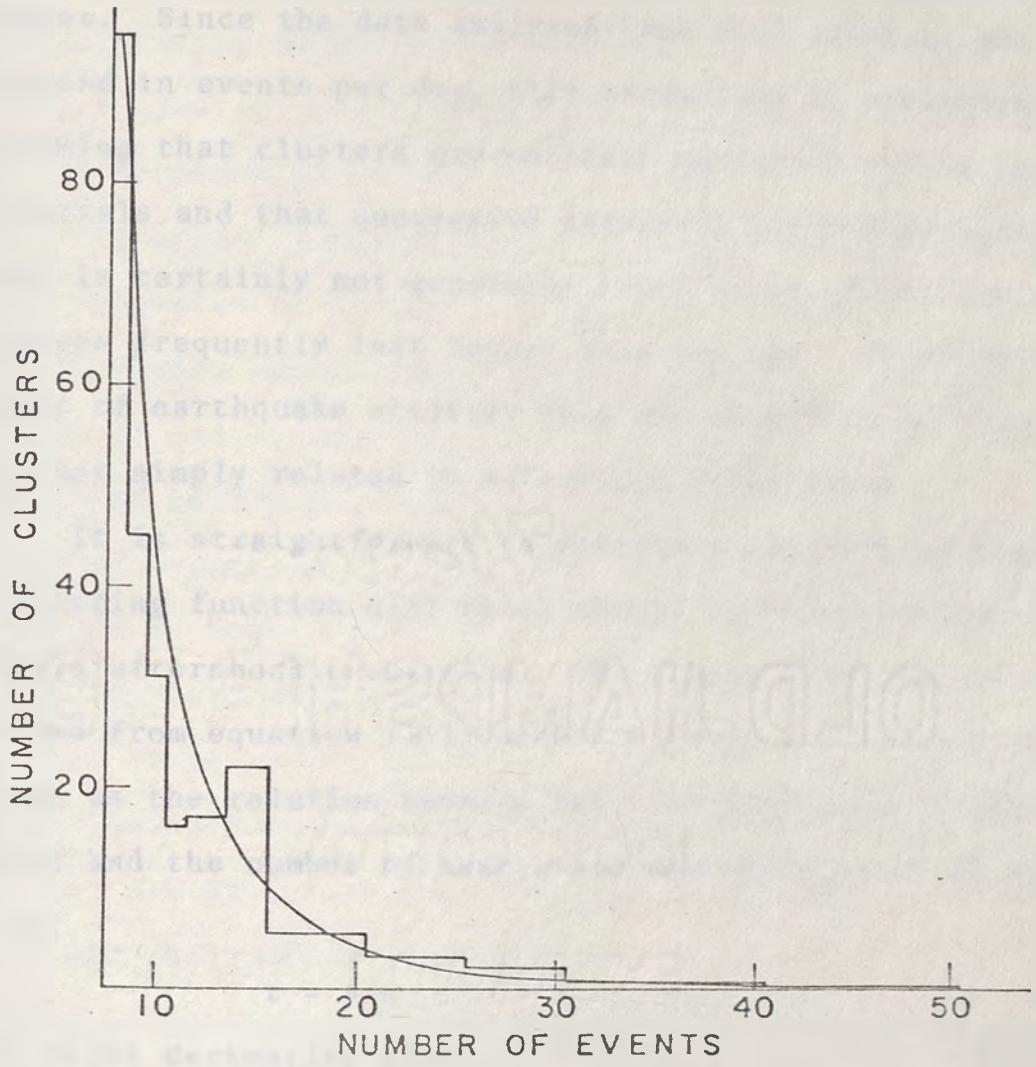

Figure 3-4. Frequency distribution of clusters of aftershocks versus the number of events per cluster. Each aftershock cluster is composed of events occurring during one day. The smooth curve is an inverse cube distribution.

Here E is a parameter describing cluster size, and $\zeta(E)$ is a normalization factor (the Riemann Zeta function).

The time distribution of events within a cluster, $\Phi(\tau)$, was assumed to be a delta function centered at the cluster center. Since the data analyzed (the NOAA catalog) was counted in events per day, this assumption is equivalent to assuming that clusters are entirely contained within one-day intervals and that successive intervals are independent. This is certainly not generally true, since aftershock sequences frequently last longer than one day. Thus the features of earthquake activity that are described by this model are not simply related to aftershock occurrences.

It is straightforward to determine the sort of daily clustering function q(N) which should be expected from a single aftershock occurrence. The simple Omori law is obtained from equation (3-1) with $\beta = 0$ and $p = 1$; it is here shown as the relation between the time after the trigger event and the number of events per day which occur at that time:

$$t = A/n \quad . \tag{3-8}$$

The first derivative gives

$$\Delta t = A/n^2 \tag{3-9}$$

when the change in number of events per day, Δn, is equal to one. Since Δt is the number of days that corresponds to a change in daily rate of occurrence of one per day at a particular value of n events per day, this is the distribution

function for a single aftershock sequence corresponding to equation (3-7). Thus the distribution of days with a given number of events is proportional to the inverse square of the number of events per day. In other words, if every day's activity during an aftershock sequence is considered as a separate cluster, the cluster size distribution is in the form of equation (3-7) with E = 2. This is seen in Figure 3-5. The solid lines represent aftershock sequences following earthquakes of indicated magnitude. To parallel the work of Shlien and Toksoz, the horizontal axis represents numbers of earthquakes per day. The initial values (the right-hand points in Figure 3-5) are proportional to the number of events in the first day after the main shock, and are found by Mogi (1967), Utsu (1969), and others, to generally increase with increasing magnitude of the main shock, but with large variations for a given magnitude. The A values chosen for these sequences, as given in the figure caption, are arbitrary. In Figure 3-5, the value of the slope for the individual sequences is E = 2.

The equation (3-9) may be summed for a combination of aftershock sequences, as shown in Figure 3-5. The individual sequences were combined in two ways. For the case in which there was a large earthquake and aftershock sequence, one magnitude 8.0 sequence was combined with two magnitude 7.0, twenty magnitude 6.0, and two hundred magnitude 5.0 sequences. The cutoff magnitude of 5.0 for this example is represented by

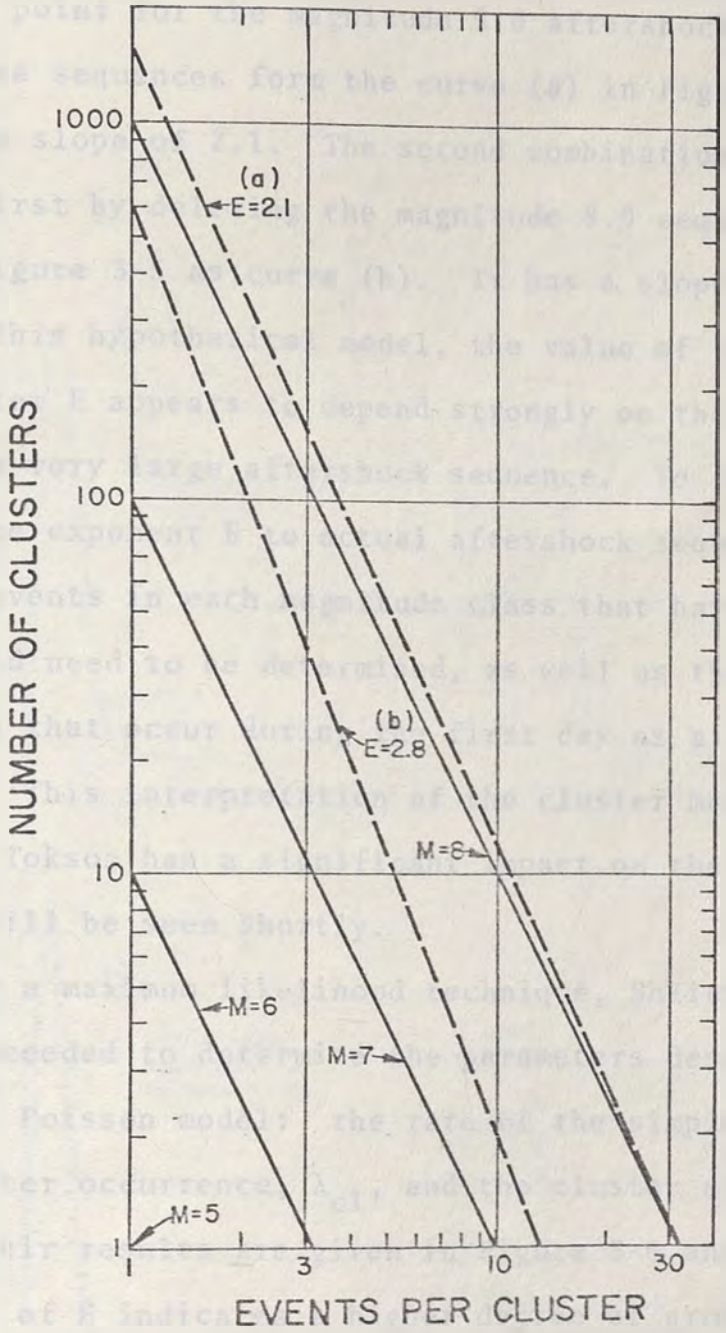

Figure 3-5. Log-log plot of number of clusters of aftershocks versus number of events per cluster. Solid lines are for aftershock sequences per equation (3-9), with Zeta distribution parameter E=2. Number of events per cluster for cluster size of one are arbitrarily selected and decrease by one-half order of magnitude for each magnitude unit decrease. Dotted lines are for summed combinations of aftershock sequences. Curve (a) is composed of one M=8, two M=7, 20 M=6, and 200 M=5 sequences; curve (b) is the same as (a) without the M=8 sequence.

the single point for the magnitude 5.0 aftershock data. The sum of these sequences form the curve (a) in Figure 3-5, which has a slope of 2.1. The second combination is formed from the first by deleting the magnitude 8.0 sequence and is shown in Figure 3-5 as curve (b). It has a slope of 2.8. Thus, for this hypothetical model, the value of the clustering parameter E appears to depend strongly on the occurrence of a single very large aftershock sequence. To relate the value of the exponent E to actual aftershock sequences, the number of events in each magnitude class that have aftershocks would need to be determined, as well as the number of aftershocks that occur during the first day as a function of magnitude. This interpretation of the cluster model used by Shlien and Toksoz has a significant impact on their conclusions, as will be seen shortly.

Using a maximum likelihood technique, Shlien and Toksoz (1970a) proceeded to determine the parameters describing the generalized Poisson model: the rate of the simple Poisson cluster center occurrence, λ_{cl}, and the cluster size parameter, E. Their results are given in Figure 3-6 and Table 3-1. A low value of E indicates a higher degree of grouping of events in time, while a high value means that the distribution approaches that of a simple Poisson model. The P values again indicate quality of fit to the null hypotheses.

There are several observations which may be drawn from Table 3-1. For worldwide activity, the value of E increases

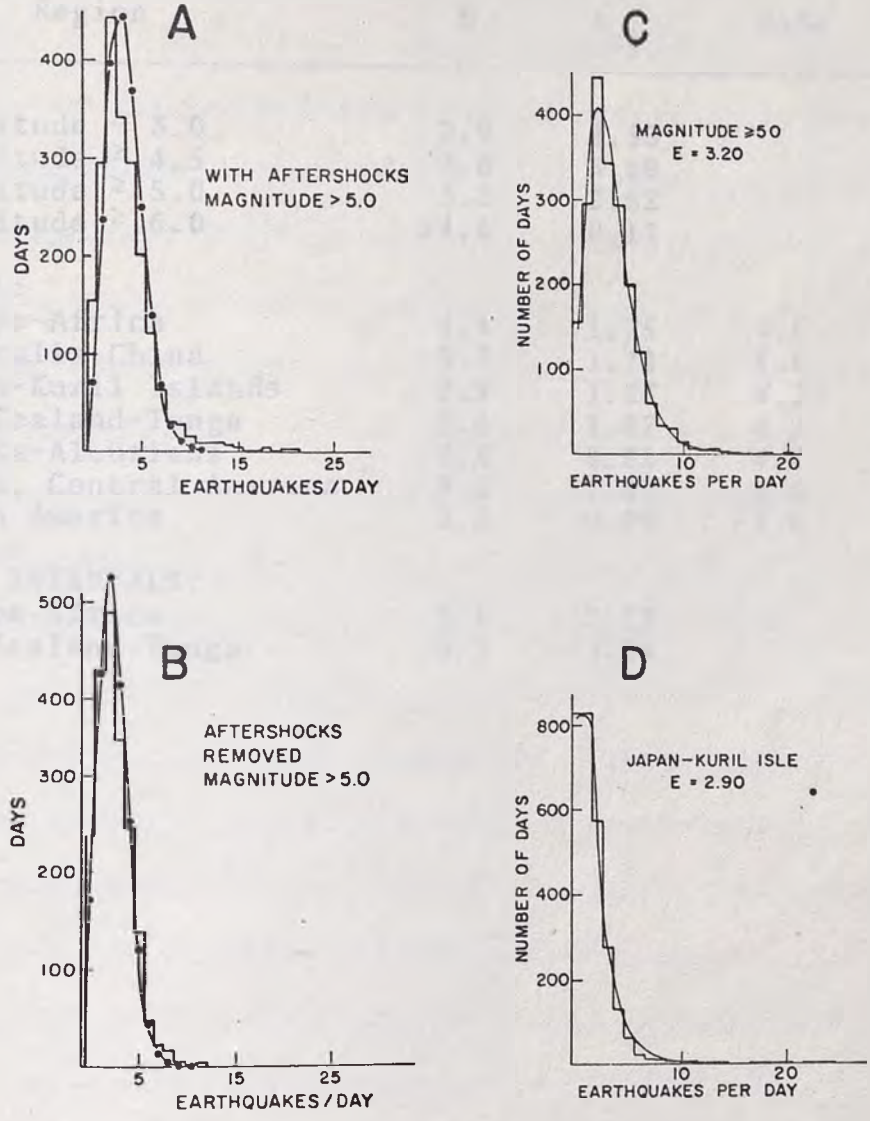

Figure 3-6. Frequency distribution of the number of days versus number of earthquakes occurring per day for the following samples: (a) worldwide, with aftershocks; (b) worldwide, with aftershocks removed; (c) worldwide, with magnitude greater than 5.0; (d) Japan and the Kuril Islands.

TABLE 3-1

Region	E	λ_{cl}	Mode	P
WORLD:				
Magnitude ≥ 3.0	2.9	8.80		0.001
Magnitude ≥ 4.5	3.0	5.69		0.1
Magnitude ≥ 5.0	3.2	2.62		0.65
Magnitude ≥ 6.0	>4.4	0.17		0.40
REGIONAL:				
Europe-Africa	3.4	1.25	4.6	0.60
Australia-China	3.7	1.72	4.6	0.20
Japan-Kuril Islands	2.9	1.23	4.2	0.0001
New Zealand-Tonga	3.4	1.87	4.3	0.07
Alaska-Aleutians	2.4	0.81	4.4	0.001
North, Central America	3.2	1.87	4.5	0.14
South America	3.5	0.99	4.6	0.01
TWO-DAY INTERVALS:				
Europe-Africa	3.1	2.23		0.01
New Zealand-Tonga	3.3	3.64		0.39

as the magnitude cutoff increases; in other words, larger events are in general more independent than smaller events. As noted earlier, this fact has been known for many years; large independent events trigger aftershock sequences composed of smaller events. In the regional analyses, it should be recalled that no cutoff magnitude was applied to the catalogs Shlien and Toksoz used. In another paper, Shlien and Toksoz (1970b) found large regional differences in the magnitude at which most events were detected (the mode). In all cases the mode values were less than the worldwide cutoff magnitude M_o = 4.75 determined by Knopoff and Gardner (1972). In fact, the difference between the average world rate of all events (14.19 per day) and the rate for events with magnitude greater than 4.5 (7.76 per day) suggests that about half of the events used in the Shlien and Toksoz (1970a) regional analysis were smaller than the completely recorded cutoff magnitude. Thus, for the worldwide data modeled, there is a bias to smaller events nearer seismic stations. Within each of the zones, recording installations are unevenly distributed, not necessarily in correspondence with the distribution of earthquake activity. Therefore, in some regions the locales of high rates of occurrence may be over-represented, while in other regions the numbers of smaller events detected may be relatively low. This effect may influence the variations in E from region to region.

A more significant effect may also be observed. In Figure 3-2, showing daily rates of occurrence for the world, there are three "spikes," corresponding to large aftershock sequences following the M = 8.1 Kuril Islands earthquake of 13 October 1963, the Alaskan earthquake of 28 March 1964, and an event in the Rat Islands on 4 February 1965. The very high daily counts following these earthquakes would definitely dominate the distribution of "clusters" and thus produce the low E values of 2.4 and 2.9 for Alaska and Japan, respectively. The effect of a single large sequence is shown in Figure 3-5. These values approach the value E = 2 that applies to a single sequence (equation 3-9).

Shlien and Toksoz (1970a) did note that the cluster model they used, in which $\Phi(\tau)$ is a delta function, also causes the cluster size parameter E to be sensitive to the time interval used. They found that the use of a two-day interval lowered the value of E. As expected, longer time intervals emphasize longer aftershock sequences that will lower the E value in equation (3-7).

Summary

It may be concluded that the Shlien and Toksoz (1970a) generalized Poisson model is not particularly satisfactory because it does not very closely relate the actual time series of events within a large region (composed of aftershock sequences, constant occurrence periods, swarms, and so forth) to the occurrence frequency of daily numbers of

events. This does not minimize the ability of the two-parameter (λ_{c1}, E) model to statistically describe the daily rate pattern, which can be done quite accurately, as Shlien and Toksoz (1970a) demonstrated. However, the significant parameter that they identified (E) is controlled chiefly by large aftershock sequences and does not provide increased seismological understanding. It may be possible to find other probability models which also fit the observed distributions. The disadvantage is that the seismological value of the data is almost completely eliminated when basic features of the occurrence pattern are masked as in the Shlien and Toksoz model.

To allow a more meaningful and extensive modeling capability, spatial coordinates and energy need to be incorporated with the temporal dimension. Vere-Jones (1970) also mentions these extensions of generalized time-series clustering models, but he notes that the necessary probabilistic techniques for discussion multi-dimensional point processes are still in "a somewhat exploratory stage."

CHAPTER IV. MICROEARTHQUAKE CLUSTERING

It is appropriate, at this point, to review the axiomatic basis of Poisson probability models. From Chapter I, the four axioms from which the simple, one-dimensional Poisson process may be derived can be written as follows for earthquake time-series:

1_T. there is no causal connection among the earthquakes in a time-series N(t);

2_T. the probability of occurrence of an earthquake in a given time interval is greater than zero and is equal to the product of the average rate of occurrence of earthquakes and the duration of the time interval;

3_T. it is not possible for earthquakes to happen simultaneously;

4_T. the distribution of earthquakes is stationary with respect to time.

In the preceding chapter, a number of instances of non-Poisson statistical behavior were described, and examples of attempts to model such behavior, particularly those of Inouye (1937), Jeffreys (1938), and Shlien and Toksoz (1970a), were reviewed. In modeling specific earthquake time-series that do not conform with the assumptions of the Poissonian axioms, it is clear that axioms 1_T and 4_T are no longer applicable and it is necessary to provide additional parameters to enable a successful non-Poisson model. Inouye (1937) noted that the data he was examining did not fit axiom 4_T, so he used a model

(equation 3-2) with a varying rate of occurrence that voided axiom 2_T. A number of other authors, including most recently Vere-Jones and Davies (1966) and Shlien and Toksoz (1970a) have approached the probability modeling of earthquake time-series with a multiparametered mathematical methodology. It is seen how this approach can lead to somewhat non-meaningful descriptions of the earthquake process. The trigger models, which contravene axiom 3_T, have been applied to earthquake data in such a way as to favor statistical data-fitting over an approach guided by the qualitative features of the time-series data and the physics of earthquake occurrence.

With a significantly differing methodology, a number of previous researchers have attempted to identify or investigate explicitly the elements of earthquake occurrence that do behave in a Poisson manner. Knopoff and Gardner (1972) assumed some arbitrary criteria to exclude relatedness among earthquakes in order to define a Poisson data set. Jeffreys (1938) and Lomnitz and Hax (1966) used a time transformation so as to apply axiom 2_T and define a Poisson model of aftershock occurrence.

In this chapter, the second methodology is applied to earthquakes in the range M = 0 to 4.0. In particular, statistical data from central Nevada and central California microearthquake studies are analyzed, and it is found that microearthquakes occur in a compound process somewhat like that of larger events ($M \geq 4.5$) that involves a Poissonian sequence

with non-Poisson aftershock behavior superimposed. For microearthquakes, an approximately constant-rate Poisson process of independent events is found, with some of these events accompanied by secondary "clusters" of dependent events. The dependent events are not like aftershock sequences, however, in several details of their occurrence. Henceforth, the term "cluster" will apply only to the groups of related microshocks.

Microearthquake Cluster Identification

There have been only a few previous examinations of the independence of microearthquakes, again with varying conclusions. Iida (1939) studied small, instrumentally recorded events in a local area in Japan and concluded that their interoccurrence times were well described by an exponential distribution, indicating their randomness. It is noticeable from Iida's data, though, that there are more short time intervals than expected for a Poisson distribution. Singh and Sanford (1972) also noted a tendency for microearthquakes near Socorro, New Mexico, to cluster in time. Following the Alaskan earthquake of 1964, Page (1968) examined microaftershocks in eighteen S-P distance ranges for 102 hours beginning 22 days after the main event. He concluded that in only two distance ranges, each being one S-P second in size, could the assumption of a Poisson distribution of occurrence times be rejected. Page associated these two discrepancies with small aftershock sequences or swarms. In summary, nonrandomness has been observed in several microearthquake samples, but not investigated in detail.

In the following sections, microearthquake samples from Nevada and California that were described in Chapter I are analyzed for dependence among events, using the Poisson model with generalizations to disclose the nature of the observed relatedness. The procedures used focus on analysis of the earthquake locations and magnitude as well as the time-series to determine the secondary distributions describing clustering, rather than attempts to fit arbitrarily chosen probability models for the time-series alone.

Central Nevada Microearthquakes. The first events examined occurred near the SMN array (Figure 1-1) during a period of 60 days. Magnetic tape recordings were made of signals from three vertical-component seismometers arranged as a tripartite array plus a three-component set of instruments at the center of the array. The tapes were played out continuously on a multi-channel chart recorder to facilitate counting events and measuring amplitudes. From the recorded group of earthquakes a limited spatial sample was chosen containing only events with S-P times between 1.5 and 2.2 seconds, corresponding to focal distances of about 11 to 16 kilometers. The cut-off amplitude was determined from the low-amplitude roll-off point of the log-amplitude frequency distribution curve; events with peak-to-peak amplitudes greater than five times background level (5 X 1.0 mm) were found to form a complete catalog. Based on previous field recordings with the same equipment (Ryall and others, 1968), estimated Richter

magnitudes of the events ranged from about -1/4 to 2.0. The sample thus selected consisted of 856 events recorded during 59.55 days, corresponding to a mean rate of 0.60 events per hour.

The observed time sequence was initially compared with the simple Poisson process

$$P(x,t) = \frac{e^{-\lambda t}(\lambda t)^x}{x!} \quad . \tag{1-2}$$

The number of events in consecutive 12-hour periods were counted and are shown in Figure 4-1a along with the theoretical curve calculated from equation (1-2) using the observed mean rate λ = 7.20 events per 12 hours. As a rough measure of goodness-of-fit, the χ^2 test was used and gave a probability of less than 0.5% for this curve. The points of worst χ^2 fit are the intervals containing fourteen or more events. This observation is similar to earlier ones made by Page (1968), and others.

To further isolate the non-Poisson behavior, the time interval distribution of the data was examined to see how closely it fit the exponential distribution expected for a Poisson process. From the probability density function,

$$f(t) = \lambda e^{-\lambda t} \quad , \tag{1-4}$$

one can calculate the distribution of time intervals, F, for intervals of duration between t_1 and t_2:

$$F(t_1,t_2) = \int_{t_1}^{t_2} f(t)\, dt = e^{-\lambda t_1} - e^{-\lambda t_2} \quad . \tag{4-1}$$

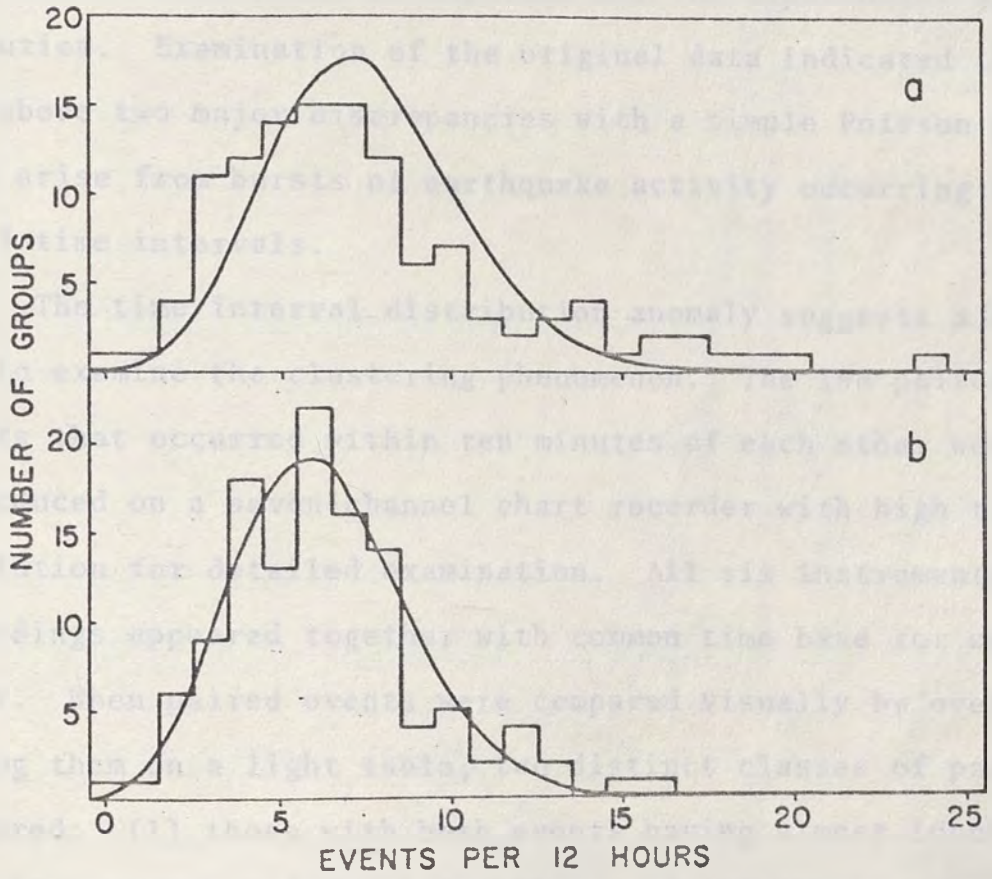

Figure 4-1. Observed (bar graph) and calculated (solid line) Poisson distributions for (a) all microearthquakes in the selected time sequence, mean rate λ = 7.20 events/12 hours, and (b) the same events counted as a cluster sequence, mean rate λ_c = 6.27 clusters/12 hours.

Figure 4-2 shows this distribution calculated for multiples of five minutes along with the outline bar plot indicating the observed time interval distribution. The calculated exponential curve for these events is an especially poor fit for the shortest time intervals. For events occurring within five minutes of each other there are 108, or 204%, more events than the 45 that would be expected for the exponential distribution. Examination of the original data indicated that the above two major discrepancies with a simple Poisson process arise from bursts of earthquake activity occurring during small time intervals.

The time-interval distribution anomaly suggests a direct way to examine the clustering phenomenon. The 196 paired events that occurred within ten minutes of each other were reproduced on a seven-channel chart recorder with high time resolution for detailed examination. All six instrumental recordings appeared together with common time base for each event. When paired events were compared visually by overlaying them on a light table, two distinct classes of pairs appeared: (1) those with both events having almost identical signal character and focal location, and (2) those with markedly different character and location. For the similar events, in some cases there were reversals of sense of first motion for various instruments of the array; e.g. the north-south trace for one event would be the mirror image about the zero line for the other, or the sense of motion on various of

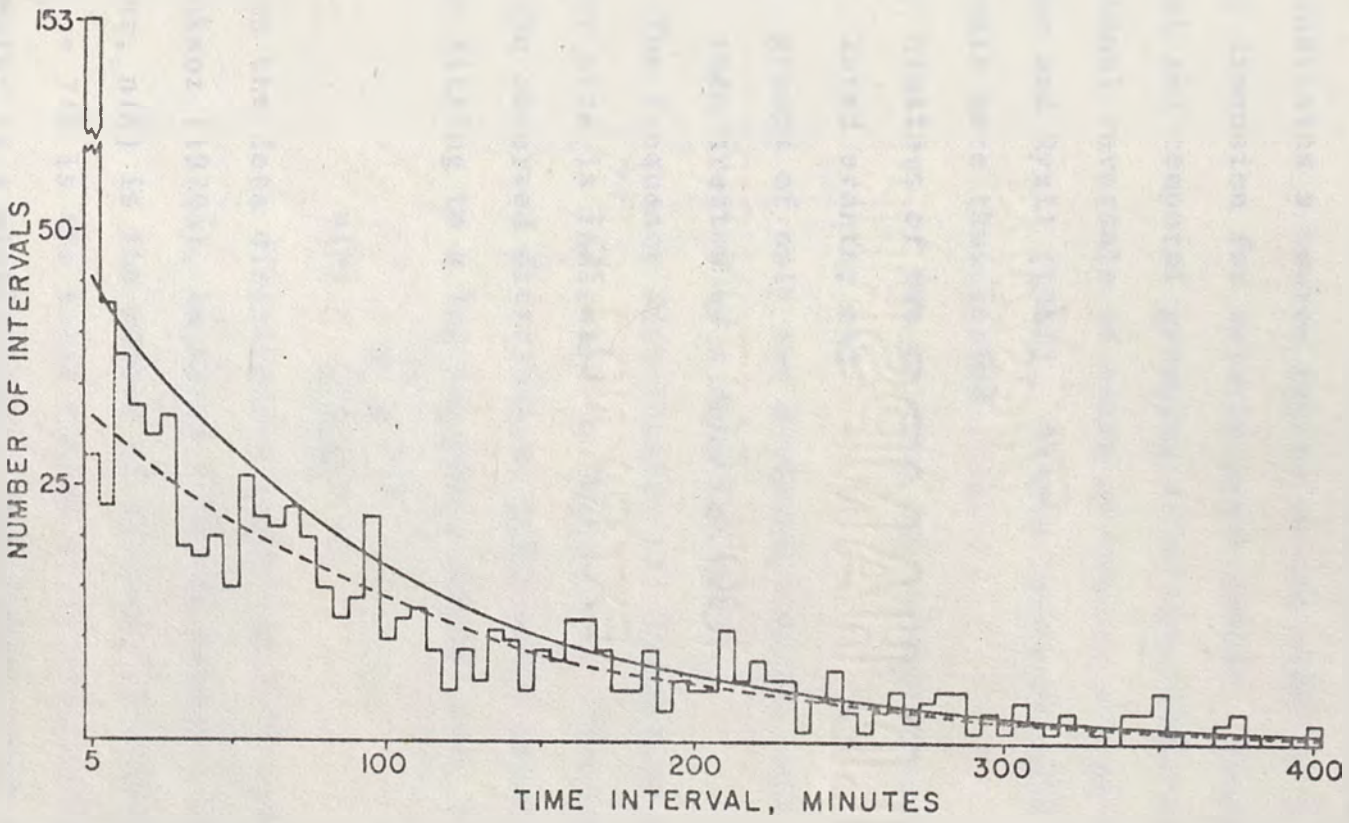

Figure 4-2. Distribution of time intervals between successive microearthquakes (entire bar plot) and clustering centers (dashed bars in first two intervals). The solid and dashed curves indicate the calclated exponential distributions for microearthquakes and clusters, respectively. Time intervals are plotted in successive 5-min units, as 0-5 sec, 5-10 sec, ...

the array legs might change from event to event. But the traces could still be overlain with minimal (less than 0.02 seconds) difference in arrival time at each array instrument. This indicates a source region on the order of a few hundred meters dimension for related pairs events. Examples of this spatial and temporal grouping of microearthquakes at SMN, with occasional reversals of sense of motion, was also noted by Stauder and Ryall (1967). Events occurring with short time intervals were thus sorted into:

1) clusters of two or more (up to fourteen) closely related events; and
2) groups of only two differing shocks, each of which was then treated as a separate event.

The frequency distribution of clusters as a function of cluster size is indicated in Figure 4-3. The smooth curve fits the observed distribution quite well, as determined by linear fitting to a log-log plot, and is given by

$$n(N) = \frac{N_o N^{-3.5}}{\zeta(3.5)} \quad . \qquad (4\text{-}2)$$

This is the Zeta distribution (equation 3-7) used by Shlien and Toksoz (1970a), in which N is the number of events per cluster, n(N) is the number of clusters containing N events, and $N_o = 746$ is the total number of cluster centers. A cluster center is a statistically independent group containing one or more earthquakes, with the 196 paired events forming clusters of two or more earthquakes. As before, the parameter

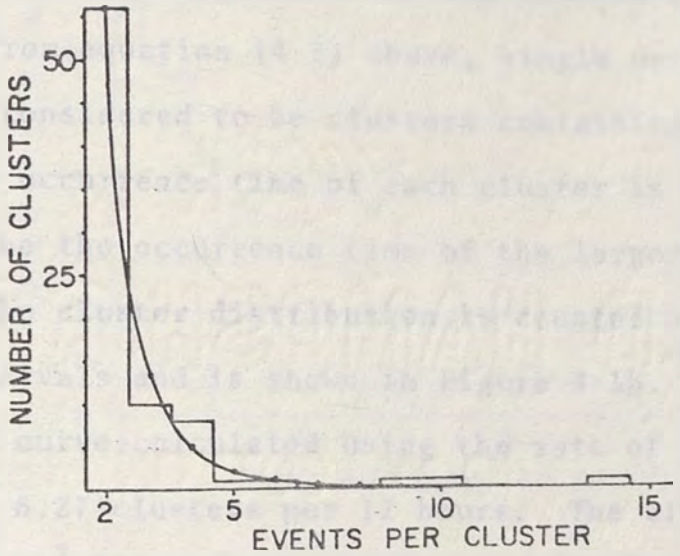

Figure 4-3. Distribution of the number of clusters versus the number of events per cluster. The smooth curve is the power law $N^{-3.5}$.

E = 3.5 describes the cluster size distribution.

In terms of the generalized Poisson model, the time sequence of the SMN microearthquake sample may be tested for resolution into a simple Poisson distribution of clustering centers and a secondary distribution (the Zeta distribution) of numbers of clustered events. The secondary distribution as found in equation (4-2) seems quite adequate, so the clustered groups of events are reduced to single cluster centers and the resulting distribution of cluster centers is tested for the null hypothesis of the Poisson distribution. Note that from equation (4-2) above, single unrelated earthquakes are considered to be clusters containing only one event. The occurrence time of each cluster is taken arbitrarily to be the occurrence time of the largest event in the cluster. The cluster distribution is counted in successive 12-hour intervals and is shown in Figure 4-1b. Also shown is the Poisson curve calculated using the rate of cluster occurrence, $\lambda_c = 6.27$ clusters per 12 hours. The cluster distribution has a χ^2 probability of 35%, a far better fit than was found for single events in Figure 4-1a. The generalized Poisson model with parameters λ and E is thus found to be a statistically good model.

The interoccurrence time distribution for clusters also indicates a closer agreement with a simple Poisson process. Figure 4-4b shows this distribution for clusters, on an expanded time scale, with its much closer agreement with the

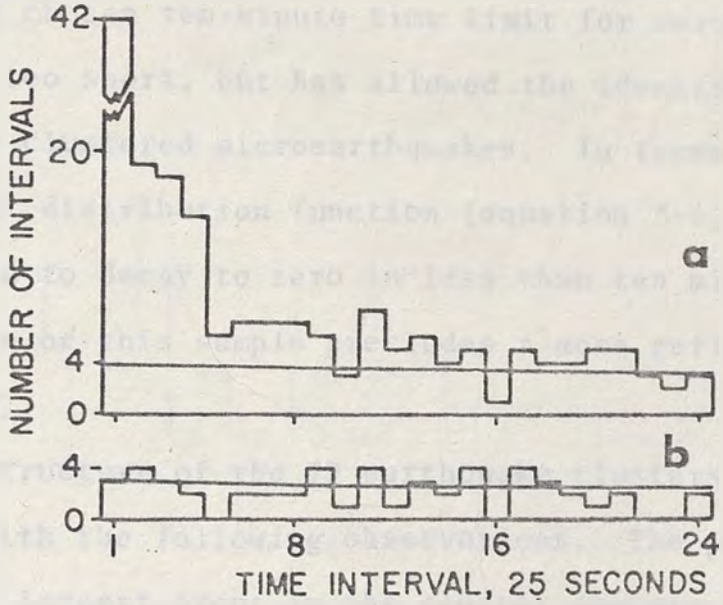

Figure 4-4. (a) Distribution of time intervals of earthquakes for the first 10 min of Figure 4-2 counted for a more detailed time scale. (b) Time interval distribution for clusters with a detailed time scale. The solid lines are the associated calculated exponential distributions. The time interval scale is in successive 25-sec units, as 0-25 sec, 25-50 sec, ...

theoretical exponential distribution calculated from equation (4-1) with parameter λ_c. Figure 4-4a shows the original distribution of Figure 4-2 for comparison. In Figure 4-2 the dashed bars and curve indicate the empirical and theoretical cluster occurrence interval distributions. The discrepancies between the empirical and theoretical distributions, particularly in the first ten or so interval groups, suggest that there are still some inadequacies in the cluster model. The arbitrarily chosen ten-minute time limit for relatedness is apparently too short, but has allowed the identification of most of the clustered microearthquakes. In terms of the general cluster distribution function (equation 3-6), $\Phi(\tau)$ has been assumed to decay to zero in less than ten minutes. The limited size of this sample precludes a more refined description of $\Phi(\tau)$.

The structure of the 79 earthquake clusters has been examined, with the following observations. The position in time of the largest event in the cluster appears to be random for all group sizes from two to fourteen events. The clusters are not spatially restricted within the data sample, for the clustered events exhibit the same S-P distribution as do the non-clustered events. Similarly, the log N(A) versus log A curve is not noticeably different for the clustered events from that of the entire sequence. In a greatly magnified plot of the first 120 seconds of the interoccurrence time distribution for events within clusters (Figure 4-5), the two most

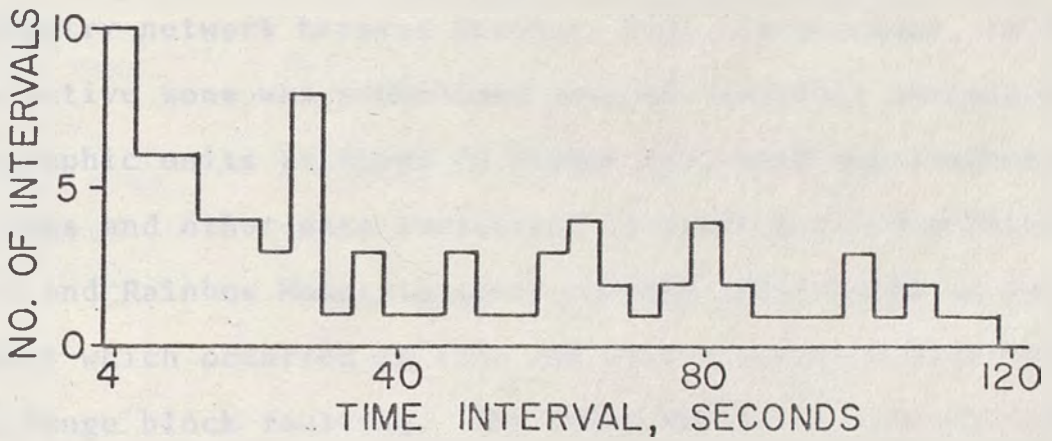

Figure 4-5. Distribution of time intervals for the first 120 seconds of Figure 4-2 counted in successive 4-second intervals, as 0-4 sec, 4-8 sec, ...

likely groups of time intervals are 0 to 4 seconds and 24 to 28 seconds, as noted by the two highest peaks. Study of the California data will supply more information on intra-cluster structure.

Nevada Regional Variations. The possibility of near-regional differences in clustering patterns was considered for earthquakes that occurred during a two-year period in the Nevada seismic zone from Fairview Peak south to Fish Lake Valley (Figure 1-1). The events are in the magnitude range 2.0 to 4.2 and were located using the University of Nevada state-wide telemetry network between October, 1969 and December, 1971. The active zone was subdivided into six distinct seismic or geographic units as shown in Figure 1-1, with the characterizations and other data summarized in Table 4-1. The Fairview Peak and Rainbow Mountain zones contain aftershocks of earthquakes which occurred in 1954 and were associated with Basin and Range block faulting. The Cedar Mountains zone delineates the active area of the 1932 magnitude 7.2 event. Gianella and Callaghan (1934) interpreted the mapped surface faulting as a product of southeastern horizontal displacement of the Cedar Mountains-Paradise Range block. The area surrounding and including the Excelsior Mountains is characterized by complex transverse range structure and dispersed seismicity, although the composite focal mechanism for events in this zone is very well and consistently determined and is quite similar to that of the Fairview Peak zone (Ryall and others, 1972). The

TABLE 4-1

Location	Type of Zone	No. of Events	Rate, event/day	Minimum Magnitude
Fairview Peak	Aftershocks of 1954, range front fault	106	0.134	2
Rainbow Mtn.	Aftershocks of 1954, range front fault	36	0.046	2
Excelsior Mtns. area	Dispersed zone	141	0.178	2
Cedar Mtns.	Aftershocks of 1932, rift valley	44	0.056	2
Bishop area	Dispersed zone	38	0.048	2-1/2
Fish Lake Valley	Near-historic faulting, range front fault	55	0.070	2-1/2

events in the Fish Lake Valley, while not explicitly known to be aftershocks, occur along a clearly defined range front fault with near-historic surface displacement. The 40-kilometer-wide gap in the zone near the north end of the valley (a large swarm of events is the northernmost activity) has been noted by Gumper and Scholz (1971) and Ryall and others (1972). Activity to the north and west of Bishop, California, is also dispersed and not associated with any specific surface features. This zone is northwest of the termination of surface faulting of the 1872 Owens Valley earthquake.

Interoccurrence times for the six zones are plotted in Figure 4-6 with the associated simple exponential distributions indicated by solid curves. Intervals are measured in multiples of one day. For these six zones there is not enough data to allow estimation of the E parameter. However, several distinct qualitative features are apparent: Cedar Mountains, Rainbow Mountain, Fairview Peak, and the Excelsior Mountains area show similar clustering features, with two to three times as many events in the 0 to 1 day interval group as would be expected for a randomly occurring sample. Because of its large area the Excelsior Mountains area was further subdivided (not shown here) with almost exactly the same clustering features appearing for each subzone as for the entire zone. The Fish Lake Valley activity is dominated by clusters, with ten times as many events in the shortest interval class. More

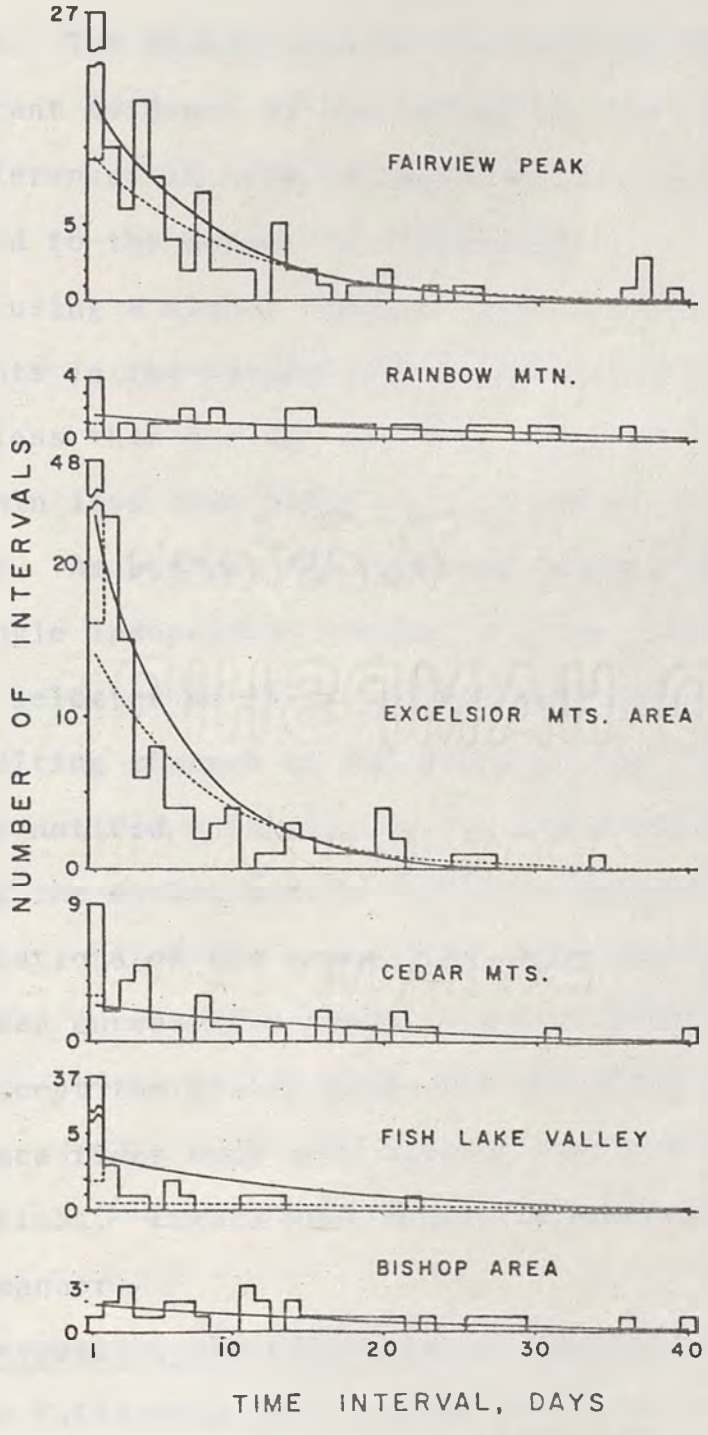

Figure 4-6. Time interval distributions in units of 1 day for larger events ($2 < M < 4.2$) in six parts of the Nevada seismic zone. The solid curves are the associated calculated exponential distributions. Dashed bars and curves are for the sequences with clustered events reduced to single events.

than 60% of the entire Fish Lake Valley sample occurred in clusters. The Bishop area to the west, however, shows no significant evidence of clustering for the two-year period. The differences in type of source area (Table 4-1) appear unrelated to the degree of clustering.

By using a visual overlay comparison of seismograms, the events in the Nevada region with occurrence times differing by less than one day and that occurred at the same focus (to within less than about one kilometer) are identified as clusters. As before, the clusters are considered to represent single independent events, and the time interval of one day was selected so as to include most of the related events. The resulting changes in the distributions for cluster centers are noticed primarily in the first interval group as shown by the dashed bar in the first columns of Figure 4-6. Recalculations of the exponential distributions are shown by the dashed curves when there is a noticeable change. In all cases except the Bishop area, the resulting distributions of occurrence times much more closely approach distributions of random times. Events near Bishop already occurred in a random manner.

Microearthquake Clustering in Central California

The California data samples discussed in Chapter I are examined in a manner similar to the Nevada samples. To select the samples for time-series analysis, it is necessary to determine the cutoff magnitudes above which the samples are

complete. As discussed in Chapter II and shown in Figure 2-3, picking M_o is made difficult by biased magnitude values. Since the b-value for the active fault zones in central California has been found to be between 0.8 and 0.9 (Eaton and others, 1970), it was assumed here that the five curves in Figure 2-3 should have slopes in this range. For each curve the value of b using the maximum likelihood method was determined as a function of magnitude, and the cutoff magnitude was chosen from this function as the magnitude at which the slope value fell below 0.8. For the five zones in Figure 2-3, the magnitude cutoffs thus calculated are as follows: Calaveras, 0.85; Sargent, 0.85; San Andreas north, 1.65; San Andreas, 1.35; and central California, 1.15. Admittedly, these cutoffs are not accurate nor are they statistically proper. The arbitrary values do, however, define the data sets to be approximately complete.

The time intervals between successive events larger than the cutoff magnitudes in each zone were computed, and the frequency distributions for three of the zones are shown in Figure 4-7. Calculated exponential distributions based on the average occurrence rates are shown by the solid curves. As in the previously examined areas in Nevada, clustering is evidenced in each of these three zones within the central California active region. The numbers of small time intervals exceed what is expected for a random distribution of events in time by factors of ten or more.

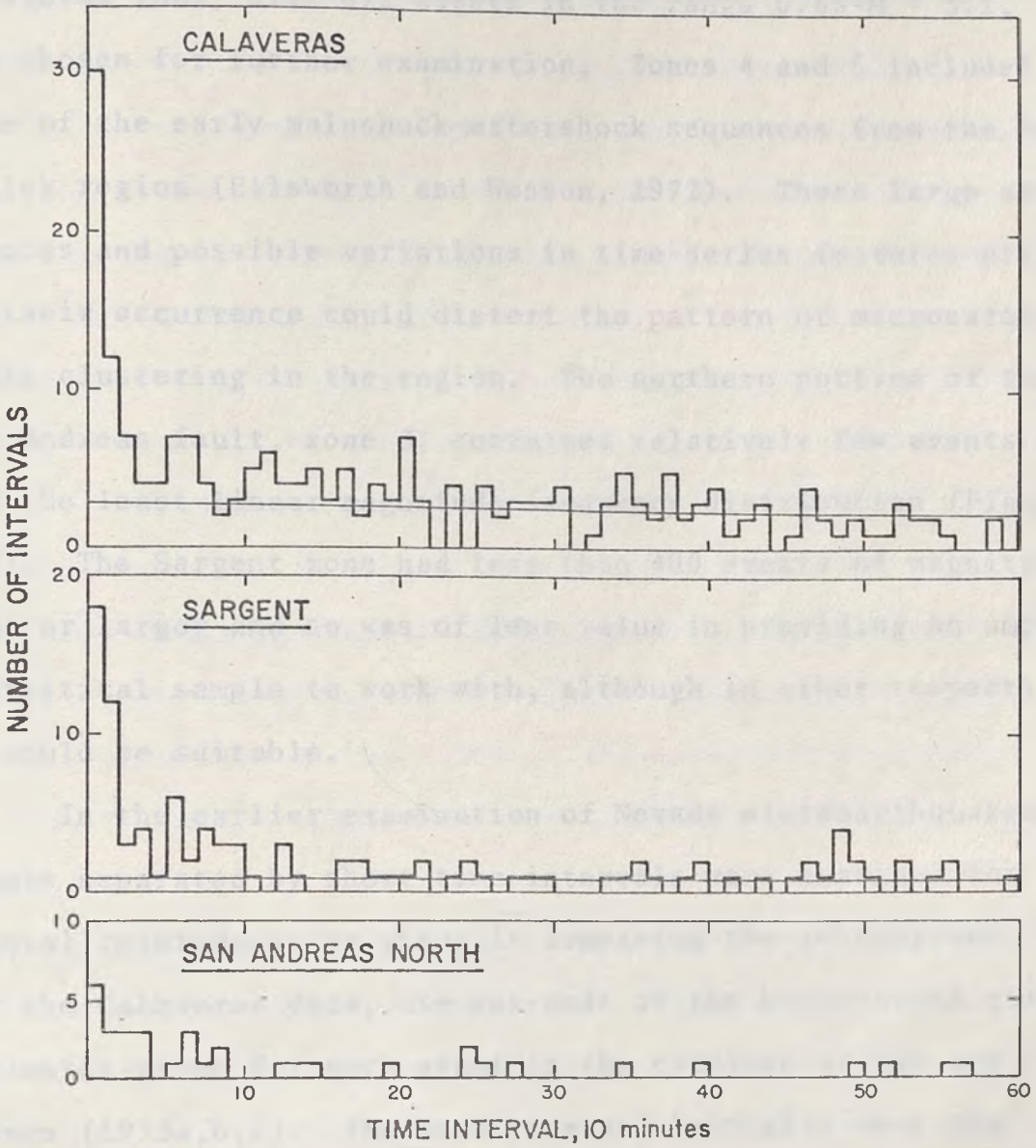

Figure 4-7. Bar graphs of time interval distributions in units of 10 minutes for three regions in central California. Solid curves are the associated calculated exponential distributions.

Calaveras Clustering. Only one of the samples, that from the Calaveras zone, with 672 events in the range $0.85 < M \leq 3.1$, was chosen for further examination. Zones 4 and 5 included some of the early mainshock-aftershock sequences from the Bear Valley region (Ellsworth and Wesson, 1972). These large sequences and possible variations in time-series features prior to their occurrence could distort the pattern of microearthquake clustering in the region. The northern portion of the San Andreas fault, zone 3, contained relatively few events and had the least linear magnitude frequency distribution (Figure 2-3). The Sargent zone had less than 400 events of magnitude 0.85 or larger and so was of less value in providing an ample statistical sample to work with, although in other respects it would be suitable.

In the earlier examination of Nevada microearthquakes, events separated by short time intervals were examined for spatial relatedness by visually comparing the seismograms. For the Calaveras data, use was made of the hypocentral error estimates given for each event in the catalogs of Lee and others (1972a,b,c). The data examined initially were the pairs of events with time separation less than thirty minutes, a time interval adequate to include all the pairs of earthquakes in the spike in Figure 4-7. For each event, the square root of the sum of the squares of the epicentral and depth errors was calculated as a measure of the event focal location error. Then the sum of the error measures for each pair of

events was plotted against focal separation calculated from the given focal coordinates, as shown in Figure 4-8. It is found that the pairs are clearly divided into two groups: (1) those with separation less than the summed error measures plus one kilometer; and (2) those with separation much greater than the focal errors. The dashed line in Figure 4-8 indicates this boundary, with the scatter in the clustered event locations being interpreted as an indication of the actual location accuracy of the catalog events (± < 1 kilometer).

It is apparent that a clustering process quite similar to that occurring in central Nevada is taking place along the Calaveras fault in central California. Most events that occur within several tens of minutes of each other and that have focal separations on the order of the size of the source dimension for a M = 1.0 to 2.0 earthquake are taken to be clustered.

Cluster Occurrence Statistics. The criterion of spatial relatedness obtained above was used to identify as clusters all pairs or larger groups of events that occurred within one kilometer of each other. Within the Calaveras zone, 85 such clusters were selected and contained from two to eighteen microearthquakes and lasted up to five days. A variety of statistical features were examined in this sample of clusters.

The cluster size distribution function for three different maximum cluster durations is shown in Figure 4-9 and has the functional description of equation (3-7). For clusters

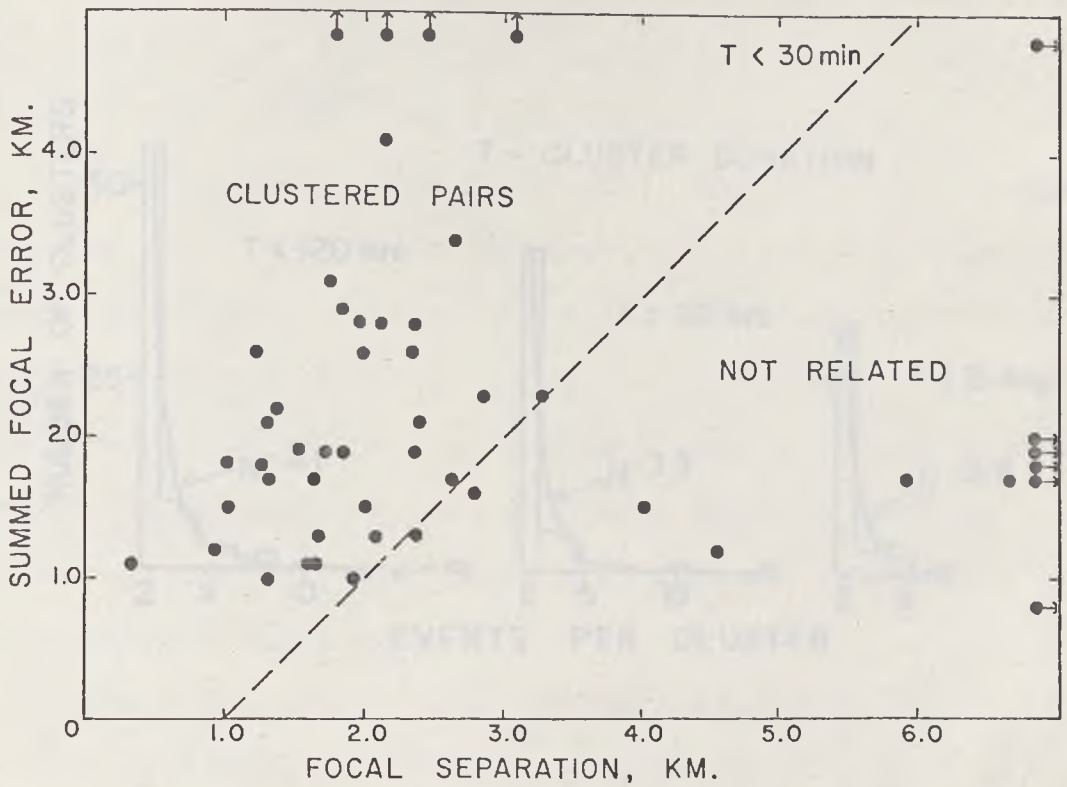

Figure 4-8. For pairs of events in the Calaveras sample with time difference less than 30 minutes, the square root of the sum of the squares of epicentral and focal depth are summed and plotted with respect to focal separation. Dashed line separating clustered pairs from non-clustered events was arbitrarily drawn.

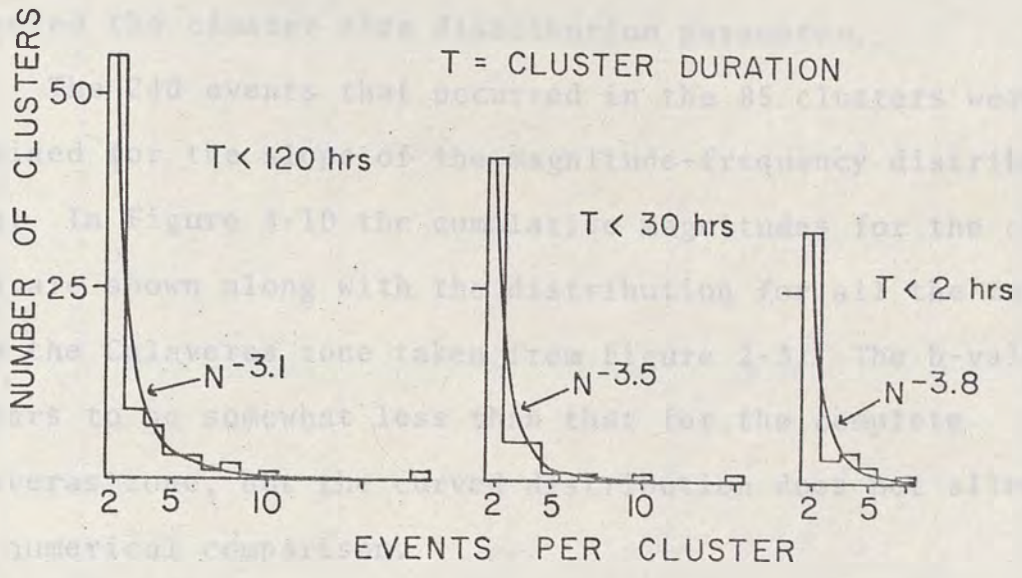

Figure 4-9. Histograms of the distribution of the number of clusters versus the number of events per cluster for three sets of clusters with maximum cluster duration less than 120 hours, 30 hours, and 2 hours, respectively. Smooth curves are power laws fit to log-log plots.

lasting less than 30 hours, the distribution is

$$q(N) = \frac{428}{N^{3.5}} \quad .$$

The exponent of the distribution function, E = 3.5, is the same as that found for Slate Mountain, Nevada, microearthquakes. As can be seen in Figure 4-9, arbitrary shortening or lengthening of the maximum cluster duration strongly affected the cluster size distribution parameter.

The 240 events that occurred in the 85 clusters were examined for the slope of the magnitude-frequency distribution. In Figure 4-10 the cumulative magnitudes for the clusters are shown along with the distribution for all the data from the Calaveras zone taken from Figure 2-3. The b-value appears to be somewhat less than that for the complete Calaveras zone, but the curved distribution does not allow any numerical comparison.

The distribution of energy release within the 85 clusters was examined by plotting the position of the largest magnitude event within each cluster, as shown in Figure 4-11. The first column indicates that 31 clusters had the largest event occur within the first half of the number of events of the cluster. The third column shows the number of clusters (28) with the greater energy release in the second half of the cluster. The central column indicates 26 clusters with less than 0.1 magnitude unit difference in cluster halves. This pattern of symmetrical energy release among clustered events

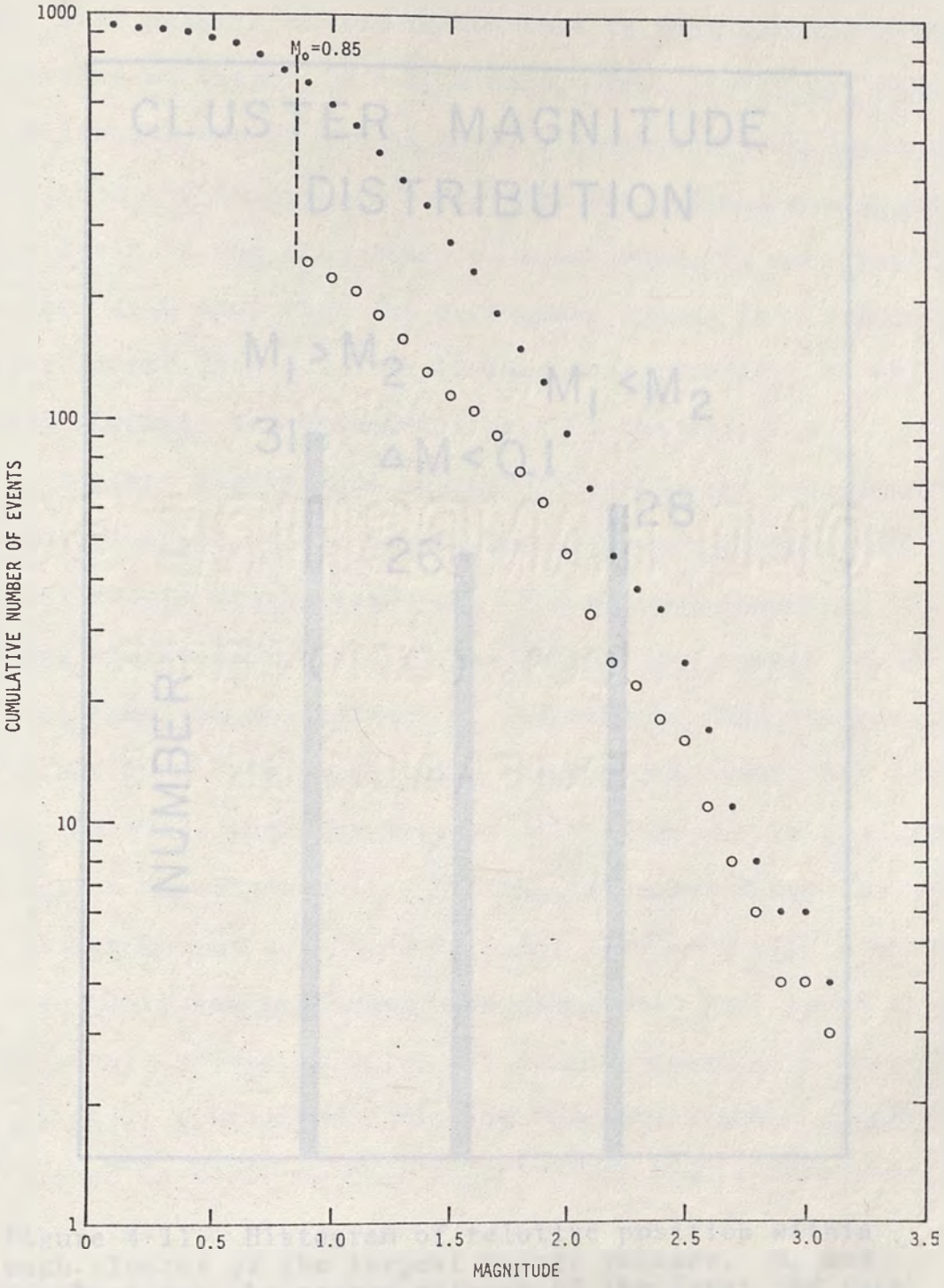

Figure 4-10. Cumulative magnitude-frequence plot of all Calaveras data from Figure 2-3 (solid circles) and clustered events only (open circles).

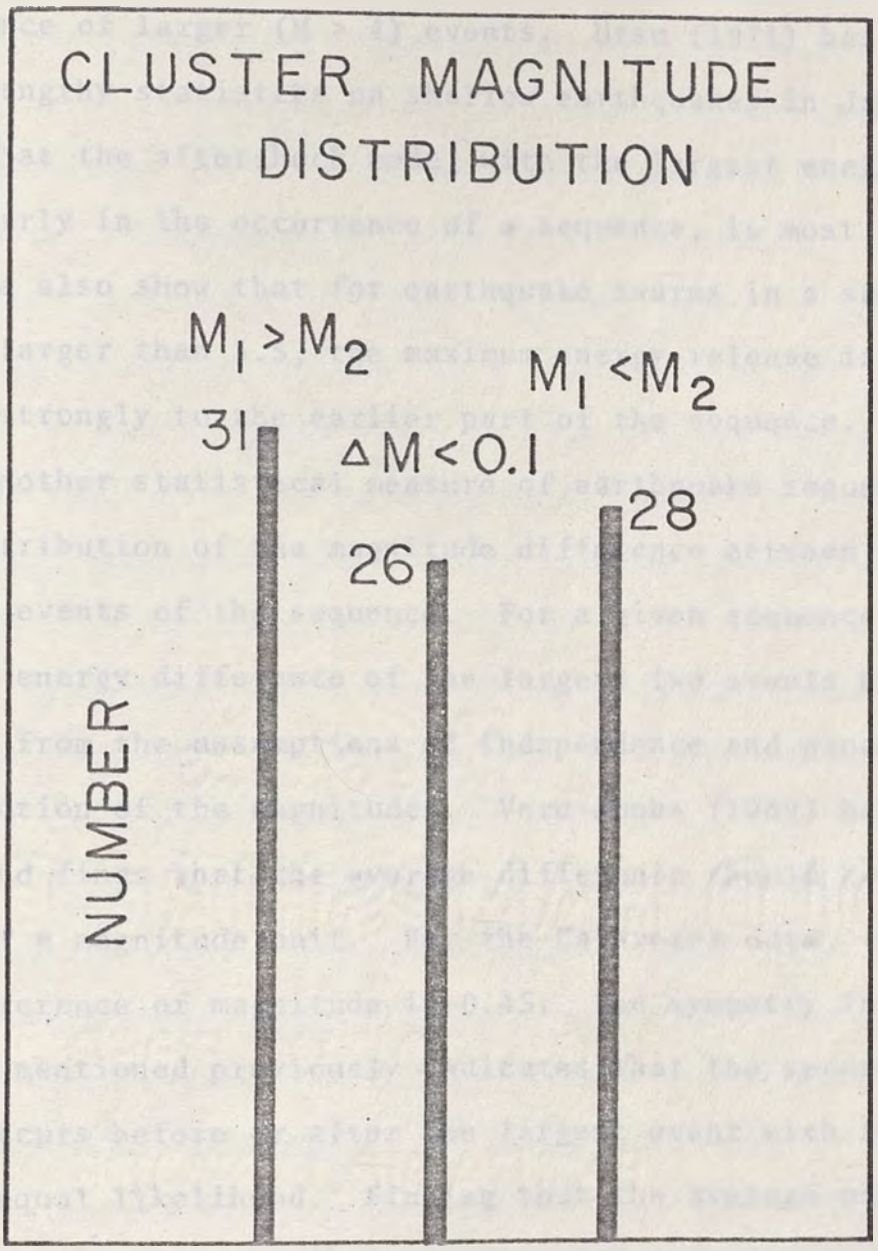

Figure 4-11. Histogram of relative position within each cluster of the largest energy release. M_1 and M_2 represent the energy release of the first and last halves of each cluster, respectively. The central column indicates the number of clusters with less than 0.1 magnitude difference between M_1 and M_2.

was also noted for microearthquake clusters in Nevada (page 96). This pattern stands in contrast to that noted for the occurrence of larger (M > 4) events. Utsu (1971) has tabulated lengthy statistics on shallow earthquakes in Japan and finds that the aftershock mode, with the largest energy release early in the occurrence of a sequence, is most typical. His data also show that for earthquake swarms in a sample with events larger than 5.5, the maximum energy release is still biased strongly to the earlier part of the sequence.

Another statistical measure of earthquake sequences is the distribution of the magnitude difference between the two largest events of the sequence. For a given sequence, the average energy difference of the largest two events may be derived from the assumptions of independence and exponential distribution of the magnitudes. Vere-Jones (1969) has done this, and finds that the average difference should be about one-half a magnitude unit. For the Calaveras data, the average difference of magnitude is 0.45. The symmetry in energy release mentioned previously indicates that the second largest event occurs before or after the largest event with approximately equal likelihood. Finding that the average magnitude difference is close to that expected for independent events suggests that magnitude independence is another characteristic of clusters, with the largest event of the sequence being independent of the others.

A commonly observed characteristic of aftershock

occurrence is the hyperbolic decay of number of events with time, equation (3-1). In order to examine the temporal character of the clustering process, a clear understanding of the definition of cluster duration is needed. From Figure 4-7, the predominant duration can be seen to be relatively short, yet spatial relatedness for some Calaveras events apparently occurs for at least five days. In order to avoid the problem of having to define an "end" to a cluster, the time difference between the two largest events in each cluster was used as a variable indicating the duration of clustering. The difference times for the 85 clusters are plotted cumulatively in Figure 4-12. In the upper graph, the linear portion indicates a hyperbolic fit to the initial portion of the data, out to about 36 hours. The slope of the line represents a time decay of cluster duration proportional to $t^{-1.2}$. The lower graph of Figure 4-12 represents the same data points plotted on a semi-log scale. The approximately linear relationship for clusters with longer durations begins near four hours and represents an exponential decay. A somewhat similar change from hyperbolic and exponential decay was noted for aftershock occurrence at approximately 100 days after the main event (Mogi, 1962).

In Figure 4-13 the spatial occurrence of clusters is compared with the occurrence of unclustered single events. The events and clusters were counted in intervals along the zone defined by 3-kilometer changes in latitude. The two

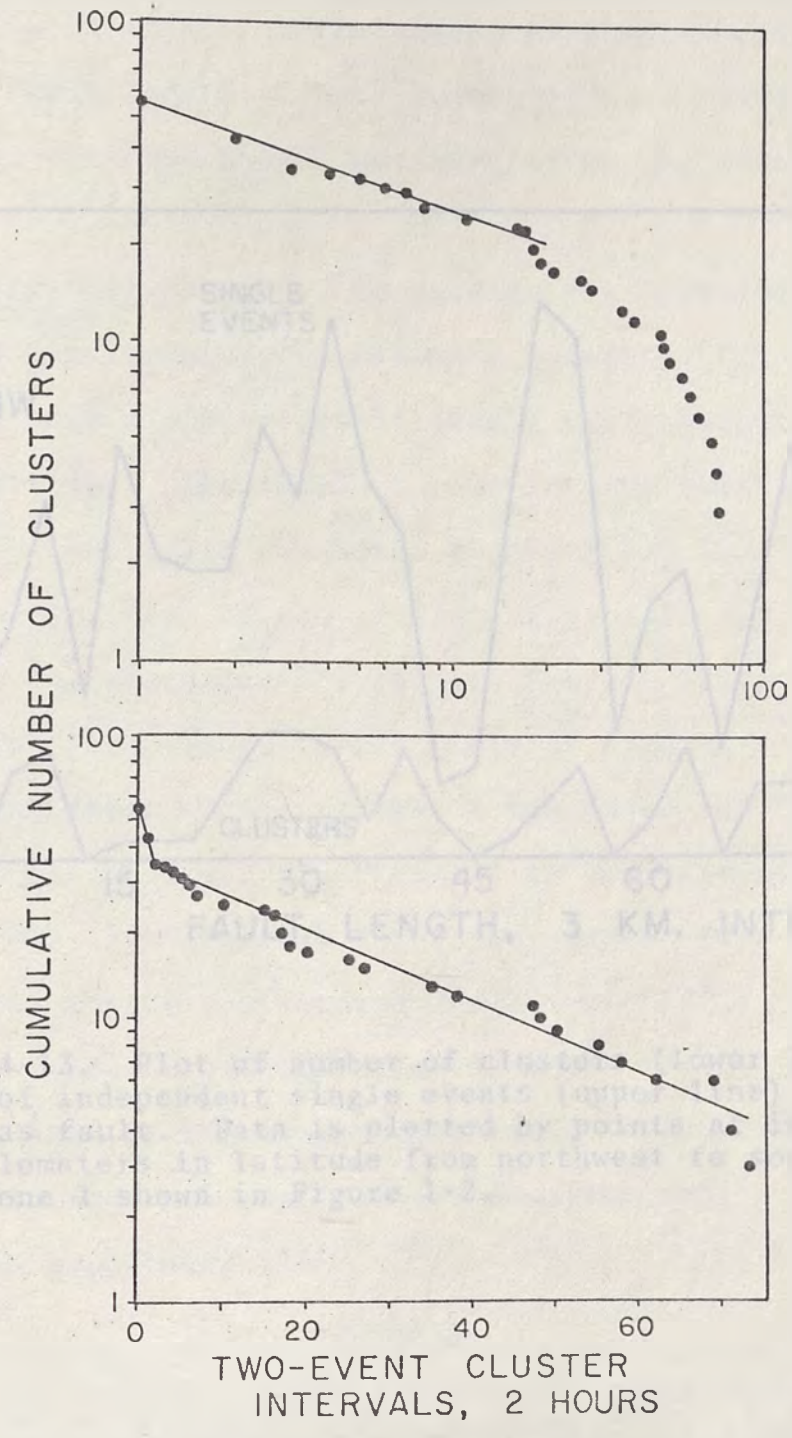

Figure 4-12. Plots of time differences between two largest events in Calaveras clusters. Upper figure is plotted on log-log scale; lower figure is plotted on semi-log scale. Horizontal scale is in units of two hours.

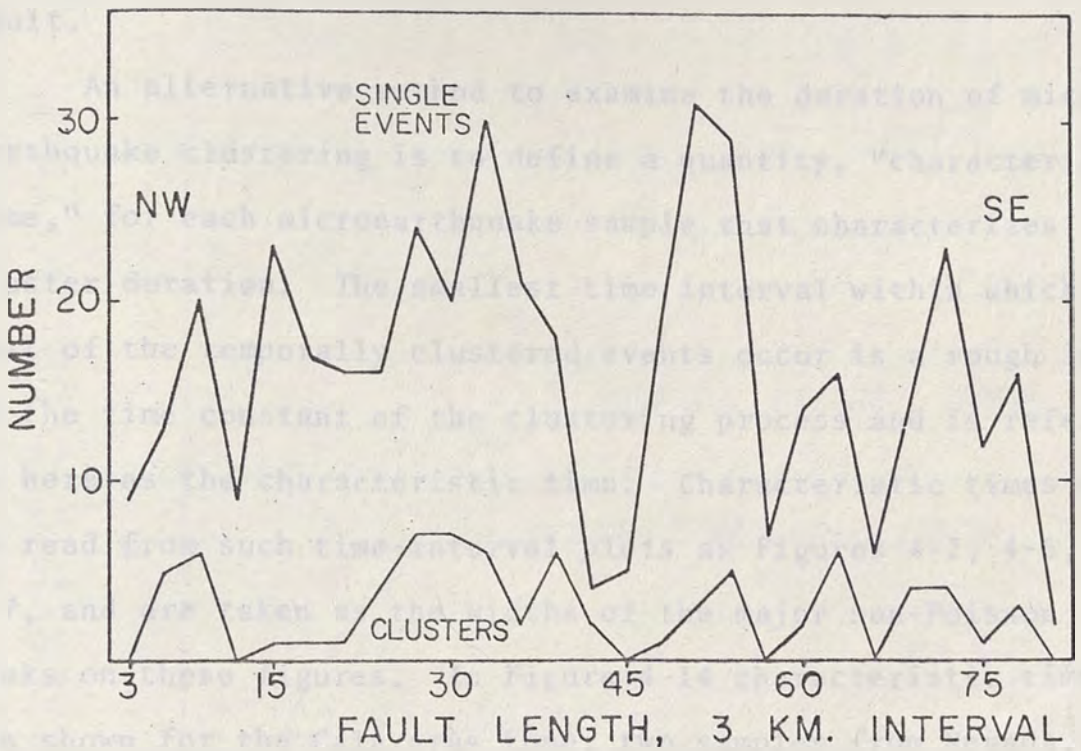

Figure 4-13. Plot of number of clusters (lower line) and number of independent single events (upper line) along the Calaveras fault. Data is plotted by points at intervals of 3 kilometers in latitude from northwest to southeast along zone 1 shown in Figure 1-2.

distributions correlate well visually, with the level of clustering being 20 to 30% of the number of single events all along the fault length. Thus clustering is a fairly constant fraction of microearthquake activity along the Calaveras fault.

An alternative method to examine the duration of microearthquake clustering is to define a quantity, "characteristic time," for each microearthquake sample that characterizes cluster duration. The smallest time interval within which most of the temporally clustered events occur is a rough index of the time constant of the clustering process and is referred to here as the characteristic time. Characteristic times may be read from such time-interval plots as Figures 4-2, 4-6, and 4-7, and are taken as the widths of the major non-Poisson peaks on these figures. In Figure 4-14 characteristic times are shown for the Calaveras zone, two samples from Nevada, two samples from Russia (Gaisky and Zhalkovsky, 1972), and large Japanese earthquakes including aftershocks (Utsu, 1970). The horizontal axis is the minimum magnitude in each sample. This limited data suggests that cluster duration scales exponentially with magnitude.

Summary

In this chapter, occurrences of microearthquakes in areas of California and Nevada were examined for their spatial and temporal relationships. This resulted in the identification and definition of microearthquake occurrence as a

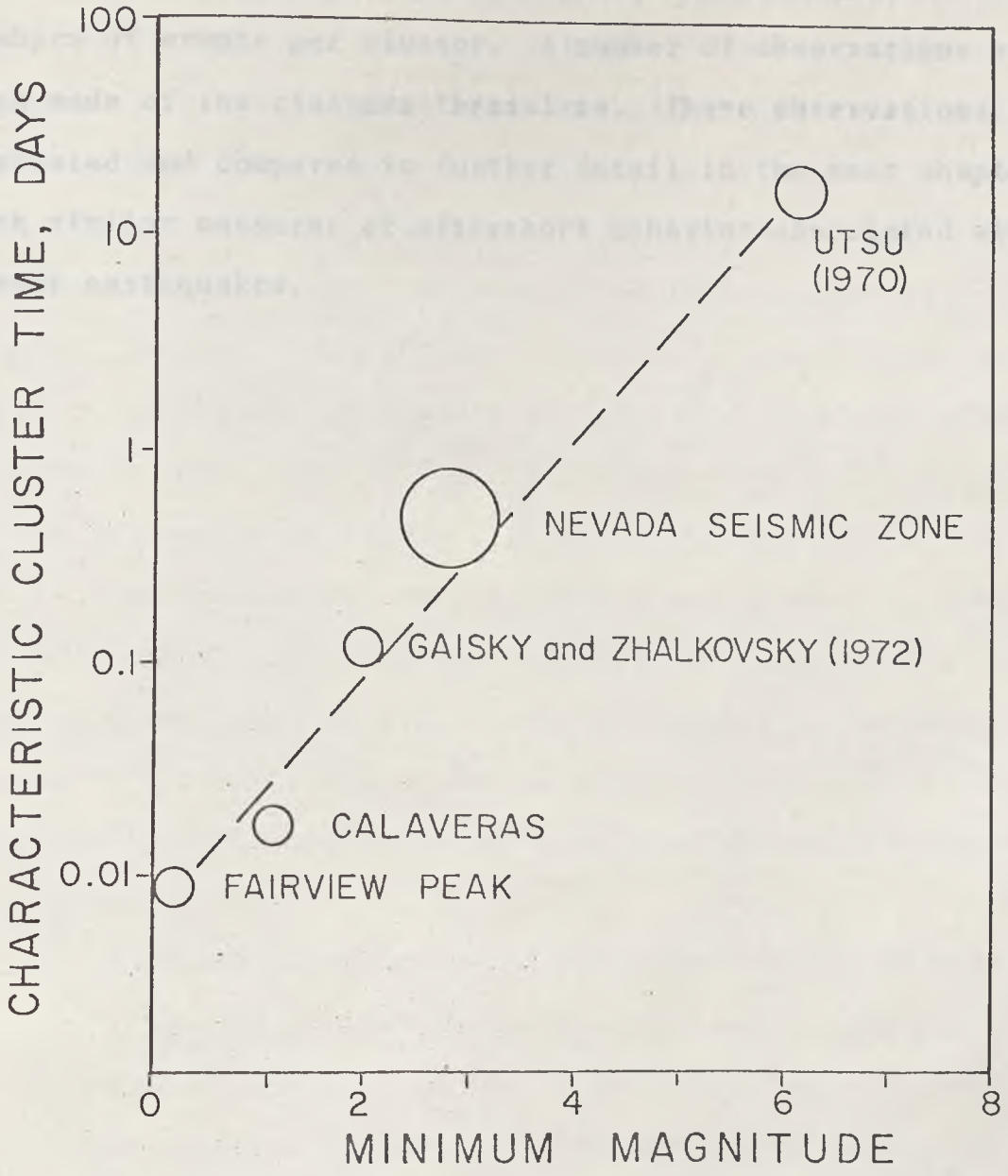

Figure 4-14. Characteristic cluster time as a function of minimum magnitude for each sample shown. Symbol size is larger for less well-defined values of characteristic time.

compound process consisting of (1) a Poisson distribution in time of cluster centers, and (2) a Zeta distribution of the numbers of events per cluster. A number of observations were then made of the clusters themselves. These observations are evaluated and compared in further detail in the next chapter with similar measures of aftershock behavior associated with larger earthquakes.

CHAPTER V. DISCUSSION AND SUMMARY

Comparisons with Aftershock Statistics

In the analyses and discussions of the preceding two chapters, it was proposed that earthquake time-series can be described by three processes; Poisson occurrence of random events, aftershocks following a "trigger" event, and micro-earthquake clustering. The second of these processes, aftershocks, has been studied statistically in considerable detail, with a quite thorough summary of aftershock statistics presented by Utsu (1969, 1970, 1971, 1972). Since microearthquake clustering is also a significantly non-Poisson process, it is most natural to compare these two processes in detail to identify similarities and differences. Some of the following comparisons were discussed in Chapter IV and will be summarized here in the following items. Table 5-1 itemizes the similarities and differences between aftershocks and clusters.

1. For both aftershocks and clusters, the volume within which the aftershocks or clusters occur appears to be scaled according to magnitude of the largest number of the group. Numerous studies have found that aftershocks define the approximate slip surface of the triggering event (Utsu, 1961, 1969), although the aftershock zone may grow somewhat with time after the main shock. The source dimensions associated with clustered earthquakes in the magnitude range 0 to 3

TABLE 5-1

Similarities Between Aftershocks and Clusters

1. Both occur in focal region approximately defined by source volume of largest event in sequence, which is proportional to magnitude.
2. Both decay in level of activity approximately hyperbolically with time.
3. Duration time of both sequences is proportional to magnitude, as defined by "characteristic time."
4. Group size distribution proportional to N^{-E}.

Differences

Aftershocks	Clusters
1. Occur following earthquakes of magnitude greater than 4.0 to 5.0.	1. Occur for earthquakes of magnitude 0 to near 4.0.
2. Likelihood of aftershock sequence occurrence increases with magnitude of main shock to near 100% above magnitude 7.0 or so.	2. Clustering occurrence varies regionally, but is an approximately constant fraction of activity in each zone.
3. Main shock acts as "trigger" for sequence.	3. Magnitude values within clusters are independent of each other.
4. Main shock is "trigger" event and dominates energy release.	4. Energy release average is symmetric about center event of cluster--no "trigger" event.

are of the same or smaller size, tens to hundreds of meters, as the relative location accuracies of the clustered events. Thus for clustering the degree of spatial relatedness can be estimated to be approximately within the source dimension of the largest event of the cluster.

2. The temporal decay in relatedness is approximately hyperbolic both for aftershocks (Omori's law, equation 3-1) and for clusters (Figure 4-12). The possible change in the distribution for clusters beyond 36 hours is not considered significant and may be due to inadequate data.

3. For the Calaveras sample, clustering affects a rather constant fraction of the total number of earthquakes (Figure 4-13), about 25%. The spatial distribution of clustering as shown in Figure 4-13 also indicates that clustering is a usual element of earthquake occurrence all along the zone studied and does not occur in a limited spatial area. The fraction of larger earthquakes that are followed by aftershocks increases from some small fraction of earthquakes near magnitude 4.0 to essentially 100% for events of magnitude 6.0 and greater. The Calaveras sample analyzed in this paper was not of sufficient size to look at possible relationships between clustering and magnitude in the range M = 1.0 to 3.0. It would not be surprising to

find that there was a moderate increased likelihood of occurrence of related events with magnitude in that range. Among the Nevada samples, there were marked regional differences in the fraction of events that occurred in clusters.

4. The quantity "characteristic time," which was defined in Chapter IV as a measure of the duration of the most obvious period of temporal relatedness, appears to scale according to magnitude (Figure 4-14). The difficulty of definition of cluster duration and the variability of duration of aftershock sequences (Utsu, 1961, 1969) again suggest caution in presuming a substantial degree of accuracy to Figure 4-14, but the trend of the relationship is quite clear.
5. For both aftershocks and clusters, the average magnitude difference of about 1/2 magnitude unit between the two largest earthquakes of the group is predicted based on the assumption of magnitude independence (Vere-Jones, 1969). The observed average difference for clusters is 0.45, in good agreement, but the observed average difference for larger mainshock-aftershock sequences is substantially larger (about 1) and does not appear to be subject to biasing due to magnitude cutoff value, M_o (Utsu, 1969). For clustered events, the occurrence of an apparently large number of pairs of events with very small magnitude

difference (Figure 4-11) does not indicate that these pairs of similar events are related in an unusual manner. The magnitudes of clustered earthquakes appear to be independent of each other, while the two largest events in the initial portions of a mainshock-aftershock sequence do not appear to be independent.

6. The most prominent and consistent difference between clustering and aftershock occurrence lies in the pattern of energy release within the two groups. In an aftershock sequence or swarm of moderate or large earthquakes, the major energy release is at or near the first part of the sequence. For clusters, however, the maximum energy release is symmetrically distributed on the average about the middle of the cluster (Figure 4-11).

Physical Models for Earthquake Clustering: Two Hypotheses

Microearthquake clustering appears to be the small-scale analog of the aftershock process associated with larger earthquakes. The many statistical features shared by clustering and aftershocks suggest that any physical model that is generally applied to the aftershock process should also apply to clustering.

Clearly, some sort of time-dependent process triggered by a main shock is the most significant feature of aftershock occurrence. In various models proposed for aftershocks, such

as Benioff (1951), Scholz (1968), Burridge and Knopoff (1967), Dieterich (1972), and Nur and Booker (1972), there is a viscous element to produce time dependency in the model. These include creep behavior of rock, static fatigue, time-dependent friction, or pore fluid migration. To a more or less adequate extent, the above models all predict the occurrence of conditions allowing for continued stress release that decreases in amount proportional to 1/t following a main event. However, the key features of cluster occurrence that must be adequately considered in order to develop a successful model are the lack of a triggering event and the symmetry of stress release.

In Figure 4-11 it was noted that a predominant pattern of stress release in clusters is the occurrence of two earthquakes (the two largest events in the cluster) with quite similar magnitudes, differing by less than one-half magnitude unit. For pairs of clustered events, as noted in Chapter IV, the arrival-time differences on array stations were as small as the timing accuracy of the records, and the detailed character of the seismograms were so similar that they could be overlaid and matched peak-for-peak well into the codas. Due to the frequency response of the recording systems, this suggests a relative location accuracy of better than 50 meters. The small magnitude difference and very similar locations suggest that such clustered events represent repeated slip of approximately the same area, displacement, and

stress drop on either the exact same fault surface or on two parallel fault surfaces separated by at most a few tens of meters. The occurrence of a pair of clustered events thus appears to indicate the reloading of the slip surface following the first event to essentially its original stress level within the seconds or minutes before the occurrence of the second event. This process does not involve a "trigger" event but instead requires a mechanism for rapid viscoelastic stress recovery such as that proposed by Benioff (1951) and used by Dieterich (1972). Because of the similarity in size between the average two clustered events, stress recovery must be sufficient to essentially fully reload the slip surface. Stress recovery to nearly the original conditions also allows the following earthquake to occur with a magnitude value that is statistically independent of the preceding event.

The observed upper magnitude limit to clustering, between magnitude 3.0 and 4.0, may be due to a loss in capacity for near-complete stress recovery to occur for larger events. As the source volume grows much larger than a dimension of several hundred meters, it begins to interact with the boundary conditions of the associated fault zone or the thickness of the brittle crust itself. The result of such boundary effects may be to reduce to capacity for the initial slip surface to be restressed by the surrounding stress field and thus to remove the potential for clustering.

An alternative approach to interpreting the occurrence of microearthquake clustering is in terms of Mogi's (1963) classification of fracture patterns. He found that different types of laboratory-generated microshock patterns depend on the structural state of the material and the spatial distribution of the applied stresses. In particular, a fairly homogeneous material to which a uniform stress is applied will exhibit a distinct main shock followed by a time-decaying aftershock sequence. However, a highly heterogeneous medium when uniformly stressed shows no main fracture, but breaks with many smaller shocks concentrated in time. This second pattern is also observed for a very concentrated stress appearing in a less heterogeneous medium. Mogi (1967) relates these laboratory models to the seismicity of Japan, and notes that swarm-type events up to M = 5.0 to 6.0 occur predominantly in volcanic regions and several other tectonic areas which are highly fractured. Earthquake swarms are also noted as a primary occurrence pattern along oceanic ridges (Sykes, 1970; Francis and Porter, 1971), where the source region is also highly fractured with a concentrated (linear) stressed region. A similar explanation may be applied to microearthquake clustering. On the scale of the source dimensions of magnitude 5.0 and larger events, with fault lengths greater than several kilometers, a fracture zone such as the San Andreas appears to be a two-dimensional boundary between two elastic blocks, and aftershock occurrence

predominates. However, for magnitude zero to magnitude 3.0 events the source dimensions range from less than a kilometer to tens of meters, which is on the scale of the detailed fracturing within a fault zone. Thus, to a small event, the medium appears to be highly fractured and it is this scale-dependent heterogeneity that encourages the clustered occurrence pattern. It is observed that clustering is most pronounced in areas along the San Andreas, Calaveras, and Fish Lake Valley fault zones, and these zones are characterized by complex fracture patterns within zones hundreds to a thousand meters in width (D. B. Slemmons, personal communication, 1972).

Summary

In the preceding chapters the importance of examining the detailed application of one-dimensional probability models to magnitude- and time-series of earthquakes has been emphasized. The Poisson model has proven of great utility in isolating and permitting further study of earthquake occurrence features that are not described by the simple Poisson process.

In studying the Poisson behavior of magnitude distributions, three non-Poisson elements must be considered in order to perform a statistically proper analysis of b-values: determination of the minimum magnitude cutoff to define a complete catalog; dependencies on occurrence of the largest events; and magnitude-value biases or other sources of

nonlinear magnitude-frequency distribution. A linear distribution log N versus magnitude is produced by earthquakes with Poisson-distributed magnitudes.

For earthquake time-series, three processes based on the Poisson model appear to describe earthquake behavior. The first is a simple Poisson occurrence of independent earthquakes that has a stationary or slowly time-varying occurrence rate. The second is the triggered process of aftershock occurrence, in which one of the independent events in the simple Poisson process initiates a single sequence or multiple sequences of aftershocks. Each aftershock sequence is composed of Poisson-distributed independent events that follow an approximately hyperbolically decaying rate law, with the trigger event generally of magnitude 4.0 or larger. The third process is that of microearthquake clustering, occurring among earthquakes of magnitude up to between 3.0 and 4.0. Clustering is defined by spatial and temporal relatedness among earthquakes and is identified in the seismicially active regions of Nevada and central California. A cluster is not characterized by a trigger event, but each cluster is composed of events with magnitudes independent of one another. The cluster-size frequency distribution is described by an inverse power law with exponent near 3.5. Clustering is analogous to the aftershock process in many of its spatial and temporal features, but according to the physical models that were discussed, the cluster process may

arise from factors determined by the scale of the earthquake process for microearthquakes.

BIBLIOGRAPHY

Aki, K., 1956, Some problems in statistical seismology: Geophysical Institute, Faculty of Science, Tokyo University, v 8, pp 205-228.

———, 1965, Maximum likelihood estimate of b in the formula log N = a - bM and its confidence limits: Bulletin of the Earthquake Research Institute, v 43, pp 237-239.

———, 1969, Analysis of the seismic coda of local earthquakes as scattered waves: Journal of Geophysical Research, v 74, pp 615-631.

Asada, T., Suzuki, Z., and Tomoda, Y., 1951, Notes on the energy and frequency of earthquakes: Bulletin of the Earthquake Research Institute, v 29, pp 289 - .

Benioff, H., 1951, Earthquakes and rock creep: Bulletin of the Seismological Society of America, v 41, pp 31-62.

Bufe, C.G., 1970, Frequency-magnitude variations during the 1970 Danville earthquake swarm: Earthquake Notes, v XLI, pp 3-7.

Brune, J.N., 1970, Tectonic stress and the spectra of seismic shear waves from earthquakes: Journal of Geophysical Research, v 75, pp 4997-5009.

Burridge, R. and Knopoff, L., 1967, Model and theoretical seismicity: Bulletin of the Seismological Society of America, v 57, pp 341-371.

Cox, D.R. and Lewis, P.A.W., 1966, The Statistical Analysis of Series of Events: Methuen and Company, Ltd., London, 285 p.

Davison, C., 1938, Studies on the periodicity of earthquakes: London, (Monograph), (Catalogue of 131 earthquakes is contained).

Dieterich, J.H., 1972, Time-dependent friction as a possible mechanism for aftershocks: Journal of Geophysical Research, v 77, pp 3771-3781.

Douglas, B.M. and Ryall, A., 1972, Spectral characteristics and stress drop for microearthquakes near Fairview Peak, Nevada: Journal of Geophyiscal Research, v 77, pp 351-359.

Duda, S.J., 1965, Secular seismic energy release in the circum-Pacific belt: Tectonophysics, v 2, pp 409-452.

Eaton, J.P., O'Neill, M.E., and Murdock, J.N., 1970, Aftershocks of the 1966 Parkfield-Cholame, California, earthquake: a detailed study: Bulletin of the Seismological Society of America, v 60, pp 1151-1197.

Ellsworth, W.L., and Wesson, R.L., 1972, Earthquakes near Bear Valley, California: Transactions, American Geophysical Union, v 53, p 1042 (abstract).

Evernden, J.F., 1970, Study of regional seismicity and associated problems: Bulletin Seismological Society of America, v 60, pp 393-446.

Francis, T.J.G., and Porter, I.T., 1971, A statistical study of mid-Atlantic ridge earthquakes: Geophysical Journal, v 24, pp 31-50.

Gaisky, V.N., and Zhalkovsky, N.D., 1972, Spatial and temporal distribution of the foci of earthquakes of different strength: Physics of the Solid Earth, v 11, pp 71-76.

Gianella, V.P., and Callaghan, E., 1934, The Cedar Mountain, Nevada, earthquake of December 20, 1932: Bulletin of the Seismological Society of America, v 24, pp 345-384.

Gumper, F.J., and Scholz, C., 1971, Microseismicity and tectonics of the Nevada seismic zone: Bulletin of the Seismological Society of America, v 61, pp 1413-1432.

Gutenberg, B., and Richter, C.F., 1944, Frequency of earthquakes in California: Bulletin of the Seismological Society of America, v 34, pp 185-188.

Hahn, G.J., and Shapiro, S.S., 1967, Statistical Models in Engineering: Wiley and Sons, New York, 355 p.

Hamilton, R.M., Smith, B.E., Fischer, F.G., and Papanek, P.J., 1972, Earthquakes caused by underground nuclear explosions on Pahute Mesa, Nevada Test Site: Bulletin of the Seismological Society of America, v 62, pp 1319-1341.

Hanks, T.C., and Wyss, M., 1972, The use of body-wave spectra in the determination of seismic-source parameters: Bulletin of the Seismological Society of America, v 62, pp 561-589.

Iida, K., 1939, Observations sur les Séismes energistrés par microsismographe construit dernièrement. (2): Bulletin of the Earthquake Research Institute, v 17, pp 741-782. (In Japanese with French abstract.)

Inouye, W., 1932, Statistical investigation on earthquake numbers: Bulletin of the Earthquake Research Institute, v 10, pp 43-54.

———, 1937, Statistical investigation of earthquake frequencies: Bulletin of the Earthquake Research Institute, v 15, pp 142-169.

Isacks, B., and Oliver, J., 1964, Seismic waves with frequencies from 1 to 100 cycles per second recorded in a deep-mine in northern New Jersey: Bulletin of the Seismological Society of America, v 54, pp 1941-1980.

Ishimoto, M., and Iida, K., 1939, Observations sur les séismes energistrés par le microsismographe construit dernièrement: Bulletin of the Earthquake Research Institute, v 17, pp 443-478.

Jeffreys, H., 1938, Aftershocks and periodicity in earthquakes: Gerl. Beitr. Geophys., v 53, pp 111-139.

Kishinouye, F., 1948, Statistical investigations of monthly numbers of earthquake felt at Tokyo: Bulletin of the Earthquake Research Institute, v 26, pp 73-80.

Knopoff, L., and Gardner, J.K., 1969, Homogeneous catalogues of earthquakes: Proceedings, National Academy of Science, v 63, pp 1051-1054.

———, 1972, Higher seismic activity during local night on the raw worldwide earthquake catalogue: Geophysical Journal of the Royal Astronomical Society, v 28, pp 311-313.

Lee, W.H.K., Bennett, R.E., and Meagher, K.L., 1972, A method of estimating magnitude of local earthquakes from signal duration: U.S. Geological Survey open-file report, 28 p.

Lee, W.H.K., Eaton, M.S., and Brabb, E.E., 1971, The earthquake sequence near Danville, California: Bulletin of the Seismological Society of America, v 61, pp 1171-1194.

Lee, W.H.K., Meagher, K.L., Bennett, R.E., and Matamoros, E.E., 1972c, Catalog of earthquakes along the San Andreas fault system in central California for the year 1971: U.S. Geological Survey open-file report, 67 p.

Lee, W.H.K., Roller, J.C., Bauer, P.G., and Johnson, J.D., 1972a, Catalog of earthquakes along the San Andreas fault system in central California for the year 1969: U.S. Geological Survey open-file report, 48 p.

Lee, W.H.K., Roller, J.C., Meagher, K.L., and Bennett, R.E., 1972b, Catalog of earthquakes along the San Andreas fault system in central California for the year 1970: U.S. Geological Survey open-file report, 73 p.

Lomnitz, C., 1966, Magnitude stability in earthquake sequences: Bulletin of the Seismological Society of America, v 56, pp 247-249.

Lomnitz, C., and Hax, A., 1966, Clustering in aftershock sequences, in The Earth Beneath the Continents, pp 502-508. J.S. Steinhart and T. Jefferson Smith (Eds.). Washington: American Geophysical Union.

Malone, S.D., 1972, Earth strain measurements in Nevada and possible effects on seismicity due to the solid earth tides: Technical Report, Seismological Laboratory, University of Nevada, Reno, 139 p.

Mogi, K., 1962, On the time distribution of aftershocks accompanying the recent major earthquakes in and near Japan: Bulletin of the Earthquake Research Institute, v 40, pp 107-124.

———, 1963, Some discussions on aftershocks, foreshocks, and earthquake swarms - the fracture of a semi-infinite body caused by an inner stress origin and its relation to earthquake phenomena, 3: Bulletin of the Earthquake Research Institute, v 41, pp 615-658.

———, 1967, Earthquakes and fractures: Tectonophysics, v 5, pp 35-55.

———, 1968, Migration of seismic activity: Bulletin of the Earthquake Research Institute, v 46, pp 53-74.

Nasu, N., 1929, On the aftershocks of the Tango earthquake: Bulletin of the Earthquake Research Institute, v 6, pp 245-332.

Nur, A., and Booker, J.R., 1972, Aftershocks caused by pore fluid flow?: Science, v 175, pp 885-887.

Page, R., 1968, Aftershocks and microaftershocks of the great Alaska earthquake of 1964: Bulletin of the Seismological Society of America, v 58, pp 1131-1168.

Parzen, E., 1962, Stochastic Processes: Holden-Day, Inc., San Francisco, California, 324 p.

Richter, C.F., 1935, An instrumental earthquake magnitude scale: Bulletin of the Seismological Society of America, v 25, pp 1-32.

———, 1958, Elementary Seismology: Freeman, San Francisco, California, 768 p.

Ryall, A., and Malone, S.D., 1971, Earthquake distribution and mechanism of faulting in the Rainbow Mt.--Dixie Valley--Fairview Peak area, central Nevada: Journal of Geophysical Research, v 76, pp 7241-7248.

Ryall, A., and Savage, W.U., 1969, A comparison of seismological effects for the Nevada underground test Boxcar with natural earthquakes in the Nevada region: Journal of Geophysical Research, v 74, pp 4281-4289.

Ryall, A., Savage, W.U., and Slemmons, D.B., 1972, Seismic potential in the western Basin and Range/eastern Sierra Nevada region, Nevada and California: (abstract) Transactions, American Geophysical Union, v 53, p 442.

Ryall, A., Slemmons, D.B., and Gedney, L.D., 1966, Seismicity, tectonism and surface faulting in the western United States during historic time: Bulletin of the Seismological Society of America, v 56, pp 1105-1135.

Ryall, A., VanWormer, J.D., and Jones, A.E., 1968, Triggering of microearthquakes by earth tides, and other features of the Truckee, California, earthquake sequence of September, 1966: Bulletin of the Seismological Society of America, v 58, pp 215-248.

Savage, W.U., 1971, Microearthquake clustering near Fairview Peak, Nevada, and in the Nevada seismic zone: Journal of Geophysical Research, v 77, pp 7049-7056.

Scholz, C.H., 1968, The frequency-magnitude relation of microfracturing in rock and its relation to earthquakes: Bulletin of the Seismological Society of America, v 58, pp 399-415.

Shlien, S., and Toksoz, M.N., 1970a, A clustering model for earthquake occurrences: Bulletin of the Seismological Society of America, v 60, pp 1765-1787.

———, 1970b, Frequency-magnitude statistics of earthquake occurrences: Earthquake Notes, v XLI, pp 5-18.

Smith, B.E., Coakley, J.M., and Hamilton, R.M., 1972, Distribution, focal mechanisms, and frequency of earthquakes in the Fairview Peak area, Nevada, near the time of the BENHAM explosion: Bulletin of the Seismological Society of America, v 62, pp 1223-1240.

Songh, S., and Sanford, A.R., 1972, Statistical analysis of microearthquakes near Socorro, New Mexico: Bulletin of the Seismological Society of America, v 62, pp 917-926.

Stauder, W., and Ryall, A., 1967, Spatial distribution and source mechanism of microearthquakes in central Nevada: Bulletin of the Seismological Society of America, v 57, pp 1317-1345.

Suyehiro, S., 1966, Difference between aftershocks and foreshocks in the relationship of magnitude to frequency of occurrence for the great Chilean earthquake of 1960: Bulletin of the Seismological Society of America, v 56, pp 185-200.

———, 1970, Difference in the relationship of magnitude to frequency of occurrence between aftershocks and foreshocks for an earthquake of magnitude 5.1 in central Japan: Annual Report of the Director, Department of Terrestrial Magnetism, Carnegie Institute, Washington, D.C., pp 475-482.

Suzuki, Z., 1958, A statistical study of the occurrence of small earthquakes III: Sci. Rep. Tohoku Univ., 5th Series, Geophys., v 10, pp 15-27.

Sykes, L.R., 1970, Earthquakes, swarms and sea-floor spreading: Journal of Geophysical Research, v 75, pp 6598-6611.

Thatcher, W., 1973, A note on discrepancies between local magnitude (M_L) and microearthquake magnitude scales: Bulletin of the Seismological Society of America, v 63, pp 315-319.

Utsu, T., 1961, A statistical study on the occurrence of aftershocks: Geophysical Magazine published by the Japan Meteorological Agency, v 30, pp 523-605.

———, 1962, On the nature of three Alaskan aftershock sequences of 1957 and 1958: Bulletin of the Seismological Society of America, v 52, pp 279-297.

———, 1965, a Method of determing the value of b in a formual log n = a - bM showing the magnitude-frequency relation for earthquakes (in Japanese with English abstract): Geophysical Bulletin, Hokkaido University, Japan, v 13, pp 99-103.

———, 1966, A statistical significance test of the difference in b-value between two earthquake groups: Journal of Physics of the Earth, v 14, pp 37-40.

———, 1967, Some problems of the frequency distribution of earthquakes in respect to magnitude (I): Geophysical Bulletin, Hokkaido University, Japan, v 17, pp 85-112.

———, 1969, Aftershocks and earthquake statistics (I) - Some parameters which characterize an aftershock sequence and their interrelations: Journal of the Faculty of Science, Hokkaido University, Japan, Series VII, v III, pp 129-195.

———, 1970, Aftershocks and earthquake statistics (II): Journal of the Faculty of Science, Hokkaido University, Japan, Series VII, v III, pp 197-266.

———, 1971, Aftershocks and earthquake statistics (III) - Analyses of the distribution of earthquakes in magnitude, time, and space with special consideration to clustering characteristics of earthquake occurrence: Journal of the Faculty of Science, Hokkaido University, Japan, Series VII, v III, pp 379-441.

———, 1972, Aftershocks and earthquake statistics (IV) - Analyses of the distribution of earthquakes in magnitude, time, and space with special consideration to clustering characteristics of earthquake occurrence: Journal of the Faculty of Science, Hokkaido University, Japan, Series VII, v IV, pp 1-42.

VanWormer, J.D., 1967, Solid earth tides as a triggering mechanism for earthquakes: MacKay School of Mines Technical Report 5, University of Nevada, Reno.

Vere-Jones, D., 1969, A note on the statistical interpretation of Bath's law: Bulletin of the Seismological Society of America, v 59, pp 1535-1541.

———, 1970, Stochastic models for earthquake occurrence: Journal of the Royal Statistical Society, v B32, pp 1-62.

Vere-Jones, D., and Davies, R.B., 1966, A statistical survey of earthquakes in the main seismic region of New Zealand - Part 2 - Time series analyses: New Zealand Journal of Geology and Geophysics, v 9, pp 251-284.

Vere-Jones, D., Turnovsky, S., and Eiby, G.A., 1964, A statistical survey of earthquakes in the main seismic region of New Zealand: New Zealand Journal of Geology and Geophysics, v 7, pp 722-744.

Von Mises, R., 1964, Mathematical Theory of Probability and Statistics: Academic Press, New York.

Wanner, E., 1937a, Zur statistik der erdbeden I: Gerl. Beitr. Geophys., v 50, pp 85-99.

———, 1937b, Zur statistik de erdbeden II: Gerl. Beitr. Geophys., v 50, pp 223-228.

Wyss, M., 1973, Towards a physical understanding of the earthquake frequency distribution: Geophysical Journal of the Royal Astronomical Society, v 31, pp 341-359.